BioMed Research International

Medicinal Practice of Bioactive Compounds (Natural/Synthetic): An Insight into Gastrointestinal Disorders

Guest Editors: Mahmood Ameen Abdulla, Ibrahim Banat, and Patrick Naughton

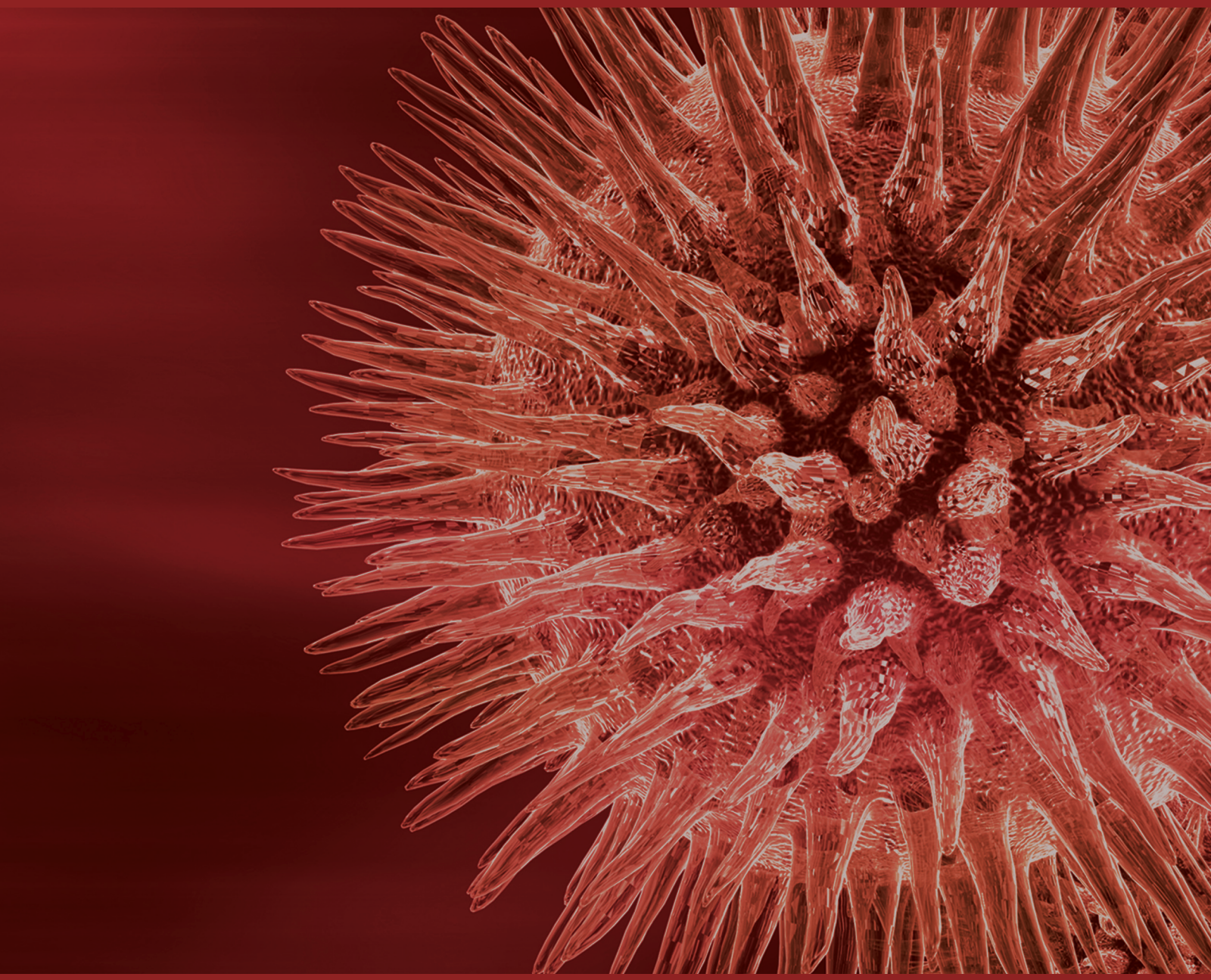

Medicinal Practice of Bioactive Compounds (Natural/Synthetic): An Insight into Gastrointestinal Disorders

BioMed Research International

Medicinal Practice of Bioactive Compounds (Natural/Synthetic): An Insight into Gastrointestinal Disorders

Guest Editors: Mahmood Ameen Abdulla, Ibrahim Banat, and Patrick Naughton

Contents

Medicinal Practice of Bioactive Compounds (Natural/Synthetic): An Insight into Gastrointestinal Disorders, Mahmood Ameen Abdulla, Ibrahim Banat, and Patrick Naughton
Volume 2014, Article ID 401698, 1 page

***In Vivo* Evaluation of Ethanolic Extract of *Zingiber officinale* Rhizomes for Its Protective Effect against Liver Cirrhosis**, Daleya Abdulaziz Bardi, Mohammed Farouq Halabi, Nor Azizan Abdullah, Elham Rouhollahi, Maryam Hajrezaie, and Mahmood Ameen Abdulla
Volume 2013, Article ID 918460, 10 pages

Schiff Base Metal Derivatives Enhance the Expression of HSP70 and Suppress BAX Proteins in Prevention of Acute Gastric Lesion, Shahram Golbabapour, Nura Suleiman Gwaram, Mazen M. Jamil Al-Obaidi, A. F. Soleimani, Hapipah Mohd Ali, and Nazia Abdul Majid
Volume 2013, Article ID 703626, 7 pages

Rikkunshito, a Japanese Kampo Medicine, Ameliorates Decreased Feeding Behavior via Ghrelin and Serotonin 2B Receptor Signaling in a Novelty Stress Murine Model, Chihiro Yamada, Yayoi Saegusa, Koji Nakagawa, Shunsuke Ohnishi, Shuichi Muto, Miwa Nahata, Chiharu Sadakane, Tomohisa Hattori, Naoya Sakamoto, and Hiroshi Takeda
Volume 2013, Article ID 792940, 9 pages

Preparation and Characterization of a Gastric Floating Dosage Form of Capecitabine, Ehsan Taghizadeh Davoudi, Mohamed Ibrahim Noordin, Ali Kadivar, Behnam Kamalidehghan, Abdoreza Soleimani Farjam, and Hamid Akbari Javar
Volume 2013, Article ID 495319, 8 pages

Preventive Inositol Hexaphosphate Extracted from Rice Bran Inhibits Colorectal Cancer through Involvement of Wnt/β-Catenin and COX-2 Pathways, Nurul Husna Shafie, Norhaizan Mohd Esa, Hairuszah Ithnin, Abdah Md Akim, Norazalina Saad, and Ashok Kumar Pandurangan
Volume 2013, Article ID 681027, 10 pages

Hindawi Publishing Corporation
BioMed Research International
Volume 2014, Article ID 401698, 1 page
http://dx.doi.org/10.1155/2014/401698

Editorial

Medicinal Practice of Bioactive Compounds (Natural/Synthetic): An Insight into Gastrointestinal Disorders

Mahmood Ameen Abdulla,[1] Ibrahim Banat,[2] and Patrick Naughton[2]

[1] *Department of Biomedical Sciences, Faculty of Medicine, University of Malaya, 50603 Kuala Lumpur, Malaysia*
[2] *School of Biomedical Sciences, Faculty of Life and Health Sciences, University of Ulster, Coleraine BT52 1SA, UK*

Correspondence should be addressed to Mahmood Ameen Abdulla; ammeen@um.edu.my

Received 3 February 2014; Accepted 3 February 2014; Published 7 April 2014

During the past two decades, the identification of new scientific developments to improve outcomes in gastrointestinal disorders has been attractive to many researchers. Pharmaceutical industries are now more motivated to introduce novel therapeutic remedies in the treatment of gastrointestinal disorders. Such disorders have increased at an exponential rate in various patient communities and both natural and synthetic compounds have been investigated for their potential biological activity in the treatment of these gastrointestinal disorders.

Several interesting works were assessed in this special issue. Amongst them five articles were chosen based on their critical findings in gastrointestinal disorders.

The effects of rikkunshito on the decrease in food intake were assessed after induction of stress in mice and showed improvement in the decrease of food intake probably via serotonin 2B receptor antagonism of isoliquiritigenin. In another work, the preventive effect of inositol hexaphosphate extract of rice bran on colon cancer was assessed. The results showed significant reduction in the expression of β-catenin and COX-2 in colon tumors. The Schiff base metal derivatives also may enhance the expression of HSP70 and suppress the expression of BAX proteins in an acute hemorrhagic gastric ulcer model. Another animal study assessed the hepatoprotective activity of the ethanolic extract of rhizomes of *Z. officinale* against thioacetamide-induced hepatotoxicity in rats. The floating dosage form of an anticancer drug was prepared in another study entitled "Preparation and Characterization of a Gastric Floating Dosage Form of Capecitabine." The work characterized the sustained release tablet in terms of total floating time, dissolution, friability, hardness, drug content, and weight uniformity to compare the prepared formulation with the commercial tablet in terms of drug release, and to evaluate the stability of the formulation.

By presenting these articles, we hope that this issue incorporates new scientific evidence and emerging developments as the basis of rational treatment in medicinal practice using novel therapeutics (natural or synthetic compounds) in the treatment of gastrointestinal disorders.

Mahmood Ameen Abdulla
Ibrahim Banat
Patrick Naughton

Hindawi Publishing Corporation
BioMed Research International
Volume 2013, Article ID 918460, 10 pages
http://dx.doi.org/10.1155/2013/918460

Research Article

In Vivo Evaluation of Ethanolic Extract of *Zingiber officinale* Rhizomes for Its Protective Effect against Liver Cirrhosis

Daleya Abdulaziz Bardi,[1] Mohammed Farouq Halabi,[1] Nor Azizan Abdullah,[2] Elham Rouhollahi,[2] Maryam Hajrezaie,[1,3] and Mahmood Ameen Abdulla[1]

[1] *Department of Biomedical Science, Faculty of Medicine, University of Malaya, 50603 Kuala Lumpur, Malaysia*
[2] *Department of Pharmacology, Faculty of Medicine, University of Malaya, 50603 Kuala Lumpur, Malaysia*
[3] *Institute of Biological Science, Faculty of Science, University of Malaya, 50603 Kuala Lumpur, Malaysia*

Correspondence should be addressed to Mahmood Ameen Abdulla; ammeen@um.edu.my

Received 28 June 2013; Revised 25 October 2013; Accepted 29 October 2013

Academic Editor: Ibrahim Banat

Zingiber officinale is a traditional medicine against various disorders including liver diseases.The aim of this study was to assess the hepatoprotective activity of the ethanolic extract of rhizomes of *Z. officinale* (ERZO) against thioacetamide-induced hepatotoxicity in rats. Five groups of male *Sprague Dawley* have been used. In group 1 rats received intraperitoneal (i.p.) injection of normal saline while groups 2–5 received thioacetamide (TAA, 200 mg/kg; i.p.) for induction of liver cirrhosis, thrice weekly for eight weeks. Group 3 received 50 mg/kg of silymarin. The rats in groups 4 and 5 received 250 and 500 mg/kg of ERZO (dissolved in 10% Tween), respectively. Hepatic damage was assessed grossly and microscopically for all of the groups. Results confirmed the induction of liver cirrhosis in group 2 whilst administration of silymarin or ERZO significantly reduced the impact of thioacetamide toxicity. These groups decreased fibrosis of the liver tissues. Immunohistochemistry assessment against proliferating cell nuclear antigen did not show remarkable proliferation in the ERZO-treated rats when compared with group 2. Moreover, factions of the ERZO extract were tested on Hep-G2 cells and showed antiproliferative activity (IC_{50} 38–60 μg/mL). This study showed hepatoprotective effect of ERZO.

1. Introduction

Ginger or *Zingiber officinale* (family: Zingiberaceae) is a perennial reed-like plant with annual leafy stems. The plant is about a meter tall. The fragrant perisperm of Zingiberaceae is used as sweetmeats by the Bantu tribe [1]. Ginger is traditionally used as a common condiment for various foods and beverages such as soup, ginger ale, ginger bread, ginger snaps, parkin, ginger biscuits, and speculoos. Ginger rhizomes contain a number of pungent constituents and active ingredients [2]. The steam distillation of ginger powder is used to produce ginger oil and contains high amount of sesquiterpene hydrocarbons, predominantly zingiberene [3]. Gingerol is of the major pungent compounds in ginger and can be altered to shogaols, zingerone, and paradol [4] which takes part in several activities such as hepatoprotective [5], antiparasitic [6], antiflarial [7], antimicrobial [8], antidiabetic [9], and radioprotective [10]. Ginger also has a potential remedy against cardiovascular disease [11] and can prevent the development of morphine analgesic tolerance and physical dependence in rats [12]. The plant contains high level of total phenolic and flavonoid, responsible for its high antioxidant activities [13] (for reviews see [14, 15]).

Liver disease is still a worldwide health problem. It develops in about one-third of patients with chronic liver diseases [16] with considerable level of morbidity and mortality [17]. Liver cirrhosis is an irreversible process characterized by excess extracellular matrix (ECM) deposition in the liver accompanied with scar formation and destruction of the liver architecture [18]. During liver cirrhosis, the normal tissue is replaced with the scar tissue, which can block the blood flow of the liver. Liver cirrhosis also attenuates the liver's functions. The liver by itself is able to regenerate the damaged parts, but, during end-stage cirrhosis, the liver is not capable of renovating the damaged cells. Etiology of the liver cirrhosis has a wide spectrum including viruses,

toxins, drugs, and life style [19]. Despite several efforts in drug discovery, treatment for liver cirrhosis is still a concern. In fact complementary and alternative medicine is one of the promising resources for treatment of liver cirrhosis. In traditional remedies herbal drugs have been used for the treatment of liver ailments. Many medicinal plants have been introduced with hepatoprotective potential such as *Vitex negundo* [20], *Boesenbergia rotunda* [21], *Phyllanthus niruri* [22], *Ipomoea aquatic* [23], and *Orthosiphon stamineus* [24]. The phytochemicals phenolic compounds exhibit antioxidant properties that scavenge the free radicals and ROS [25]. Antioxidant activity is important in the treatment of liver cirrhosis [26, 27]. Thioacetamide (TAA) is a hepatotoxic chemical and is widely used in induction of hepatic necrosis. Moreover, thioacetamide causes oxidative stress during its metabolism by microsomal CYP2E1. These effects together cause acute hepatitis which consequently leads to apoptosis of liver cells. Several phytochemicals have been reported in *Z. officinale* with hepatoprotective activity. For instance, in liver, cineole may inhibit CYP2E1 [28] and tocopherol and hepatocyte lipid peroxidation [29]. Inhibition of active caspase-3, capsaicin, possesses hepatoprotective effect through its antioxidant and free radical scavenging mechanisms [30]. Hepatoprotective activity of the ethanolic extract of rhizomes of *Z. officinale* (ERZO) has not been reported specifically. Thus, the present study was to assess the hepatoprotective effect of ERZO against TAA-induced liver cirrhosis in rats.

2. Materials and Methods

2.1. Chemicals. In this study we used TAA (Sigma-Aldrich, Germany) for induction of liver cirrhosis in the rats. Silymarin, a standard drug, was purchased from International Laboratory USA. Ethanol (95%; industrial graded; R&M chemical, UK) and 10% Tween-20 (Merck, Germany), concentrated formalin (38–40%; Merck, Germany), Di-natrium hydrogenphosphat (Merck, Germany), sodium dihydrogen phosphate monohydrate (Sigma-Aldrich, Germany), toluene (Merck, Germany), xylene (BDH Laboratory supplies, England), and other ordinary laboratory materials were also obtained for this experiment.

2.2. Preparation of the Plant Extract. Fresh rhizome of the plant was purchased from a commercial company (Ethno Resources Sdn Bhd, Selangor, Malaysia) and was identified by the voucher specimen deposited at the Herbarium of Rimba Ilmu, Institute of Science Biology, University of Malaya. The rhizome was dried and ground into fine powder using an electrical blender. Fine powder (100 g) was homogenized in ethanol (95%; 500 mL) and left in a conical flask at room temperature for 3 days. Then, the mixture was filtered through a fine muslin cloth and a filter paper (Whatman No. 1). Using the Eyela rotary evaporator (Sigma-Aldrich, USA) the extract became concentrated. The extract was then lyophilized and yielded ERZO. Tween-20 (10%) was used to dissolve the extract in the concentrations of 50 mg/mL and 100 mg/mL. In this study doses of 250 mg/kg and 500 mg/kg were considered for the oral administration of ERZO.

Liquid-liquid partitioning was also performed on the crude ERZO. Briefly, the extract was reconstituted with distilled water (150 mL × 3) to form a suspension. Then it partitioned with n-hexane (200 mL × 3), chloroform (200 mL × 3), and butanol (200 mL × 3) to obtain soluble fractions of n-hexane, chloroform, and butanol. The fractions were mixed well, inverting the whole separation funnel. The suspension was allowed to be separated overnight. For each solvent, the separation was performed thrice. The organic fractions were pooled and the same procedures were performed to yield the respective fractions. Each dried fraction was then dissolved in DMSO (0.5%) in different concentrations for the cell culture experiment.

2.3. Animal Experiments. The study was approved by the ethics committee for animal experimentation, Faculty of Medicine, University of Malaya, Malaysia, and the Ethic no. PM/07/05/2011/MMA (a) (R). All animals received human care according to the criteria outlined in the "Guide for the Care and Use of laboratory Animals" prepared by the National Academy of Sciences and published by the national Institute of health. The rats were provided from the Experimental Animal House, Faculty of Medicine, University of Malaya. The animals were kept at 25 ± 2°C (humidity, 50–60%) with 12 h light/dark cycle.

2.4. Acute Toxicity Test. The toxicity of the ERZO was evaluated in *Sprague Dawley* rats. The animals were treated with two distinct doses of ERZO. The animals were given standard rat pellets and tap water *ad libitum*. Thirty-six rats (18 males and 18 females), weighed 150–180 g, were assigned into 3 groups named control group (Tween-20 10% w/v; 5 mL/kg), low dose group (ERZO, 2 g/kg), and high dose group (ERZO, 5 g/kg). Prior to the dosing, the rats fasted (food but water) overnight. Food was withheld for a further 3 to 4 hours after dosing. Each group received their respective administration, orally. Then, the animals were observed high frequently for 48 h for any sign of abnormality. The rats were monitored for 14 days for any sign of toxicity. The animals were sacrificed on the 15th day. Histological, hematological, and serum biochemical parameters were also assessed [31].

2.5. Induction of Liver Injury. Thirty male SD rats (6–8 weeks old; weighted 150–180 g) were obtained from the Experimental Animal House, Faculty of Medicine, University of Malaya. The rats were randomly divided into 5 groups of 6 rats and kept individually in a cage with wide-mesh wire bottom (i.e., to prevent coprophagia during the experiment). Group 1 received i.p. injection of normal saline, thrice weekly, and oral admonition of distilled water (5 mL/kg), daily. Groups 2–5 were injected with 200 mg/kg TAA (i.p.), thrice weekly as previously described [32]. Group 2 received oral administraion of distilled water (5 mL/kg). Group 5 received silymarin (50 mg/kg) as standard drug. Groups 4 and 5 were fed daily with 250 mg/kg and 500 mg/kg of ERZO. The animals were given water ad libitum. The body weights of the animals were recorded weekly. The duration of the experiment was 8 weeks, according to the previous published work [24].

The rats fasted for 24 h after receiving their respective treatments. Then the animals were euthanized with ketamine (30 mg/kg) and xylazil (3 mg/kg) and diethyl ether inhalation. For each rat, the abdomen and thoracic cavities were opened. The internal organs were checked to be assured that the other organs appear intact, microscopically. The liver was washed with ice-cold normal saline and phosphate buffered saline (PBS; pH 7.4). The organ was carefully dissected and assessed grossly. The liver's weight was recorded for each animal. The tissues were preceded for immunohistology evaluations and antioxidant activities. Blood was sampled through jugular vein to assess the liver's function.

2.6. Biochemical Parameters for Liver Function. Blood analysis was performed at the Clinical Diagnosis Laboratory of University of Malaya Hospital. The main biochemical parameters to assess the liver function were aspartate aminotransferase (AST), alanine aminotransferase (ALT), alkaline phosphatase (ALP), gamma glutamyl transferase (GGT), globulin, conjugated bilirubin, total bilirubin, albumin, and total protein.

2.7. Histopathology of Liver Tissues. Liver tissues were fixed in 10% formalin. The fixed tissues were processed using an automated tissue processing machine (Leica, Germany) and were embedded in paraffin (Leica, Germany). Sections of 5 μm thickness were prepared for each liver tissue. The sections were processed for hematoxylin and eosin (H&E) and Masson's Trichrome (MT) staining. Another set of sections were prepared for immunohistochemistry study of the tissues and mitotic indexing. The liver tissues were further assessed for histopathological examination in a blinded fashion.

2.8. Immunohistochemistry and Mitotic Index. The sections were heated at 60°C for 60 min in an oven (Venticell, MMM, Einrichtungen, Germany). Then the tissues were deparaffinized with xylene. The dehydrating step was performed with graded alcohols (absolute alcohol, 95% and 70% alcohol). Antigen retrieval was performed with 10 mM sodium citrate buffer boiling in a microwave (Sanyo, Super Showe wave, Japan). The sections were placed in TBS contained Tween-20 (0.05%). The staining steps were performed according to the manufacturer's instructions (DakoCytomation, USA). In short, endogenous peroxidase was quenched by peroxidase blocking solution. Then the sections were incubated with proliferating cell nuclear antigen (PCNA; 1 : 200), a biotinylated primary antibodies, for 15 min. Then, streptavidin-HRP was added and incubated for 15 min. The sections were incubated with diaminobenzidine-substrate chromagen DAB for 5 min. The sections were then dipped in weak ammonia (0.037 M/L). Under light microscopy, PCNA positive tissues were stained brown with blue background.

Cell proliferation was assessed though counting the number of mitotic cells per high-power field (HPF) at the magnification of 100x. For each slide 10 randomly selected fields were counted. The mitotic index (MI) was defined as the number of mitotic cells per 1,000 hepatocytes in paraffin-embedded liver samples stained with H&E [33].

2.9. Superoxide Dismutase and Malondialdehyde in Liver Tissue. The tissue samples were homogenized in cold 20 mM HEPES buffer (1 mM EGTA, 210 mM mannitol, and 70 mM sucrose; pH 7.2) using tephlon homogenizer (Polytron, Heidolph RZR 1, Germany). The cell debris was separated by centrifugation (Heraeus, Germany) at 1,500 g for 5 min (4°C). The supernatants were used for the estimation of SOD activity (Cayman Chemical Company, USA). The MDA level was also measured by thiobarbituric acid (TBARS) according to the manufacturer protocol (Cayman Chemical Company, USA).

2.10. Cell Culture and Cytotoxicity of ERZO's Fractions. There were four different fractions, ZC, ZX, ZB, and ZW, representing chloroform, n-hexane, butanol, and aqueous fractions of *Z. officinale*, respectively. A human liver carcinoma cell line (Hep-G2) was obtained from American Type Culture Collection (ATCC, USA). The 3-(4, 5-dimethylthiazol-2-yl)-2, 5-diphenyl tetrazolium bromide (MTT assay) was used to assess the number of viable cells which has been adapted to measure the growth of cells *in vitro*. According to modified protocol [34], the assay was adapted to 96-well cell culture plates. Approximately, 5000 cells per well were seeded one day before the experiment. Cell lines were cultured in RPMI-1640 growth medium, supplemented with ERZO's fractions at different concentrations (3–200 μg/mL), 10% (v/v) sterile fetal bovine serum (FBS, PAA Lab, Austria), 100 mg/mL streptomycin and 100 U/mL penicillin (PAA Lab, Austria), and 50 mg/mL fungizone (Sigma Aldrich). The cultures were incubated in 5% CO_2 incubator at 37°C in a humidified atmosphere. The cells were harvested by detaching the cells from the culture flask using 1-2 mL of trypsin after the flask get confluent enough with the cells. The harvested cells were transferred aseptically into 50 mL sterile falcon tube and washed with physiological buffer (pH 7.2) under spinning at 1200 rpm for 2 minutes. The supernatant was discarded, and the cells pellet was mixed with 1 mL of sterile media and was mixed to form a cell suspension. Harvested cells were seeded into a 96-well culture plates at 100 μL/well and allowed to adhere overnight. ERZO's fractions were predissolved in dimethyl sulphoxide (DMSO) and diluted to different concentration spanning from 3–200 μg/mL. Blank DMSO was used as a control. Cells were incubated with the samples (three wells on a plate for each concentration) for 24 to 72 h. Thereafter, 10 μL of MTT (5 mg/mL) (Sigma) was added to each well and the plates were incubated at 37°C for 4 h. The media were then gently removed, and about 200 mL of DMSO was added to dissolve the formazan crystals. The MTT formazan production was quantified spectrophotometrically at 570 nm using a microplate reader (GF-M3000) for acidified isopropanol and at 555 nm for DMSO. OD reading was referenced to 700 nm to eliminate the background effect. The percentage cell viability was calculated according to the following equation:

$$\text{Cell viability\%} = \left(\frac{\text{Abs}_{570}\ \text{treated}}{\text{Abs}_{570}\ \text{untreated}}\right) \times 100. \quad (1)$$

The IC_{50} value was calculated using the line graph which was drawn with % inhibition and sample concentration.

Table 1: Effects of ERZO on body weight, liver weight, and liver index.

Animal groups	Body weight (gm)	Liver weight (gm)	Liver index (LW/BW %)
Normal control	347 ± 6.65^{b}	10.33 ± 1.15	2.95 ± 0.22^{b}
TAA control	172 ± 6.47^{a}	12.61 ± 0.41	7.38 ± 0.36^{a}
HD 500 mg/kg	217 ± 3.44^{ab}	10.14 ± 0.53^{b}	4.66 ± 0.21^{ab}
LD 250 mg/kg	231 ± 8.76^{ab}	11.78 ± 0.18	5.11 ± 0.19^{ab}
Silymarin 50 mg/kg	374 ± 8.16^{b}	10.66 ± 1.69	2.99 ± 0.32^{b}

Data are expressed as mean ± SEM. Means among groups ($n = 6$ rats/group) show significant difference.

[b]$P < 0.05$ compared to TAA control group, and [a]$P < 0.05$ compared to normal control group.

2.11. Statistical Analysis. In this study statistical analysis was done using one-way analysis of variance (ANOVA) followed by Bonferroni's post hoc test (SPSS ver. 20; SPSS Inc., USA). The P value less than 0.05 was considered significant.

3. Results

3.1. Acute Toxicity Tests. The animals pretreated with ERZO (2 g/kg and 5 g/kg) remained alive and did not manifest any significant visible sign of toxicity within the experimental period. There was no clinical and behavioral abnormality. Histological assessment also confirmed that the extract is safe in doses less than 5 g/kg within 15 days.

3.2. Liver Injury and the Effects of ERZO on Liver. Figure 1 shows gross appearance of the liver for each group. Liver in all of the groups except group 2 possessed generally smooth surfaces without significant irregularities or sign of nodules. Table 1 lists the body weight and the liver weight for each rat during the experiment. Group 1 demonstrated a normal growth pattern for healthy rats. Administration of TAA to group 2 lowered the body weight dramatically. The administration of ERZO (250 mg/kg and 500 mg/kg) was comparable with the effects observed in group 3 (silymarin treated group).

3.3. Biomedical Parameter for Liver Function. According to Tables 2 and 3, group 2 exhibits the highest levels of ALP, ALT, AST, GGT, globulin, total bilirubin, and conjugated bilirubin but albumin and total protein were the lowest among the groups. ERZO (250 mg/kg) showed that the level of ALP, ALT, AST, GGT, globulin, total bilirubin, and conjugated bilirubin were reduced significantly, whilst albumin content was significantly elevated. In these groups, ERZO could significantly restore the biochemical parameters to the levels comparable with silymarin (the standard drug).

3.4. Histopathological Study. A histological image is shown in Figure 2. Regular cellular architecture with distinct normal plates of hepatocytes separated by sinusoidal capillaries and central vein was remarkable in group 1 (Figure 2(a)). In TAA control group (group 2), the liver was enlarged with numerous micro- and macronodules accompanied with disrupted cellular architecture due to the presence of regenerating nodules. The liver was sectioned by fibrous septa extending from the central vein to portal triad. The liver in group 2 showed extensive hepatic damage with necrosis and severe proliferation of bile duct. Moreover, there were microvesicular and macrovesicular centrilobular type fatty changes. Intense inflammation consisting of granulocytes and mononuclear cells around the central vein and in portal areas and congestion appeared to be significant. The livers in groups 3–5 showed a relative protection against the hepatic lesions induced by TAA. There was less disruption of the hepatic cellular structure with mild fibrotic septa. Lymphocyte infiltration in these groups was not significant. They also showed occupied region of the liver by regenerative parenchyma nodules surrounded by septa of fibrous tissue with a remarkable increase in fat storing cells, Kupffer cells, and bile ductules (Figures 2(c), 2(d), and 2(e)).

Masson's trichrome staining was performed to evaluate the degree of fibrosis. As shown in Figure 3(a), liver section from group 1 had no collagen deposition. Group 2 showed proliferation of bile duct with dense fibrous septa and increased deposition of collagen fibers around the congested central vein, which indicate a severe fibrosis (Figure 3(b)). The rat treated with 250 mg/kg and 500 mg/kg of ERZO showed less fibrous septa and irregular regenerating nodules (Figures 3(d) and 3(e)). The collagen deposition patterns appeared comparable among groups 3–5. These observations confirmed the hepatoprotection activity of ERZO.

3.5. Regulation of PCNA and Mitotic Index. Using immunohistochemical staining against PCNA and mitotic index, the proliferating cells were highlighted in the liver tissue sections (Figure 4 and Table 4). Normal hepatocytes as appeared in group 1 did not have PCNA positive cells. Moreover, this group did not possess significant number of mitotic cells. Similarly, group 3 had no sign of PCNA staining. In comparison, group 2 showed upregulation of PCNA as a proliferative factor for the renovation of the damage tissues caused by TAA. Administration of ERZO significantly declined the mitotic index with low level of PCNA.

3.6. SOD and MDA Content of Liver Homogenate. The antioxidant activity for group 2 showed that SOD was significantly reduced when compared with group 1. The treated groups with ERZO (250 mg/kg and 500 mg/kg) or silymarin restored the SOD level significantly (Figure 5). MDA level of liver homogenate was significantly high in group 2 but administration of ERZO considerably lowered the level of MDA. These results were comparable with the silymarin-treated group (Figure 6).

3.7. Cytotoxicity Effect of ERZO's Fractions on Hep-G2. In vitro evaluation of ERZO's fractions against human liver carcinoma cell line is presented in Table 5. It is observed that ZX fraction at low concentration <50 mg/mL has the highest inhibition activity with corresponding 59% inhibition and

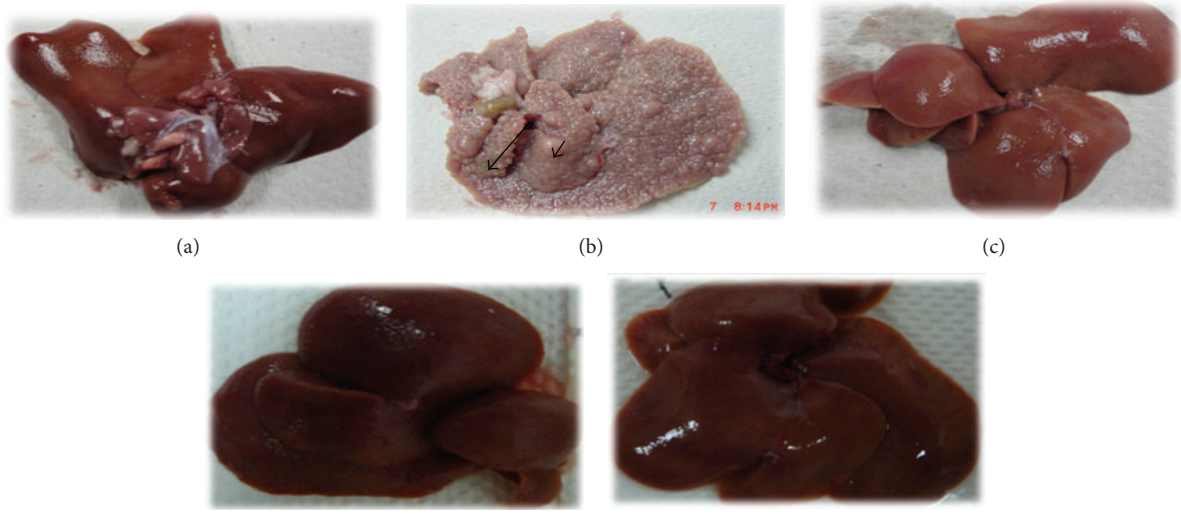

(a) (b) (c)

(d) (e)

Figure 1: Gross morphology shows the effects of ERZO on thioacetamide TAA induced liver damage in rats. (a) Normal control group shows a regular and smooth surface. (b) Animals treated with TAA show many micronodules (arrowhead) and macronodules in the liver (arrow). (c) Animals treated with TAA + silymarin showing normal smooth surface. (d) Animals treated with TAA + ERZO 250 mg/kg and (e) animals treated with TAA + ERZO 500 mg/kg. Both low dose and high dose of ERZO were having normal smooth surface and nearly preserve the liver normal anatomical shape and appearance.

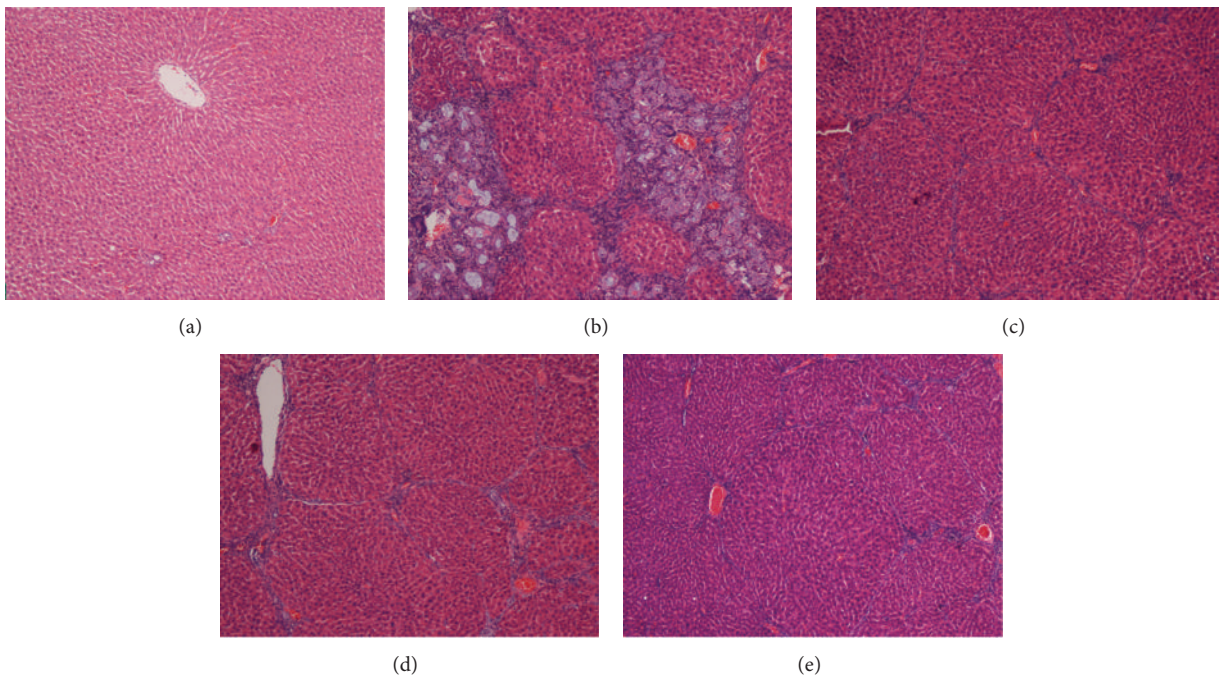

(a) (b) (c)

(d) (e)

Figure 2: Micrograph presents the histopathological sections of the livers taken from rats in different experimental groups. (a) Normal histological structure and architecture were seen in livers of the normal control group. (b) Severe structural damage and formation of pseudolobules with thick fibrotic septa with proliferation of bile duct and centrilobular necrosis were present in the liver of the TAA control group. (c) Mild inflammation but no fibrotic septa were depicted in the liver of the hepatoprotective rat treated with TAA + silymarin. (d) Partially preserved hepatocyte and architecture with small area of necrosis and narrow fibrotic septa existed in the liver of the rat treated with TAA + 250 mg/kg of the ERZO. (e) Partially preserved hepatocyte and architecture with small areas of mild necrosis were observed in the liver of the rat treated with TAA + 500 mg/kg of the ERZO (H&E stain original magnification 10x).

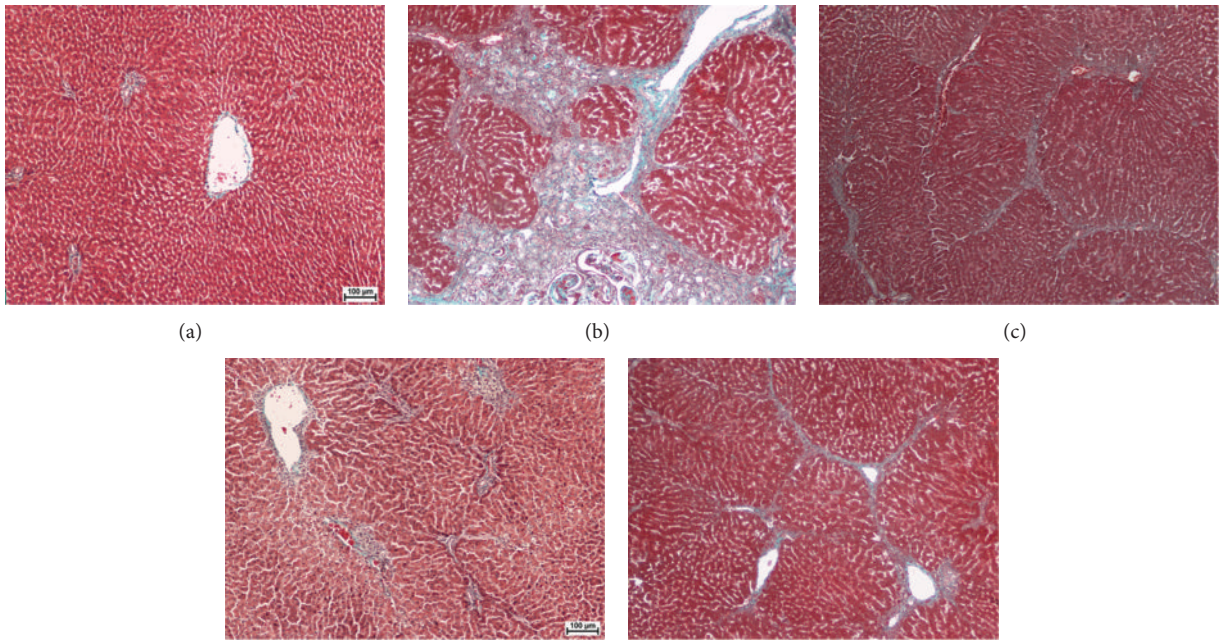

Figure 3: Photomicrograph shows histopathological sections of the livers sampled from different experimental groups. (a) Normal control group shows normal liver architecture. (b) TAA control group shows proliferation of bile duct, dens fibrous septa, and collagen fibers. (c) Rat treated with TAA + silymarin shows minimal fibrous septa and collagen fibers. (d) Rat treated with TAA + 250 mg/kg of the ERZO shows minimal fibrous septa and irregular regenerating nodules. (e) Rat treated with TAA + 500 mg/kg of ERZO shows minimal fibrous septa and collagen fibers. Masson's Trichrome stain (original magnification 10x).

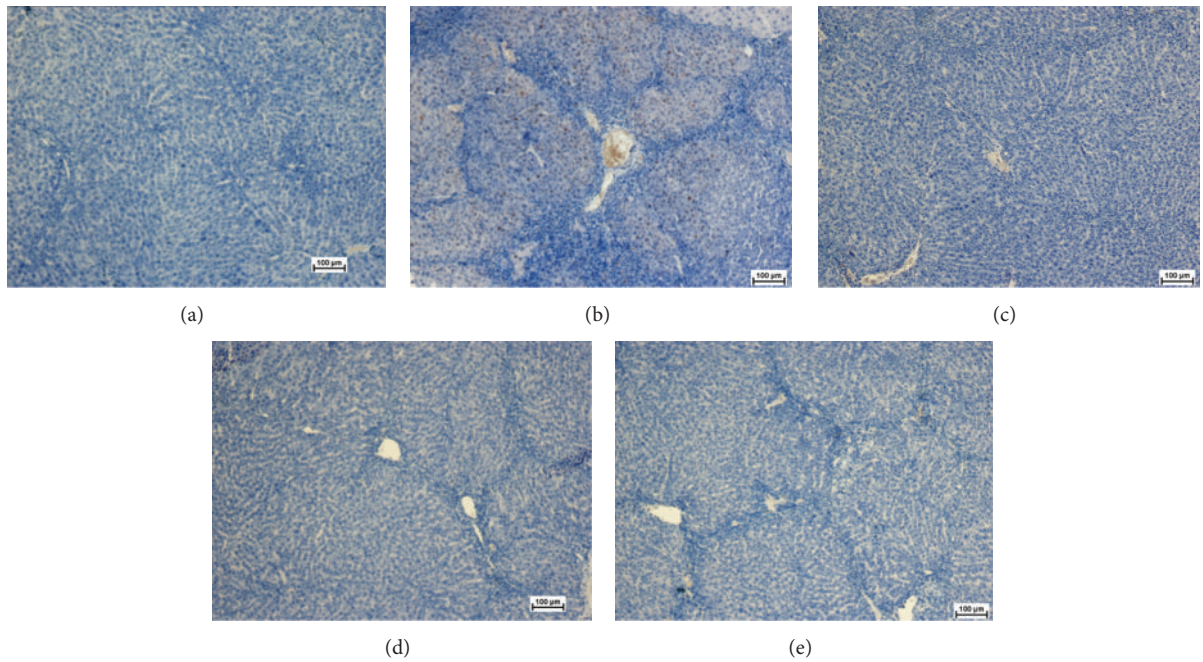

Figure 4: Photomicrograph shows histopathological sections of the livers sampled from different experimental groups using an anti-PCNA antibody. (a) Normal control group was stained without adding the primary antibody and shows normal liver architecture with no signs of PCNA expression. (b) TAA control group showed many hepatocytes nuclei positive for PCNA monoclonal antibody. (c) TAA + silymarin treated rats with no expression of PCNA in hepatocytes. (d) TAA + 250 mg/kg of ERZO and (e) TAA + 500 mg/kg of ERZO group showed nearly normal liver architecture with no signs of PCNA expression (immunohistochemistry, 10x).

Table 2: Effect of TAA, silymarin, and ERZO on biochemical parameters in the serum of experimental rats.

Animal groups	T. protein (g/L)	Albumin (g/L)	Globulin (g/L)	T. bilirubin (umol/L)	Conjugated bilirubin (umol/L)
Normal control	68.67 ± 1.4^{b}	12.83 ± 1.70^{b}	54.50 ± 0.54^{b}	2.66 ± 0.5^{b}	1 ± 0.00^{b}
TAA control	60.83 ± 0.47^{a}	7.83 ± 0.40^{a}	68.66 ± 3.44^{a}	9 ± 0.21^{a}	5.3 ± 0.00^{a}
HD 500 mg/kg	67.66 ± 0.41	12 ± 0.63^{b}	54.16 ± 1.72^{b}	5 ± 1.26^{a}	3 ± 0.22^{ab}
LD 250 mg/kg	65.33 ± 0.33	11.50 ± 1.04^{b}	51.50 ± 2.85^{b}	7.33 ± 1.21^{a}	3.5 ± 0.61^{a}
Silymarin 50 mg/kg	67.33 ± 0.95^{b}	11.83 ± 1.83^{b}	54.33 ± 3.61^{b}	5.66 ± 1.86	3 ± 0.36^{a}

Data are expressed as mean ± SEM. Means among groups ($n = 6$ rats/group) show significant difference.
$^{b}P < 0.05$ compared to TAA control group, and $^{a}P < 0.05$ compared to normal control group.

Table 3: Effects of pretreatment with TAA, silymarin, and ERZO on serum liver biomarkers of experimental rats.

Animal groups	ALP (IU/L)	ALT (IU/L)	AST (IU/L)	GGT (IU/L)
Normal control	100.67 ± 4.96^{b}	64 ± 1.26^{b}	174.5 ± 8.11^{b}	5 ± 0.00^{b}
TAA control	243.83 ± 18.33^{a}	209.83 ± 5.23^{a}	322.16 ± 6.17^{a}	12 ± 0.00^{a}
HD 500 mg/kg	119.67 ± 3.72^{ab}	63.83 ± 7.25^{b}	180.83 ± 1.94^{b}	6.67 ± 0.55^{ab}
LD 250 mg/kg	218.83 ± 16.58^{a}	82.5 ± 3.09^{ab}	227.83 ± 4.62^{b}	6.83 ± 0.16^{b}
Silymarin 50 mg/kg	132.66 ± 10.44^{b}	70.3 ± 4.92^{b}	184.33 ± 7.9^{b}	7 ± 0.00^{ab}

Data are expressed as mean ± SEM. Means among groups ($n = 6$ rats/group) show significant difference.
$^{b}P < 0.05$ compared to TAA control group, and $^{a}P < 0.05$ compared to normal control group.

Table 4: Effects of pretreatment with TAA, silymarin, and ERZO on mitotic index.

Animal groups	Mitotic index
Normal control	0
TAA control	2.8 ± 1.15^{a}
HD 500 mg/kg	0.5 ± 0.16
LD 250 mg/kg	0.7 ± 0.08
Silymarin 50 mg/kg	0.4 ± 0.02

Data are expressed as mean ± SEM. Means among groups ($n = 6$ rats/group) show significant difference; $^{a}P < 0.05$ compared to normal control group.

Table 5: Antiapoptotic efficacy of ERZO's fractions by MTT assay on Hep-G2 cell line.

ERZO fractions	IC50 (μg/mL)
ZX	38
ZC	42
ZB	60
ZW	>200

IC_{50} of 38 μg/mL. However, beyond 50 μg/mL, ZB fraction showed the lowest efficacy with corresponding 67% inhibition and IC_{50} of 60 μg/mL. In comparison to ZB fraction, ZC fraction was observed to be more potent on Hep-G2 cell line achieving a maximum inhibition of about 92% and IC_{50} of 42 μg/mL. The percentage inhibition appeared to continue to increase with increasing concentration up to 200 μg/mL. However, the aqueous fraction ZW performance was found to have an $IC_{50} > 200$ μg/mL.

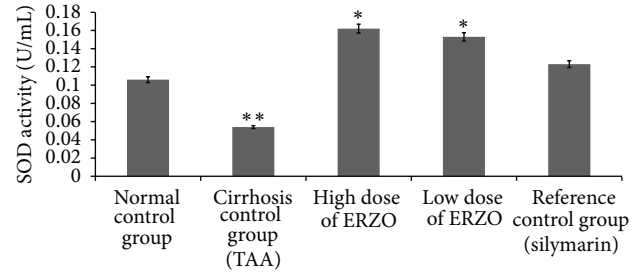

Figure 5: Effect of ERZO on SOD level in the liver tissue. Data are expressed as mean ± SEM. Means among groups ($n = 6$ rate/group) show significant difference, $^{*}P < 0.05$ compared to TAA control group, and $^{**}P < 0.05$ compared to normal control group.

4. Discussion

Several models have been introduced in induction of hepatic injuries [35]. TAA, a most common agent used for induction of liver cirrhosis in animal studies, converts into a toxic reactive metabolite named N-acetylp-benzoquinone imine (NAPBI) and halogenates free radical in hepatic cytochrome p450 [36]. A single dose of TAA causes centrilobular necrosis and subsequent regenerative response in animals [37]. Oral administration of TAA to rodents causes apoptosis and necrosis. In fact, thioacetamide can cause liver cirrhosis and hepatocarcinoma [38, 39], hepatocellular carcinomas, hepatocellular neoplasms, bile duct, and cholangiocellular neoplasms [34]. TAA is specific for the liver and regiospecific for the perivenous hepatocytes with a long window period between necrogenic effects and liver failure [37]. In this study, acute toxicity test showed that ERZO was not toxic <5 mg/kg and did not cause any sign of toxicity or mortality

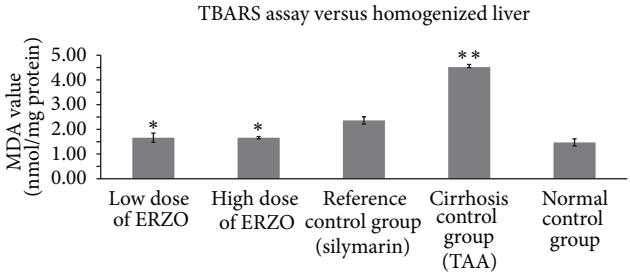

FIGURE 6: Effect of ERZO on MDA level in the liver tissue. Data are expressed as mean ± SEM. Means among groups ($n = 6$ rate/group) show significant difference, $^{*}P < 0.05$ compared to TAA control group, and $^{**}P < 0.05$ compared to normal control group.

within 14 days of the experiment. This observation was in accordance with the previous studies on *Z. officinale* [40, 41]. Rats in group 2 showed hepatomegaly. The increased liver weight/body weight ratio in TAA-treated animal was due to the accumulation of fat and degeneration in the liver. This result was in agreement with a previous report on the increased liver weight/body weight ratio [42]. Our result showed that ERZO could significantly accelerate the recovery of the liver damage. Liver cirrhosis caused hepatomegaly but in this experiment treatment with ERZO significantly prevents the effect of TAA as previously described [24]. The reduction of body weight seen in ERZO treatments might be due to the reduction of hyperlipidemic [43].

TAA enhanced the levels of serum biochemical parameters such as globulin, total bilirubin, and conjugated bilirubin but lowered total protein and albumin as previously reported [44]. The serum biochemical level for ALT, AST, and ALP is in accordance with the extent of liver damage [45]. These results confirmed previous works [41, 44]. The elevation in AST and ALT reflects hepatocellular injury while ALP is linked to the GGT elevation [46]. ERZO reduced the level of ALP as previously reported by Ajith et al. 2007 [47].

Histological evaluation showed protective effect of ERZO against TAA-induced liver cirrhosis. TAA by its nature induces liver cirrhosis in rats. A normal liver has a regular and smooth surface, but in liver cirrhosis it appeared rough and nodular with formations of micronodules and macronodules. In the histopathology evaluation, severe structural damage, formation of irregular pseudolobules with dense fibrotic septa, and proliferation of bile ducts in presence of centrilobular and inflammatory cells were noticeable. The treatment with silymarin and ERZO (in both doses) was considerable. ERZO could enhance reconstitution of liver structure from cirrhosis. The protection level of ERZO was dosedependent as the treatment of 500 mg/kg of ERZO had more protective effect. Moreover, a remarkable reduction in liver fibrosis was observed in ERZO (especially at 500 mg/kg), as previously confirmed [44, 48]. As Masson's trichrome staining showed, minimal reduction in collagen synthesis was seen in ERZO-treated groups. In a healthy liver, no significant collagen deposition was observed. The cytoplasm of the cells appeared clear, with dilated central veins [49, 50]. Liver cirrhosis induced by TAA caused severe fibrosis especially around bile ducts where dense fibrous septa and high deposition of collagen fibers with distorted nuclei and extensively vacuolated cytoplasm were considerable. The standard drug, silymarin, reduced collagen deposition and the cells architecture was resembled. Comparably, ERZO showed a moderate deposition of collagen fibers, especially in the dose of 500 mg/kg. Our results confirmed previous reports on the reduction of necrosis and fibrosis in hepatoxic liver cells in response to phytochemical treatments [49, 50].

The inhibitory effect of ERZO on hepatic stellate cell activation was confirmed by Lee et al. 2011 [51].

PCNA, also known as cyclin, is a nuclear protein synthesized in G_1/S-phase of the cell cycle and is related to cell proliferative activity [52–54]. PCNA is polymerase S accessory protein, essential for cellular DNA synthesis [54]. Liver cirrhosis showed upregulation of PCNA, indicating extensive proliferation for the replacement of the damaged tissues. Treatment with ERZO or silymarin significantly reduced the expression of PCNA as previously reported [55]. The antioxidant test for SOD for the treated rats with ERZO showed high level of activity in comparison with the TAA control group (group 2). The SOD activity appeared similar in both groups treated with ERZO or silymarin which confirmed the previously published work [47]. Reactive oxygen species and nitric oxide are responsible for the induction of hepatocytes apoptosis [56]. Administration of ERZO significantly reduced MDA activity as previously observed in adriamycin-induced model [57].

On evaluating the antiapoptotic efficacy, Hep-G2 cell line was used in this analysis. n-Hexan fraction of ERZO proved to be more potent on Hep-G2 cell line. On the other hand, chloroform fraction of ERZO showed a moderate potency. Butanol fraction of ERZO showed lower efficacy. However, water fraction of ERZO was observed to show the lowest inhibitory activity. In general, the observed efficacy could probably be due to the phytochemical constituents of this plant. The antioxidant action of *Z. officinale* has been proposed as one of the major possible mechanisms for the protective actions of the plant against toxicity. It has been shown that [6]-gingerol is endowed with strong antioxidant action both *in vivo* and *in vitro*, in addition to strong anti-inflammatory and antiapoptotic actions. Pretreatment with [6]-gingerol reduced UVB-induced intracellular reactive oxygen species levels, activation of caspases 3, 8, and 9, and Fas expression. It also reduced UVB-induced expression and transactivation of COX-2 [58]. The hepatoprotective effect of ERZO is due to its antioxidant potency [13] dominated by monoterpenoids [59]. This could be due to the fact that flavonoids have the ability to inhibit lipid peroxidation [5]. These data suggested that ERZO is a very effective agent for the prevention of liver cirrhosis.

5. Conclusion

In the present study, the hepatoprotective activity of ERZO was explored *in vitro* and *in vivo*. Histology, ERZO slowed down liver fibrosis progression and prevents the generation of free radical induced by TAA, which provide an insight into

the mechanism of its biological action. According to these data, *Z. officinale* ingestion is safe in humans and might be a promising hepatoprotective agent.

Acknowledgments

This research was supported by the University of Malaya Grant PV046/2012A, RG 373/11HTM and University Malaya High Impact Research Grant (UM/MOHE/HIR Grant E000045-20001).

References

[1] J. M. Watt and M. G. Breyer-Brandwijk, *The Medicinal and Poisonous Plants of Southern and Eastern Africa*, 2nd edition, 1962.

[2] V. N. Dedov, V. H. Tran, C. C. Duke et al., "Gingerols: a novel class of vanilloid receptor (VR1) agonists," *British Journal of Pharmacology*, vol. 137, no. 6, pp. 793–798, 2009.

[3] V. S. Govindarajan and D. W. Connell, "Ginger—chemistry, technology, and quality evaluation: part 1," *Critical Reviews in Food Science and Nutrition*, vol. 17, no. 1, pp. 1–96, 1983.

[4] V. S. Govindarajan and D. W. Connell, "Ginger—chemistry, technology, and quality evaluation: part 2," *Critical Reviews in Food Science and Nutrition*, vol. 17, no. 3, pp. 189–258, 1983.

[5] C. Ezeonu, P. A. C. Egbuna, L. U. S. Ezeanyika, C. G. Nkwonta, and N. D. Idoko, "Antihepatotoxicity studies of crude extract of *Zingiber officinale* on CCl_4 induced toxicityand comparison of the extract's fraction D hepatoprotective capacity," *Research Journal of Medical Sciences*, vol. 5, no. 2, pp. 102–107, 2011.

[6] S. Forouzan, M. Bahmani, P. Parsaei et al., "Anti-parasitic activites of *Zingiber officinale* methanolic extract on *Limnatis nilotica*," *Global Veterinaria*, vol. 9, no. 2, pp. 144–148, 2012.

[7] O. M. S. Mostafa, R. A. Eid, and M. A. Adly, "Antischistosomal activity of ginger (*Zingiber officinale*) against *Schistosoma mansoni* harbored in C57BL/6 mice," *Parasitology Research*, vol. 109, no. 2, pp. 395–403, 2011.

[8] P. Karuppiah and S. Rajaram, "Antibacterial effect of *Allium sativum* cloves and *Zingiber officinale* rhizomes against multiple-drug resistant clinical pathogens," *Asian Pacific Journal of Tropical Biomedicine*, vol. 2, no. 8, pp. 597–601, 2012.

[9] Z. M. Al-Amin, M. Thomson, K. K. Al-Qattan, and M. Ali, "Anti-diabetic and hypolipidaemic properties of ginger (*Zingiber officinale*) in streptozotocin-induced diabetic rats," *British Journal of Nutrition*, vol. 96, no. 4, pp. 660–666, 2006.

[10] M. S. Baliga, R. Haniadka, M. M. Pereira, K. R. Thilakchand, S. Rao, and R. Arora, "Radioprotective effects of *Zingiber officinale* Roscoe (ginger): past, present and future," *Food & Function*, vol. 3, no. 7, pp. 714–723, 2012.

[11] R. Nicoll and M. Y. Henein, "Ginger (*Zingiber officinale* Roscoe): a hot remedy for cardiovascular disease?" *International Journal of Cardiology*, vol. 131, no. 3, pp. 408–409, 2009.

[12] F. Darvishzadeh-Mahani, S. Esmaeili-Mahani, G. Komeili, V. Sheibani, and L. Zare, "Ginger (*Zingiber officinale* Roscoe) prevents the development of morphine analgesic tolerance and physical dependence in rats," *Journal of Ethnopharmacology*, vol. 141, no. 3, pp. 901–907, 2012.

[13] A. Ghasemzadeh, H. Z. E. Jaafar, and A. Rahmat, "Antioxidant activities, total phenolics and flavonoids content in two varieties of Malaysia young ginger (*Zingiber officinale* Roscoe)," *Molecules*, vol. 15, no. 6, pp. 4324–4333, 2010.

[14] S. Chrubasik, M. H. Pittler, and B. D. Roufogalis, "Zingiberis rhizoma: a comprehensive review on the ginger effect and efficacy profiles," *Phytomedicine*, vol. 12, no. 9, pp. 684–701, 2005.

[15] B. H. Ali, G. Blunden, M. O. Tanira, and A. Nemmar, "Some phytochemical, pharmacological and toxicological properties of ginger (*Zingiber officinale* Roscoe): a review of recent research," *Food and Chemical Toxicology*, vol. 46, no. 2, pp. 409–420, 2008.

[16] G. H. Koek, A. Bast, and A. Driessen, "Liver cirrhosis and vitamin E status," in *The Encyclopedia of Vitamin E*, R. R. Watson, Ed., CABI Publishing, 2007.

[17] T. Ueki, Y. Kaneda, H. Tsutsui et al., "Hepatocyte growth factor gene therapy of liver cirrhosis in rats," *Nature Medicine*, vol. 5, no. 2, pp. 226–230, 1999.

[18] M. Pinzani, "Liver fibrosis," in *Springer Seminars in Immunopathology*, vol. 21, pp. 475–490, Springer, 2000.

[19] M. Cruz-Pamplona, M. Margaix-Munoz, and M. G. Sarrión-Pérez, "Dental considerations in patients with liver disease," *Journal of Clinical and Experimental Dentistry*, vol. 3, no. 2, pp. 127–134, 2011.

[20] F. A. Kadir, F. Othman, M. A. Abdulla, F. Hussan, and P. Hassandarvish, "Effect of *Tinospora crispa* on thioacetamide-induced liver cirrhosis in rats," *Indian Journal of Pharmacology*, vol. 43, no. 1, pp. 64–68, 2011.

[21] S. M. Salama, M. Bilgen, A. S. Al Rashdi, and M. A. Abdulla, "Efficacy of *Boesenbergia rotunda* treatment against thioacetamide-induced liver cirrhosis in a rat model," *Evidence-Based Complementary and Alternative Medicine*, vol. 2012, Article ID 137083, 12 pages, 2012.

[22] Z. A. Amin, M. Bilgen, M.A. Alshawsh, H. M. Ali, A. H. A. Hadi, and M. A. Abdulla, "Protective role of *Phyllanthus niruri* extract against thioacetamide-induced liver cirrhosis in rat model," *Evidence-Based Complementary and Alternative Medicine*, vol. 2012, Article ID 241583, 9 pages, 2012.

[23] S. S. Alkiyumi, M. A. Abdullah, A. S. Alrashdi, S. M. Salama, S. I. Abdelwahab, and A. H. Hadi, "*Ipomoea aquatica* extract shows protective action against thioacetamide-induced hepatotoxicity," *Molecules*, vol. 17, no. 5, pp. 6146–6155, 2012.

[24] M. A. Alshawsh, M. A. Abdulla, S. Ismail, and Z. A. Amin, "Hepatoprotective effects of *Orthosiphon stamineus* extract on thioacetamide-induced liver cirrhosis in rats," *Evidence-Based Complementary and Alternative Medicine*, vol. 2011, Article ID 103039, 6 pages, 2011.

[25] G. Miliauskas, P. Venskutonis, and T. van Beek, "Screening of radical scavenging activity of some medicinal and aromatic plant extracts," *Food Chemistry*, vol. 85, no. 2, pp. 231–237, 2004.

[26] A. Rafat, K. Philip, and S. Muniandy, "Antioxidant potential and content of phenolic compounds in ethanolic extracts of selected parts of *Andrographis paniculata*," *Journal of Medicinal Plant Research*, vol. 4, no. 3, pp. 197–202, 2010.

[27] I. Stoilova, A. Krastanov, A. Stoyanova, P. Denev, and S. Gargova, "Antioxidant activity of a ginger extract (*Zingiber officinale*)," *Food Chemistry*, vol. 102, no. 3, pp. 764–770, 2007.

[28] N. H. Kim, S. H. Hyun, C. H. Jin et al., "Pretreatment with 1,8-cineole potentiates thioacetamide-induced hepatotoxicity and immunosuppression," *Archives of Pharmacal Research*, vol. 27, no. 7, pp. 781–789, 2004.

[29] V. Tayal, B. S. Kalra, S. Agarwal, N. Khurana, and U. Gupta, "Hepatoprotective effect of tocopherol against isoniazid and rifampicin induced hepatotoxicity in albino rabbits," *Indian Journal of Experimental Biology*, vol. 45, no. 12, pp. 1031–1036, 2007.

[30] M. H. Hassan, M. Edfawy, A. Mansour, and A. A. Hamed, "Antioxidant and antiapoptotic effects of capsaicin against carbon tetrachloride-induced hepatotoxicity in rats," *Toxicology and Industrial Health*, vol. 28, no. 5, pp. 428–438, 2012.

[31] S. Y. Hor, M. Ahmad, E. Farsi, C. P. Lim, M. Z. Asmawi, and M. F. Yam, "Acute and subchronic oral toxicity of *Coriolus versicolor* standardized water extract in *Sprague-Dawley* rats," *Journal of Ethnopharmacology*, vol. 137, no. 3, pp. 1067–1076, 2011.

[32] P. Ljubuncic, H. Song, U. Cogan, H. Azaizeh, and A. Bomzon, "The effects of aqueous extracts prepared from the leaves of *Pistacia lentiscus* in experimental liver disease," *Journal of Ethnopharmacology*, vol. 100, no. 1-2, pp. 198–204, 2005.

[33] M. Selzner and P.-A. Clavien, "Failure of regeneration of the steatotic rat liver: disruption at two different levels in the regeneration pathway," *Hepatology*, vol. 31, no. 1, pp. 35–42, 2000.

[34] R. Sartor, C. Thomas, S. Natural et al., *Some anti-thyroidand related substances, nitrofurans and industrial chemicals*, World Health Organisation, Geneva, Switzerland, 1974.

[35] M. Ramya, C. K. Ashok Kumar, M. Teja Sree, and K. Revathi, "A review on hepatoprotective plants," *International Journal of Phytopharmacy Research*, vol. 3, no. 2, pp. 83–86, 2012.

[36] J. Chilakapati, K. Shankar, M. C. Korrapati, R. A. Hill, and H. M. Mehendale, "Saturation toxicokinetics of thioacetamide: role in initiation of liver injury," *Drug Metabolism and Disposition*, vol. 33, no. 12, pp. 1877–1885, 2005.

[37] P. Staňková, O. Kučera, H. Lotková, T. Roušar, R. Endlicher, and Z. Červinková, "The toxic effect of thioacetamide on rat liver *in vitro*," *Toxicology in Vitro*, vol. 24, no. 8, pp. 2097–2103, 2010.

[38] S. K. Natarajan, S. Thomas, P. Ramamoorthy et al., "Oxidative stress in the development of liver cirrhosis: a comparison of two different experimental models," *Journal of Gastroenterology and Hepatology*, vol. 21, no. 6, pp. 947–957, 2006.

[39] J. Balkan, S. Dogru-Abbasoglu, O. Kanbagli et al., "Taurine has a protective effect against thioacetamide-induced liver cirrhosis by decreasing oxidative stress," *Human and Experimental Toxicology*, vol. 20, no. 5, pp. 251–254, 2001.

[40] K. Srivastava and T. Mustafa, "Ginger (*Zingiber officinale*) in rheumatism and musculoskeletal disorders," *Medical Hypotheses*, vol. 39, no. 4, pp. 342–348, 1992.

[41] A. Atta, T. A. Elkoly, S. M. Mouneir, G. Kamel, N. A. Alwabel, and S. Zaher, "Hepatoprotective effect of methanol extracts of *Zingiber officinale* and *Cichorium intybus*," *Indian Journal of Pharmaceutical Sciences*, vol. 72, no. 5, pp. 564–570, 2010.

[42] M. Galisteo, A. Suárez, M. P. Montilla, M. I. Fernandez, A. Gil, and M. C. Navarro, "Protective effects of *Rosmarinus tomentosus* ethanol extract on thioacetamide-induced liver cirrhosis in rats," *Phytomedicine*, vol. 13, no. 1-2, pp. 101–108, 2006.

[43] S. V. Kadnur and R. K. Goyal, "Beneficial effects of *Zingiber officinale* Roscoe on fructose induced hyperlipidemia and hyperinsulinemia in rats," *Indian Journal of Experimental Biology*, vol. 43, no. 12, pp. 1161–1164, 2005.

[44] J. Pal, S. P. Singh, O. Prakash, M. Batra, A. K. Pant, and C. S. Mathela, "Hepatoprotective and antioxidant activity of *Zingiber chrysanthum* Rosec. rhizomes," *Asian Journal of Traditional Medicines*, vol. 6, no. 6, pp. 242–251, 2011.

[45] S. Islam, L. Antonsson, J. Westin, and M. Lagging, "Cirrhosis in hepatitis C virus-infected patients can be excluded using an index of standard biochemical serum markers," *Scandinavian Journal of Gastroenterology*, vol. 40, no. 7, pp. 867–872, 2005.

[46] F. A. Hasan and S. Owyed, "Interpretation of liver chemistry tests," *Bulletin of the Kuwait Institute for Medical Specialization*, vol. 2, no. 1, pp. 27–31, 2003.

[47] T. A. Ajith, U. Hema, and M. S. Aswathy, "*Zingiber officinale* Roscoe prevents acetaminophen-induced acute hepatotoxicity by enhancing hepatic antioxidant status," *Food and Chemical Toxicology*, vol. 45, no. 11, pp. 2267–2272, 2007.

[48] O. K. Yemitan and M. C. Izegbu, "Protective effects of *Zingiber officinale* (Zingiberaceae) against carbon tetrachloride and acetaminophen-induced hepatotoxicity in rats," *Phytotherapy Research*, vol. 20, no. 11, pp. 997–1002, 2006.

[49] R. Nagalekshmi, A. Menon, D. K. Chandrasekharan, and C. K. K. Nair, "Hepatoprotective activity of *Andrographis paniculata* and *Swertia chirayita*," *Food and Chemical Toxicology*, vol. 49, no. 12, pp. 3367–3373, 2011.

[50] U. Suriyakalaa, J. J. Antony, S. Suganya et al., "Hepatocurative activity of biosynthesized silver nanoparticles fabricated using *Andrographis paniculata*," *Colloids and Surfaces B*, vol. 102, pp. 189–194, 2013.

[51] J. K. Lee, J. H. Kim, and H. K. Shin, "Therapeutic effects of the oriental herbal medicine Sho−saiko−to on liver cirrhosis and carcinoma," *Hepatology Research*, vol. 41, no. 9, pp. 825–837, 2011.

[52] I. O. L. Ng, E. C. S. Lai, S. T. Fan, M. Ng, A. S. Y. Chan, and M. K. P. So, "Prognostic significance of proliferating cell nuclear antigen expression in hepatocellular carcinoma," *Cancer*, vol. 73, no. 9, pp. 2268–2274, 1994.

[53] Y. Takasaki, "Anti-proliferating cell nuclear antigen (PCNA) antibody," *Japanese Journal of Clinical Medicine*, vol. 68, pp. 578–581, 2010.

[54] N. H. Waseem and D. P. Lane, "Monoclonal antibody analysis of the proliferating cell nuclear antigen (PCNA). Structural conservation and the detection of a nucleolar form," *Journal of Cell Science*, vol. 96, no. 1, pp. 121–129, 1990.

[55] M. M. E. Taha, A. B. Abdul, R. Abdullah, T. A. T. Ibrahim, S. I. Abdelwahab, and S. Mohan, "Potential chemoprevention of diethylnitrosamine-initiated and 2-acetylaminofluorene-promoted hepatocarcinogenesis by zerumbone from the rhizomes of the subtropical ginger (*Zingiber zerumbet*)," *Chemico-Biological Interactions*, vol. 186, no. 3, pp. 295–305, 2010.

[56] J. H. Wang, H. P. Redmond, Q. D. I. Wu, and D. Bouchier-Hayes, "Nitric oxide mediates hepatocyte injury," *The American Journal of Physiology*, vol. 275, no. 5, pp. G1117–G1126, 1998.

[57] S. A. Sakr, H. A. Mahran, and H. A. Lamfon, "Protective effect of ginger (*Zingiber officinale*) on adriamycin-induced hepatotoxicity in albino rats," *Journal of Medicinal Plant Research*, vol. 5, no. 1, pp. 133–140, 2011.

[58] J.-K. Kim, Y. Kim, K.-M. Na, Y.-J. Surh, and T.-Y. Kim, "[6]-gingerol prevents UVB-induced ROS production and COX-2 expression *in vitro* and *in vivo*," *Free Radical Research*, vol. 41, no. 5, pp. 603–614, 2007.

[59] Y. Sivasothy, W. K. Chong, A. Hamid, I. M. Eldeen, S. F. Sulaiman, and K. Awang, "Essential oils of *Zingiber officinale* var. rubrum Theilade and their antibacterial activities," *Food Chemistry*, vol. 124, no. 2, pp. 514–517, 2011.

Hindawi Publishing Corporation
BioMed Research International
Volume 2013, Article ID 703626, 7 pages
http://dx.doi.org/10.1155/2013/703626

Research Article

Schiff Base Metal Derivatives Enhance the Expression of HSP70 and Suppress BAX Proteins in Prevention of Acute Gastric Lesion

Shahram Golbabapour,[1,2] Nura Suleiman Gwaram,[3] Mazen M. Jamil Al-Obaidi,[4] A. F. Soleimani,[5] Hapipah Mohd Ali,[3] and Nazia Abdul Majid[2]

[1] *Department of Biomedical Science, Faculty of Medicine, University of Malaya, 50603 Kuala Lumpur, Malaysia*
[2] *Institute of Biological Sciences, Faculty of Science, University of Malaya, 50603 Kuala Lumpur, Malaysia*
[3] *Department of Chemistry, Faculty of Science, University of Malaya, 50603 Kuala Lumpur, Malaysia*
[4] *Faculty of Dentistry, Universiti Teknologi MARA, 40450 Shah Alam, Malaysia*
[5] *Institute of Tropical Agriculture, Universiti Putra Malaysia, 43400 Kuala Lumpur, Malaysia*

Correspondence should be addressed to Nazia Abdul Majid; nazia@um.edu.my

Received 26 June 2013; Accepted 22 September 2013

Academic Editor: Ibrahim Banat

Schiff base complexes have appeared to be promising in the treatment of different diseases and disorders and have drawn a lot of attention to their biological activities. This study was conducted to evaluate the regulatory effect of Schiff base metal derivatives on the expression of heat shock proteins (HSP) 70 and BAX in protection against acute haemorrhagic gastric ulcer in rats. Rats were assigned to 6 groups of 6 rats: the normal control (Tween 20 5% v/v, 5 mL/kg), the positive control (Tween 20 5% v/v, 5 mL/kg), and four Schiff base derivative groups named Schiff_1, Schiff_2, Schiff_3, and Schiff_4 (25 mg/kg). After 1 h, all of the groups received ethanol 95% (5 mL/kg) but the normal control received Tween 20 (Tween 20 5% v/v, 5 mL/kg). The animals were euthanized after 60 min and the stomachs were dissected for histology (H&E), immunohistochemistry, and western blot analysis against HSP70 and BAX proteins. The results showed that the Schiff base metal derivatives enhanced the expression of HSP70 and suppressed the expression of BAX proteins during their gastroprotection against ethanol-induced gastric lesion in rats.

1. Introduction

Wide spectrum applications of the Schiff base in biological systems have opened a new horizon in pharmaceutical researches. Schiff bases are usually synthesized through the condensation process of primary amines and active carbonyl groups. Furthermore, indole derivatives have critical roles in variety of biological activities. In novel therapeutics, the development of hybrid molecules consisting different pharmacophores in one frame may lead to remarkable pharmacological effects. The coadministration of the moieties, acting by different mechanisms, may have a synergistic effect with higher activities [1]. The pharmacological activity of Schiff bases metal complexes is solely attributed to the metal, its ligands, or both. Two important factors such as maximum thermodynamic stability and large degree of selectivity are crucial in the design of Schiff base metal complexes or ligands for pharmaceutical application. Various metal complexes have been introduced for their potential therapeutic applications. Possessing various biological activities, some of the first row transition metals are important in metalloproteins. The chemistry of the metal complexes of Schiff bases containing nitrogen and other donors is well described by Tarafder and colleagues [2]. Various Schiff base complexes have shown variety of properties such as anticancer [3–5], antimicrobial, antifungal [6, 7], antiviral [8] and antioxidant, and anti-inflammatory activity [9]; also see [10]. It is believed that some complexes are more effective in metal complexes

than free ligands [11]. Recent studies showed that Schiff base complexes also have remarkable effects against peptic ulcer [12–17].

Peptic ulcer is a result of imbalance between aggressive factors and protective factors. Ethanol has been widely used to induce acute hemorrhagic gastric lesions in animal model studies. Ethanol as an aggressive factor can induce apoptosis in the gastric mucosa. In both prokaryotic and eukaryotic cells, these proteins are classified according to their size [18]. Small heat shock proteins with molecular mass between 15 and 30 kDa act as molecular chaperones in the unfolding and refolding reactions [19, 20]. Heat shock proteins also are important in the translocation of polypeptides across mitochondria membranes [21], nucleus [22], and endoplasmic reticulum [23]. Upregulation of HSPs is a protective mechanism in many biological systems. 70 kDa heat shock protein (HSP70) mediates its biological roles through an interaction with other proteins [24]. Several studies have shown that HSP70 is a type of protein in variety of biological systems. This protein could inhibit apoptosis [25], maybe through its chaperone function stress-induced apoptosis independent from the immune response [26]. This protein is also important in proteins translocation across the nucleus [22]. Heat shock proteins play a critical role in gastroprotection against acute hemorrhagic lesion of gastric mucosa. Studies showed that gastric tissues produce HSP70 as a protective mechanism against ethanolic induced gastric lesions [16, 27–29]. Tsukimi and Okabe reviewed that enhance in expression of HSP70 is an important protective mechanism in mucosal defence against ethanolic-induced lesions [30]. Several studies introduced variety of synthetic compounds and natural products that enhanced the expression of HSP70 in protection of gastric tissue [16, 28, 29, 31]. BAX, a member of Bcl-2 family, is a proapoptotic protein which induces apoptosis [32] to maintain homeostasis. The cytosol in a cell normally contains BAX protein but during apoptosis it migrates to the mitochondria [33]. Ethanol produces reactive oxygen species that increases the expression of BAX protein and causes acute hemorrhagic gastric lesions [16, 27–29]. In our previously published work, copper Schiff base complexes caused a remarkable protection against ethanolic-induced gastric ulcer [16]. The present article was to evaluate whether Schiff bases metal derivatives enhance the expression of heat shock proteins and suppress the expression of BAX proteins in prevention of acute gastric lesion. The gastroprotective properties of each Schiff base derivative complexes were not the main focus in this work.

2. Materials and Methods

2.1. Preparation of Schiff Bases. Condensation between carbonyl group and amines is possible in different reaction conditions and in different solvents [34]. The presence of dehydrating agents normally favours the formation of Schiff bases. Acid salts (usually $MgSO_4$ or Na_2SO_4) are commonly employed as a dehydrating agent. Primary alcohols such as ethanol are the main solvent for the preparation of Schiff bases. Schiff bases have been purified by crystallization methods. Chromatography of Schiff bases on silica gel might cause decomposition of the Schiff bases, through hydrolysis [35]. Stirring the crude reaction mixture in hexane or cyclohexane can purify the Schiff base in these solvents [36]. Moderate polar solvent, such as diethyl ether and dichloromethane, might enhance the purity [37]. In general, Schiff bases are stable solids and can be stored without many precautions [35]. This type of compound is known as an imine or Schiff base. Figure 1 illustrates the general structure of Schiff base derivative. In this study, four Schiff base derivatives with different metal groups named Schiff_1, Schiff_2, Schiff_3, and Schiff_4 were tested to assess the expression levels of HSP70 and BAX proteins during their gastroprotective activity.

Table 1: Specifications of groups for first and second section of the experiment.

Groups	First section	Second section
Normal group	Tween 20 (5% v/v), 5 mL/kg	Tween 20 (5% v/v), 5 mL/kg
Positive group	Tween 20 (5% v/v), 5 mL/kg	Ethanol (95% v/v), 5 mL/kg
Schiff_1	25 mg/kg*	Ethanol (95% v/v), 5 mL/kg
Schiff_2	25 mg/kg*	Ethanol (95% v/v), 5 mL/kg
Schiff_3	25 mg/kg*	Ethanol (95% v/v), 5 mL/kg
Schiff_4	25 mg/kg*	Ethanol (95% v/v), 5 mL/kg

*Dissolved in Tween 20 (5% v/v) and orally given at the dose of 5 mL/kg.

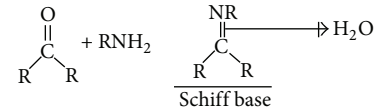

Figure 1: Reaction pathway for the Schiff base derivative.

2.2. Animals. *Sprague Dawley* (8–10 weeks old, weighted 210–230 g) rats were obtained from the Experimental Animal House, Faculty of Medicine, University of Malaya. Animal care and experimental procedures were performed in accordance with the Guide for the Care and Use of Laboratory Animals (National Institute of Health) with approval from the committee for animal experimentation, Faculty of Medicine, University of Malaya (ethic no. (ISB/30/05/2012/SG (R))). They were maintained at ~24°C with free access to standard laboratory pellet and water. 12 h before the experiment, the animals' access for food was restricted. Their access to water was also restricted from 2 h before the experiment.

2.3. Animals Experiment. In this experiment, in addition to two control groups, named the normal group ($n = 6$) and the positive group ($n = 6$), the animals were assigned to four Schiff base groups (Schiff_1, Schiff_2, Schiff_3, and Schiff_4) of 6 rats. The experimental diagram shows specifications for each group (Table 1). In brief, the experiment was divided two sections (Sections 1 and 2). An hour interval was introduced between the sections. In the first section, the normal group and the positive group received 5 mL/kg Tween 20 (5% v/v) while the other groups received 25 mg/kg of

their respective Schiff base complexes (Schiff_1 to Schiff_4) dissolved in Tween 20 (5% v/v). The animals received a volume of 5 mL/kg of their respective complexes. The animals received 5 mL/kg of ethanol (5% v/v) after 1 h but the normal group received 5 mL/kg of Tween 20 (5% v/v). The animals were euthanized after 1 h and their stomachs were dissected for further analysis.

The gastric lesion indexing was performed as described by several works [38–41]. In brief, a dissecting microscope of the lesion area (mm^2) was measured. The index was calculated as inhibition percentage, accordingly [29, 31].

2.4. Histological Observation. Gastric tissues were fixed in buffered formalin (10% v/v) for 18 h and processed by a tissue-processing machine (Leica, Germany). Sections of the stomach were prepared on proper histological slides at a thickness of 5 μm and proceeded to hematoxylin and eosin (H&E) staining and immunohistochemical staining.

Immunohistochemistry staining was performed according to the manufacturer's protocol (DakoCytomation, USA). Tissue sections were incubated with HSP70 (1 : 500) and BAX (1 : 200) biotinylated primary antibodies. Streptavidin-HRP (streptavidin conjugated to horseradish peroxidase) was incubated as a secondary antibody. Under light microscope, the secondary antibody appeared as brown stains.

2.5. Western Blotting. Stomachs of each rat were washed and tissue homogenates were prepared with phosphate buffer (50 mM, pH 7 at ~4–8°C). The homogenates were centrifuged at 4000 rpm for 20 min (4°C) and the supernatant was subjected for protein extraction using the lysis buffer (50 mM Tris-HCL pH 8.0, 120 mM NaCl, 0.5% NP-40, 1 mM PMSF), Protein extract (25 g) was separated by SDS-PAGE (10%), then transferred to a polyvinylidenedifluoride membrane (Bio-Rad), and blocked with 5% nonfat milk in TBS-Tween buffer 7 (0.12 M Tris-base, 1.5 M NaCl, 0.1% Tween 20). The membrane was incubated with the antibodies (HSP70 (1 : 1000), BAX (1 : 1000), and β-actin 1 : 10,000; Cruz Biotechnology, USA) following incubation with horseradish peroxidase conjugated secondary antibody. The bound antibody was detected with peroxidase conjugated anti-rabbit antibody (1 : 10,000) or anti-mouse antibody (1 : 10,000) followed by chemiluminescence (ECL System) and exposed by autoradiography [42].

3. Results

3.1. Lesion Indexing. Gross appearance of luminal surface of the stomach for each group that received the Schiff base complexes showed significant protection when compared with the positive group. However, the protection indexes varied among the rats that received Schiff base complexes. The protection index for Schiff_1 was 73.6% ± 5.50%; Schiff_2 68.06% ± 6.28%; Schiff_3 83.37% ± 6.85%; Schiff_4 79.83% ± 6.47%.

3.2. Histological Observation. Figure 2 shows the H&E staining of gastric tissue for each group. Histological evaluation of gastric tissues showed that ethanol imposed extensive acute haemorrhagic damages into gastric tissue of the positive group. The mucosal and submucosal tissues were disrupted by lesions. Edema was typically observable at the submucosal layer with neutrophil migration. In the experimental groups that received the Schiff base complexes, the damages were significantly reduced when compared with the positive control group. The Schiff base complexes protected the mucosal and submucosal tissues. The histology slides showed that these groups possessed moderate lesion and disruption of the histological layers. Furthermore, the edema was remarkably declined and neutrophil migration was negligible (Figure 2, left column).

3.3. Immunohistochemistry. Immunohistochemistry study showed the expression of HSP70 and BAX proteins in tissue sections of the gastric tissues among the groups. Figure 2 shows the expression of HSP70 and BAX proteins (mid and right columns, resp.) in different groups. Microscopic evaluation of the gastric sections showed that acute haemorrhagic gastric lesions induced by ethanol caused an increase in the expression of BAX protein (Figure 2(f)) and decline in the expression of HSP70 protein (Figure 2(e)). Oral administration of the Schiff base complexes enhanced the expression of HSP70 protein (Figures 2(h), 2(k), 2(m), and 2(q)) and suppressed the expression of BAX protein (Figures 2(i), 2(l), 2(o), and 2(r)). In Figure 2, the expression of these two proteins is characterized by the brown colour staining of the cytoplasm.

3.4. Western Blotting. Throughout the western blot analysis, we conducted a comparable analysis of these proteins in the tissue homogenates of each sample where the β-actin protein was considered the loading control. The result showed that HSP70 was significantly induced in those rats that received the Schiff base complexes as compared with the positive group (Figure 3). On the other hand, the expression of BAX protein was suppressed when the animals received the Schiff based complexes (Figure 3). These results confirmed the role of Schiff base complexes in the regulation of certain proteins as a protective mechanism.

4. Discussion

Ethanol intoxication caused extensive and acute haemorrhagic lesions on the luminal surface of the gastric tissue and damaged the gastric layers. Previous studies showed that such disruption caused decline in antioxidant properties of the stomach and increased in neutrophil infiltration [16, 28, 29, 31]. These studies also confirmed that ethanol reduced the expression of HSP70 protein but enhanced the regulation of BAX protein. Antiulcer properties of several agents have proven the importance of upregulation of HSP70 protein for gastroprotection. For instance, *Polygonum chinense* aqueous leaf extract and *Mucuna pruriens* at the dose of 250 mg/kg and 500 mg/kg, respectively, showed the highest expression level of HSP70 [28, 31]. Our previous study also confirmed that Schiff base derived copper (II) significantly enhanced

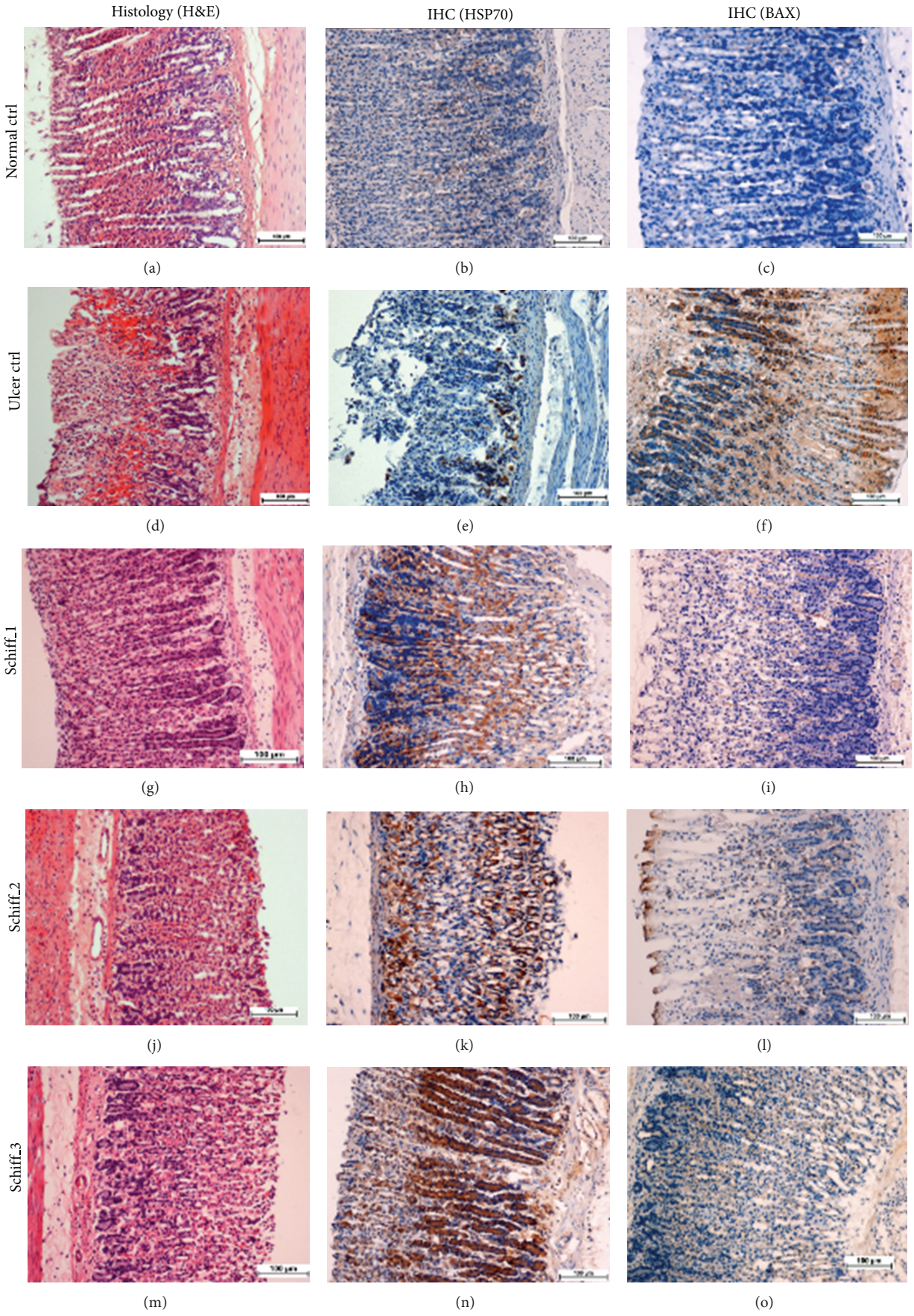

Figure 2: Continued.

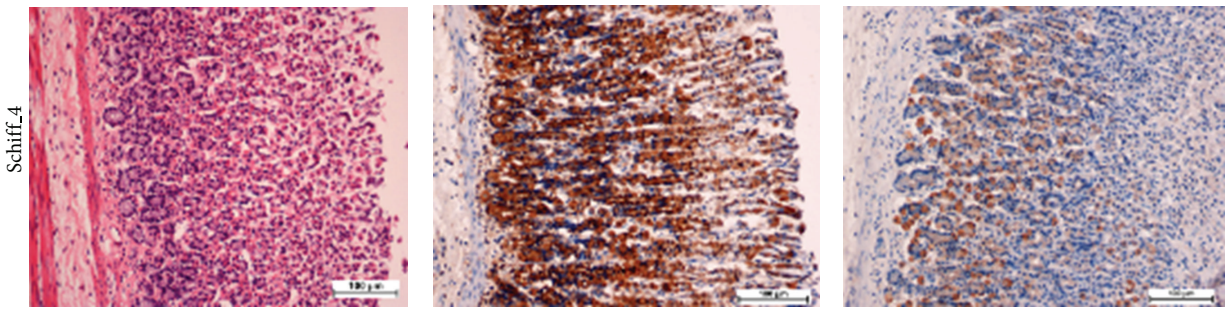

Figure 2: Microscopic study of gastric mucosa in rats (20x). Histological H&E staining of the gastric tissues (left column) and immunohistochemistry (IHC) of HSP70 and BAX proteins (mid column and right column, resp.) are shown for different experimental groups. Normal control group (1st row) shows intact gastric tissue with moderate presence of HSP70 and low presence of BAX. The ulcer control group (2nd row) shows epithelial disruption with acute hemorrhagic lesions into the mucosa. Remarkable submucosa edema and leucocyte penetration are noticeable. The presence of HSP70 is apparently suppressed while the BAX protein is considerably overwhelmed. The Schiff base derivative complexes (3rd–6th rows) show considerable protection against the mucoepithelial disruption caused by ethanol. The edema is not significant. The IHC of HSP70 and BAX shows that these proteins are meaningfully regulated by the Schiff base derivative complexes. The presence of HSP70 in considerably increased when compared to either of the control groups while that of BAX proteins is dramatically declined.

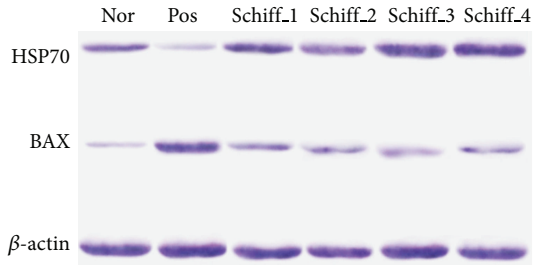

Figure 3: Western blot assay against HSP70 and BAX mouse monoclonal antibody. Corresponding β-actin blots are considered as the loading control. Nor, the normal control group, Pos, the ulcer control group.

the expression of HSP70 [16]. In all of these studies, the enhancement of HSP70 protein was parallel with the suppression of BAX protein.

In this study we assessed the protein expression levels of HSP70 and BAX proteins when the animals were administered with different Schiff base complexes. Based on our pilot study, the dose of 25 mg/kg was the optimal dose for its preventive properties. Moreover, to evaluate the biological effect of Schiff base derivative complexes, all of the Schiff base groups received the same dose (25 mg/kg) of their respective Schiff base complexes. The microscopic evaluation of the stomach for each group showed that Schiff base complexes remarkably increased the gastric protection against ethanol-induced ulcers in rats. Although the protection level of each Schiff base complexes did not appear to be similar, they showed protective property for Schiff base derivative complexes. This work mainly focussed on the expression level of HSP70 and BAX proteins in the protection against acute haemorrhagic gastric lesions. Histological examination with H&E staining confirmed the protective effect of the Schiff base complexes, accordingly. This study revealed that the Schiff base complexes inhibited neutrophil infiltration to the submucosal layer. Moreover, immunohistochemical staining against HSP70 and BAX proteins showed the effect of the Schiff base complexes in enhancement of HSP70 protein and suppression of BAX protein while the animals received their respective administration of Schiff base complexes. Western blot assay showed that the expression level of HSP70 was enhanced, in the tissue homogenates, when the rats received the respective administration of Schiff base complexes in the first section of the experiment. Expectedly, the expression level of BAX protein was suppressed upon receiving Schiff base complexes.

5. Conclusion

Schiff base derivative complexes are among the promising compounds with several biological properties. This study was conducted to evaluate the expression level of HSP70 and BAX proteins in acute haemorrhagic gastric lesions in rats administrated with Schiff base derivative complexes. The Schiff base complexes showed direct relationship with the expression level of HSP70 protein. They also showed that they might suppress the expression of BAX protein as a protective mechanism. Each Schiff base complexes showed a different level of protection but all of them had the same regulatory properties on the expression of HSP70 and BAX proteins at the dose of 25 mg/kg. Consistent with several studies on gastroprotective complexes, Schiff base derivative complexes showed prosperous protective potential through protein regulation pathways. The immunohistochemistry evaluation of gastric tissues showed the protein regulation in situ which was confirmed by western blot assay accordingly.

Conflict of Interests

The authors declare that they have no conflict of interests.

Authors' Contribution

All authors contributed equally in data acquisition. Shahram Golbabapour drafted the paper. All authors read and approved the paper.

Acknowledgments

The authors express their gratitude to the staff of the Faculty of Medicine Animal House for the care and supply of rats and to the University of Malaya for the financial supports. This research is supported by High Impact Research Grant UM-MOHE UM.C/625/1/HIR/MOHE//SC/09 from the Ministry of Higher Education, Malaysia, and by the University of Malaya Grant PG016-2012B and RG057/11BIO. The authors are deeply grateful for all the supports received from the late Professor Datuk Dr. A. Hamid A. Hadi throughout this study.

References

[1] H. Khaledi, A. A. Alhadi, W. A. Yehye, H. M. Ali, M. A. Abdulla, and P. Hassandarvish, "Antioxidant, cytotoxic activities, and structure-activity relationship of gallic acid-based indole derivatives," *Archiv der Pharmazie*, vol. 344, no. 11, pp. 703–709, 2011.

[2] M. T. H. Tarafder, M. A. Ali, D. J. Wee, K. Azahari, S. Silong, and K. A. Crouse, "Complexes of a tridentate ONS Schiff base. Synthesis and biological properties," *Transition Metal Chemistry*, vol. 25, no. 4, pp. 456–460, 2000.

[3] S. B. Desai, P. B. Desai, and K. R. Desai, "Synthesis of some Schiff bases,thiazolidinones and azetidinones derived from 2,6-diaminobenzo[1,2-d:4,5-d′] bisthiazole and their anticancer activities," *Heterocyclic Communications*, vol. 7, no. 1, pp. 83–90, 2001.

[4] A. A. Osowole, I. Ott, and O. M. Ogunlana, "Synthesis, spectroscopic, anticancer, and antimicrobial properties of some metal (II) complexes of (substituted) nitrophenol Schiff base," *International Journal of Inorganic Chemistry*, vol. 2012, Article ID 206417, 6 pages, 2012.

[5] B. Duff, V. R. Thangella, B. S. Creaven et al., "Anti-cancer activity and mutagenic potential of novel copper(II) quinolinone Schiff base complexes in hepatocarcinoma cells," *European Journal of Pharmacology*, vol. 689, no. 1–3, pp. 45–55, 2012.

[6] K. Shanker, R. Rohini, V. Ravinder, P. M. Reddy, and Y.-P. Ho, "Ru(II) complexes of N_4 and N_2O_2 macrocyclic Schiff base ligands: their antibacterial and antifungal studies," *Spectrochimica Acta A*, vol. 73, no. 1, pp. 205–211, 2009.

[7] R. A. Sheikh, M. Y. Wani, S. Shreaz, and A. A. Hashmi, "Synthesis, characterization and biological screening of some Schiff base macrocyclic ligand based transition metal complexes as antifungal agents," *Arabian Journal of Chemistry*, 2011.

[8] K. S. Kumar, S. Ganguly, R. Veerasamy, and E. de Clercq, "Synthesis, antiviral activity and cytotoxicity evaluation of Schiff bases of some 2-phenyl quinazoline-4(3)H-ones," *European Journal of Medicinal Chemistry*, vol. 45, no. 11, pp. 5474–5479, 2010.

[9] M. S. Alam, J. H. Choi, and D. U. Lee, "Synthesis of novel Schiff base analogues of 4-amino-1, 5-dimethyl-2-phenylpyrazol-3-one and their evaluation for antioxidant and anti-inflammatory activity," *Bioorganic & Medicinal Chemistry*, vol. 20, no. 13, pp. 4103–4108, 2012.

[10] A. Jarrahpour, J. Sheikh, I. Mounsi et al., "Computational evaluation and experimental in vitro antibacterial, antifungal and antiviral activity of bis-Schiff bases of isatin and its derivatives," *Medicinal Chemistry Research*, vol. 22, no. 3, pp. 1203–1211, 2013.

[11] A. Golcu, M. Tumer, H. Demirelli, and R. A. Wheatley, "Cd(II) and Cu(II) complexes of polydentate Schiff base ligands: synthesis, characterization, properties and biological activity," *Inorganica Chimica Acta*, vol. 358, no. 6, pp. 1785–1797, 2005.

[12] S. Golbabapour, N. S. Gwaram, P. Hassandarvish et al., "Gastroprotection studies of Schiff base zinc (II) derivative complex against acute superficial hemorrhagic mucosal lesions in rats," *PLoS ONE*, vol. 8, no. 9, Article ID e75036, 2013.

[13] N. S. Gwaram, L. Musalam, H. M. Ali, and M. A. Abdulla, "Synthesis of 2′-(5-chloro-2-hydroxybenzylidene) benzenesulfanohydrazide Schiff base and its anti-ulcer activity in ethanol-induced gastric mucosal lesions in rats," *Tropical Journal of Pharmaceutical Research*, vol. 11, no. 2, pp. 251–257, 2012.

[14] M. Ibrahim, H. Ali, M. Abdullah et al., "Acute toxicity and gastroprotective effect of the Schiff base ligand ^{1}H-indole-3-ethylene-5-nitrosalicylaldimine and its nickel (II) complex on ethanol induced gastric lesions in rats," *Molecules*, vol. 17, no. 10, pp. 12449–12459, 2012.

[15] R. Nirmal, C. R. Prakash, K. Meenakshi, and P. Shanmugapandiyan, "Synthesis and pharmacological evaluation of novel Schiff base analogues of 3-(4-amino) phenylimino) 5-fluoroindolin-2-one," *Journal of Young Pharmacists*, vol. 2, no. 2, pp. 162–168, 2010.

[16] M. Hajrezaie, S. Golbabapour, P. Hassandarvish et al., "Acute toxicity and gastroprotection studies of a new Schiff base derived copper (II) complex against ethanol-induced acute gastric lesions in rats," *PLoS ONE*, vol. 7, no. 12, Article ID e51537, 2012.

[17] M. S. Salga, H. M. Ali, M. A. Abdulla, and S. I. Abdelwahab, "Gastroprotective activity and mechanism of novel dichloridozinc(II)-4-(2- (5-methoxybenzylideneamino)ethyl)piperazin-1-iumphenolate complex on ethanol-induced gastric ulceration," *Chemico-Biological Interactions*, vol. 195, no. 2, pp. 144–153, 2012.

[18] R. H. Burdon, "Heat shock and the heat shock proteins," *Biochemical Journal*, vol. 240, no. 2, pp. 313–324, 1986.

[19] U. Jakob, M. Gaestel, K. Engel, and J. Buchner, "Small heat shock proteins are molecular chaperones," *Journal of Biological Chemistry*, vol. 268, no. 3, pp. 1517–1520, 1993.

[20] E. A. Craig, B. D. Gambill, and R. J. Nelson, "Heat shock proteins: molecular chaperones of protein biogenesis," *Microbiological Reviews*, vol. 57, no. 2, pp. 402–414, 1993.

[21] K. Hannavy, S. Rospert, and G. Schatz, "Protein import into mitochondria: a paradigm for the translocation of polypeptides across membranes," *Current Opinion in Cell Biology*, vol. 5, no. 4, pp. 694–700, 1993.

[22] Y. Shi and J. O. Thomas, "The transport of proteins into the nucleus requires the 70-kilodalton heat shock protein or its cytosolic cognate," *Molecular and Cellular Biology*, vol. 12, no. 5, pp. 2186–2192, 1992.

[23] R. Zimmermann, "The role of molecular chaperones in protein transport into the mammalian endoplasmic reticulum," *Biological Chemistry*, vol. 379, no. 3, pp. 275–282, 1998.

[24] A. R. Clarke, "Molecular chaperones in protein folding and translocation," *Current Opinion in Structural Biology*, vol. 6, no. 1, pp. 43–50, 1996.

[25] E. M. Creagh, R. J. Carmody, and T. G. Cotter, "Heat shock protein 70 inhibits caspase-dependent and -independent apoptosis

in Jurkat T cells," *Experimental Cell Research*, vol. 257, no. 1, pp. 58–66, 2000.

[26] D. D. Mosser, A. W. Caron, L. Bourget et al., "The chaperone function of hsp70 is required for protection against stress-induced apoptosis," *Molecular and Cellular Biology*, vol. 20, no. 19, pp. 7146–7159, 2000.

[27] R. Al Batran, F. Al-Bayaty, M. A. Abdulla et al., "Gastroprotective effects of *Corchorus olitorius* leaf extract against ethanol-induced gastric mucosal hemorrhagic lesions in rats," *Journal of Gastroenterology and Hepatology*, vol. 28, no. 8, pp. 1321–1329, 2013.

[28] I. F. Ismail, S. Golbabapour, P. Hassandarvish et al., "Gastroprotective activity of polygonum Chinense aqueous leaf extract on ethanol-induced hemorrhagic mucosal lesions in rats," *Evidence-Based Complementary and Alternative Medicine*, vol. 2012, Article ID 404012, 9 pages, 2012.

[29] K. A. Ketuly, A. H. Hadi, S. Golbabapour et al., "Acute toxicity and gastroprotection studies with a newly synthesized steroid," *PLoS ONE*, vol. 8, no. 3, Article ID e59296, 2013.

[30] Y. Tsukimi and S. Okabe, "Recent advances in gastrointestinal pathophysiology: role of heat shock proteins in mucosal defense and ulcer healing," *Biological and Pharmaceutical Bulletin*, vol. 24, no. 1, pp. 1–9, 2001.

[31] S. Golbabapour, M. Hajrezaie, P. Hassandarvish et al., "Acute toxicity and gastroprotective role of *M. Pruriens* in ethanol-induced gastric mucosal injuries in rats," *BioMed Research International*, vol. 2013, Article ID 974185, 13 pages, 2013.

[32] T. Strobel, L. Swanson, S. Korsmeyer, and S. A. Cannistra, "BAX enhances paclitaxel-induced apoptosis through a p53-independent pathway," *Proceedings of the National Academy of Sciences of the United States of America*, vol. 93, no. 24, pp. 14094–14099, 1996.

[33] K. G. Wolter, Y.-T. Hsu, C. L. Smith, A. Nechushtan, X.-G. Xi, and R. J. Youle, "Movement of Bax from the cytosol to mitochondria during apoptosis," *Journal of Cell Biology*, vol. 139, no. 5, pp. 1281–1292, 1997.

[34] H. Ohkura, D. O. Berbasov, and V. A. Soloshonok, "Chemo- and regioselectivity in the reactions between highly electrophilic fluorine containing dicarbonyl compounds and amines. Improved synthesis of the corresponding imines/enamines," *Tetrahedron*, vol. 59, no. 10, pp. 1647–1656, 2003.

[35] P. G. Cozzi, "Metal-salen Schiff base complexes in catalysis: practical aspects," *Chemical Society Reviews*, vol. 33, no. 7, pp. 410–421, 2004.

[36] M. Tümer, D. Ekinci, F. Tümer, and A. Bulut, "Synthesis, characterization and properties of some divalent metal(II) complexes: their electrochemical, catalytic, thermal and antimicrobial activity studies," *Spectrochimica Acta A*, vol. 67, no. 3-4, pp. 916–929, 2007.

[37] S. C. Menon, H. B. Singh, R. P. Patel, and S. K. Kulshreshtha, "Synthesis, structure and reactions of the first tellurium-containing macrocyclic Schiff base," *Journal of the Chemical Society*, no. 7, pp. 1203–1207, 1996.

[38] Y. Pérez, A. Oyárzabal, R. Mas et al., "Protective effect of D-002, a mixture of beeswax alcohols, against indomethacin-induced gastric ulcers and mechanism of action," *Journal of Natural Medicines*, vol. 67, no. 1, pp. 182–189, 2013.

[39] Y. Raji, W. A. Oyeyemi, S. T. Shittu et al., "Gastro-protective effect of methanol extract of *Ficus asperifolia* bark on indomethacin-induced gastric ulcer in rats," *Nigerian Journal of Physiological Sciences*, vol. 26, no. 1, pp. 43–48, 2011.

[40] V. Mishra, M. Agrawal, S. A. Onasanwo et al., "Anti-secretory and cyto-protective effects of chebulinic acid isolated from the fruits of *Terminalia chebula* on gastric ulcers," *Phytomedicine*, vol. 20, no. 6, pp. 506–511, 2013.

[41] R. Colucci, L. Antonioli, N. Bernardini et al., "Nonsteroidal anti-inflammatory drug-activated gene-1 plays a role in the impairing effects of cyclooxygenase inhibitors on gastric ulcer healing," *Journal of Pharmacology and Experimental Therapeutics*, vol. 342, no. 1, pp. 140–149, 2012.

[42] S. Mohan, S. I. Abdelwahab, B. Kamalidehghan et al., "Involvement of NF-κB and Bcl_2/Bax signaling pathways in the apoptosis of MCF_7 cells induced by a xanthone compound Pyranocycloartobiloxanthone A," *Phytomedicine*, vol. 19, no. 11, pp. 1007–1015, 2012.

Hindawi Publishing Corporation
BioMed Research International
Volume 2013, Article ID 792940, 9 pages
http://dx.doi.org/10.1155/2013/792940

Research Article

Rikkunshito, a Japanese Kampo Medicine, Ameliorates Decreased Feeding Behavior via Ghrelin and Serotonin 2B Receptor Signaling in a Novelty Stress Murine Model

Chihiro Yamada,[1] Yayoi Saegusa,[1] Koji Nakagawa,[2] Shunsuke Ohnishi,[2,3] Shuichi Muto,[2,4] Miwa Nahata,[1] Chiharu Sadakane,[1] Tomohisa Hattori,[1] Naoya Sakamoto,[3] and Hiroshi Takeda[2,3]

[1] *Tsumura Research Laboratories, Tsumura & Co., Ibaraki 300-1192, Japan*
[2] *Pathophysiology and Therapeutics, Faculty of Pharmaceutical Sciences, Hokkaido University, Sapporo, Hokkaido 060-0812, Japan*
[3] *Department of Gastroenterology and Hepatology, Hokkaido University Graduate School of Medicine, Sapporo, Hokkaido 060-8638, Japan*
[4] *Department of Medical Gastroenterology, National Hospital Organization Hokkaido Medical Center, Sapporo, Hokkaido 063-0005, Japan*

Correspondence should be addressed to Tomohisa Hattori; hattori_tomohisa@mail.tsumura.co.jp

Received 28 June 2013; Revised 21 August 2013; Accepted 29 August 2013

Academic Editor: Mahmood Ameen Abdulla

We investigated the effects of rikkunshito (RKT), a ghrelin signal enhancer, on the decrease in food intake after exposure to novelty stress in mice. RKT administration (500 mg/kg, *per os*) improved the decrease in 6 h cumulative food intake. In control mice, the plasma acylated ghrelin levels significantly increased by 24 h fasting. In contrast, the acylated ghrelin levels did not increase by fasting in mice exposed to the novelty stress. RKT administration to the novelty stress mice showed a significant increase in the acylated ghrelin levels compared with that in the distilled-water-treated control mice. Food intake after administering serotonin 2B (5-HT_{2B}) receptor antagonists was evaluated to clarify the role of 5-HT_{2B} receptor activation in the decrease in feeding behavior after novelty stress. SB215505 and SB204741, 5-HT_{2B} receptor antagonists, significantly improved the decrease in food intake after exposure to novelty stress. A component of RKT, isoliquiritigenin, prevented the decrease in 6 h cumulative food intake. Isoliquiritigenin showed 5-HT_{2B} receptor antagonistic activity *in vitro*. In conclusion, the results suggested that RKT improves the decrease in food intake after novelty stress probably via 5-HT_{2B} receptor antagonism of isoliquiritigenin contained in RKT.

1. Introduction

Stress is becoming a significant social problem [1, 2] and is known to influence gastrointestinal function [3, 4]. One of the psychological stressors experienced in daily life is exposure to social environmental changes, but no detailed investigation regarding the effects of stress associated with this exposure on feeding behavior has been conducted. The novelty-induced hypophagia test measures the suppression of food intake by exposure to a novel environment and is one of the few animal tests of anxiety [5, 6].

Central 5-hydroxytryptamine (5-HT; serotonin) functions by evoking fear and anxiety manifestations and is involved in appetite regulation. Acute 5-HT depletion decreases anxiety behavior that is measured by inhibition of food intake during exposure to novel stimuli [7]. 5-HT_{2C} receptor (5-HT_{2C}R) stimulation may decrease hunger [8, 9], and this type of receptor is expressed on corticotropin-releasing factor (CRF) neurons in the hypothalamic paraventricular nucleus and on proopiomelanocortin neurons in the arcuate nucleus [10]. In addition, stimulation of 5-HT_{2B}Rs, which are distributed throughout the gastrointestinal system,

negatively regulates eating behavior [11–13]. We previously confirmed that novelty stress decreases food intake by activating both CRF1R and 5-HT_{2C}R [14]. However, we have been unable to clarify the role of 5-HT_{2B}R activation in decreased food intake as a result of novelty stress.

Ghrelin is an orexigenic hormone produced in large quantities in the stomach [15]. Peripheral ghrelin binds to its specific growth hormone secretagogue receptor (ghrelin receptor) localized at the end of the vagus nerve around the stomach [16, 17]. Ghrelin secretion from the stomach is regulated by particular subtypes of some neurotransmitters. Activations of 5-HT_{2B}R and 5-HT_{2C}R lead to a reduction in the circulating ghrelin concentrations via a decrease in ghrelin secretion in the stomach [13]. In mice exposed to a novelty stress condition, plasma ghrelin levels decreased 3 h after stress application, and acylated ghrelin supplementation remedied this reaction [14].

Rikkunshito (RKT) is a Japanese Kampo medicine comprising ingredients that facilitate ghrelin signaling [13, 18, 19]. In gastrointestinal functional disorders, where 5-HT is excessively released, such as disorders following cancer chemotherapy [13] and SSRI administration [19], 5-$HT_{2B/2C}$R stimulation causes decreased peripheral and central ghrelin concentrations, and RKT restores decreased peripheral acylated ghrelin secretion to normal levels via antagonizing these receptors. We have already demonstrated that RKT administration improves decreased food intake in novel environmental stress mice [14], but the underlying mechanism remains to be sufficiently elucidated.

We hypothesized that the improvement effects of RKT on decreased feeding behavior caused by novelty stress may be mediated through 5-HT_{2B}R antagonism. To confirm this hypothesis, abnormal ghrelin dynamics in this stress model were clarified. In addition, to clarify the role of 5-HT_{2B}R in the decreased food intake in novelty stress, the administration of 5-HT_{2B}R antagonists was performed. Furthermore, we investigated the antagonistic effects of isoliquiritigenin, a component of RKT, on 5-HT_{2B}Rs and its influence on food intake.

2. Materials and Methods

2.1. Chemicals. SB215505 (5-HT_{2B}R antagonist) and SB204741 (5-HT_{2B}R antagonist) were purchased from Sigma-Aldrich (St. Louis, MO, USA). All chemicals were dissolved in sterilized physiological saline before use. RKT was used as a powdered extract which was obtained by spray drying the hot water extract of a mixture of eight crude drug types: sojutsu (*Atractylodis lanceae rhizoma*), ninjin (*Ginseng radix*), hange (*Pinelliae tuber*), bukuryo (*Hoelen*), taiso (*Zizyphi fructus*), chinpi (*Aurantii nobilis pericarpium*), kanzo (*Glycyrrhizae radix*), and shokyo (*Zingiberis rhizoma*). RKT and RKT components were supplied by Tsumura & Co. (Tokyo, Japan).

2.2. Experimental Animals. Male C57BL/6J mice aged 6 weeks (Charles River Laboratories Japan, Inc., Tokyo, Japan) were used. Before the experiment, five mice per cage were maintained in a room with controlled temperature and humidity under a 07:00–19:00 light cycle with free access to food and water. For novelty stress, each mouse was transferred from group-housed cages to individual cages. Control mice were housed in individual cages for 7 days before the experiment was initiated. The mice in each group were similarly handled. All experiments were performed between 09:00 and 18:00 according to the guidelines established by the Experimental Animal Ethics Committee of Tsumura & Co.

2.3. Food Intake. All protocols were performed under a 24 h fasting condition. Time-course evaluation of the effect of the novelty stress on food intake in 24 h fasted mice was undertaken 1, 2, 3, 6, and/or 24 h after exposure to the novelty stress, and the effect was calculated as the difference between the food weights before and after the feeding period at each time interval.

To clarify the orexigenic action of RKT on food intake in stressed mice, we then investigated the effects of *per os* (PO) administration of RKT (500 mg/kg) [14] (Figure 1(a)) or RKT components (8-shogaol, nobiletin, tangeretin, glycyrrhizin, glycycoumarin, and isoliquiritigenin; 4 mg/kg, Figure 1(a)). The effect of intraperitoneal (IP) administration of SB215505 (10 mg/kg) or SB204741 (10 mg/kg) on the novelty stress-induced decrease in food intake was also investigated (Figure 1(a)). The experimental doses were chosen on the basis of a previous report [13]. RKT, RKT components, SB215505, or SB204741 was administered immediately after the onset of novelty stress.

2.4. Determining Plasma Levels of Ghrelin. To clarify the alteration of peripheral ghrelin dynamics after exposure to the novelty stress, blood was collected from mice given ether anesthesia 0.5 and 3 h after the novelty stress under the 24 h fasting and freely fed conditions. Blood collection to determine plasma ghrelin levels was performed from 10:00 to 12:00. We next investigated the effect of RKT (125, 250, or 500 mg/kg, PO) on plasma ghrelin concentration levels 3 h after exposure to the novelty stress (Figure 1(b)). RKT was orally administered 1 h before exposure to the novelty stress, and blood was collected 3 h after the exposure. The results of our evaluation of the postnovelty stress time course revealed that plasma ghrelin decreased significantly after 3 h [14]. We collected blood samples 3 h after stress to clarify the relationship between this change in plasma ghrelin levels and improved food intake.

The ghrelin levels were determined using commercial ELISA kit (Mitsubishi Chemical Medience Co., Tokyo, Japan).

2.5. Extraction of Total RNA for Reverse Transcription-Polymerase Chain Reaction (PCR). The hypothalamus and stomach in mice treated with distilled water or RKT (500 mg/kg) 3 h after exposure to novelty stress were rapidly removed and immediately frozen by placing them in a tube on dry ice. Homogenization of the isolated tissue and total RNA extraction were performed according to the protocol from the RNeasy Universal Tissue Kit (Qiagen, Valencia, CA,

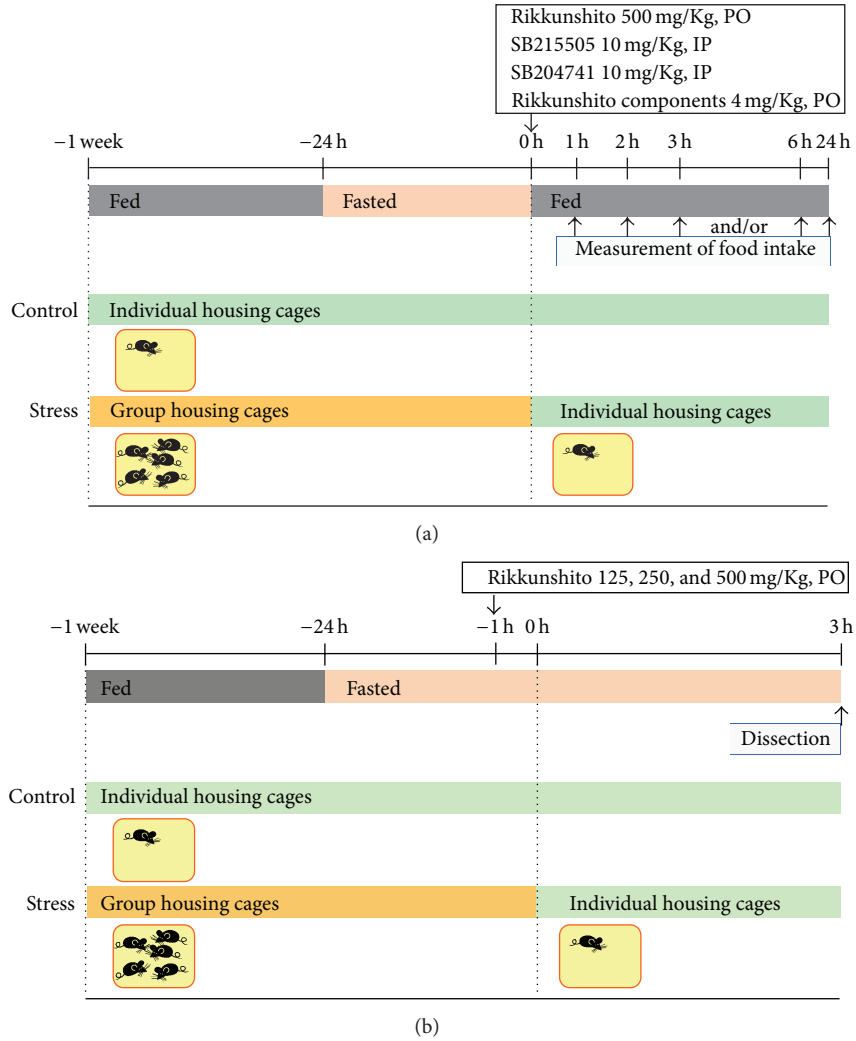

Figure 1: Experimental protocol. (a) Measurement of food intake. Cumulative food intake was measured at various time intervals after exposure to the novelty stress. (b) Measurement of plasma ghrelin and tissue mRNA levels. Blood, hypothalamus, and stomach were collected 3 h after exposure to the novelty stress.

USA), after which each sample was diluted to 100 ng/μL. The diluted total RNA was incubated at 70°C for 5 min and then cooled on ice. A TaqMan Reverse Transcription Reagent kit (Applied Biosystems, Foster City, CA, USA) was used according to the manufacturer's protocol to reverse transcribe the total RNA (1000 ng). A TaqMan Universal PCR Master Mix (Applied Biosystems) was used to perform quantitative PCR assays with a Prism 7900HT Sequence Detection System (Applied Biosystems). To correct the differences in the amount of total RNA added to each reaction, ribosomal protein S29 (RPS29) as an endogenous control was used to normalize mRNA expression. These differences were expressed by the ΔCt (Ct: threshold cycle) value: $\Delta Ct = 2^{(-|A-B|)}$, where A is the number of cycles that needed to reach the threshold for the housekeeping gene and B is the number of cycles needed for the target gene. All oligonucleotide primers and fluorogenic probe sets for TaqMan real-time PCR were manufactured by Applied Biosystems (RPS29: Mm02342448_gH, NPY: Mm00445771_m1, AgRP: Mm00475829_g1, preproghrelin: Mm00445450_m1, ghrelin receptor: Mm00616415_m1, orexin: Mm01964030_s1, leptin receptor: Mm00440174_m1, and CRF: Mm01293920_s1).

2.6. Binding Assay and Cell Function Assay for 5-HT$_{2B}$R. CHO-K1 cells stably transfected with a plasmid encoding the human 5-HT$_{2B}$R were used to prepare membranes in modified Tris-HCl buffer. A membrane protein was incubated with 1.2 nmol/mL [^{3}H]LSD for 60 min at 37°C. Nonspecific binding was estimated in the presence of 10 μmol/L serotonin. Membranes were filtered and washed, and then, the filters were assayed for radioactivity to determine the amount of specifically bound [^{3}H]LSD [20].

The antagonistic activities of compounds on human 5-HT$_{2B}$R expressed in transfected CHO-K1 cells were determined using the HTRF detection method to measure their effects on agonist-induced IP$_1$ production [21]. Cells were suspended in 10 mM HEPES buffer pH 7.4, plated in 96-well

microplates at a density of 4×10^4 cells/well, and preincubated for 5 min at room temperature in the presence of the buffer (basal control) or the test compound. Thereafter, the reference agonist 5-HT was added at a final concentration of 30 nM. Separate assay wells did not contain 5-HT for basal control measurements. After a 30 min incubation at 37°C, the cells were lysed, and the fluorescence acceptor (D2-labeled IP_1) and donor (anti-IP_1 antibody labeled with europium cryptate) were added. After a 60 min incubation at room temperature, the fluorescence transfer was measured at λ_{ex} = 337 nm and λ_{em} = 620 and 665 nm. The IP_1 concentration was determined by dividing the signal measured at 665 nm by that measured at 620 nm. Results were expressed as percent inhibition of the control response to 30 nM 5-HT. A concentration-response curve was generated to calculate the IC_{50} values.

2.7. Statistical Analysis. Statistical analyses of mean values of the two groups were performed using Student's *t*-test or Aspin-Welch's *t*-test after the *F*-test. Differences in multiple groups' mean values were assessed by Dunnett's analysis after Bartlett test. Cumulative food intake data were analyzed by repeated measures analysis of variance (ANOVA) followed by Dunnett's *post hoc* test. Data were expressed as the mean ± standard error of the mean (SEM) of each group, and *P* values < 0.05 were considered to indicate statistical significance.

3. Results

3.1. Changes in Food Intake in Mice Exposed to Novelty Stress. We investigated the effects of novelty stress on changes in food intake (Figure 2). Two-factor repeated measures ANOVA revealed that the effects of stress ($F(1, 42) = 47.93$, $P < 0.001$), time ($F(3, 42) = 1323$, $P < 0.001$), and stress × time ($F(3, 42) = 5.799$, $P = 0.0021$) were significant.

3.2. Effects of RKT on Food Intake in 24 h Fasted Mice. To clarify the effects of RKT on food intake, RKT (500 mg/kg, PO) was administered to 24 h fasted mice. Food intake was measured 2, 6, and 24 h after exposure to novelty stress. RKT administration restored the decreased food intake significantly ($F(1, 26) = 4.692$, $P = 0.0495$, Figure 3). Two-factor repeated measures ANOVA revealed that the effects of treatment × time ($F(2, 26) = 5.907$, $P = 0.0077$) were significant.

3.3. Changes in Plasma Ghrelin Levels and Effects of RKT in Mice Exposed to Novelty Stress. We measured plasma ghrelin levels to clarify whether plasma acylated ghrelin played a role in decreasing food intake in the mice exposed to novelty stress. Plasma acylated ghrelin and des-acyl ghrelin levels at 0.5 and 3 h under ad libitum feeding were not significantly different between the control and novelty stress groups. Under the 24 h fasting condition, plasma acylated ghrelin levels in the stress group were not significantly increased compared with those under ad libitum feeding; however, the des-acyl ghrelin level significantly increased, while still being lower than that in the control group (0.5 h; $P < 0.001$, 3 h; $P < 0.001$, Figure 4).

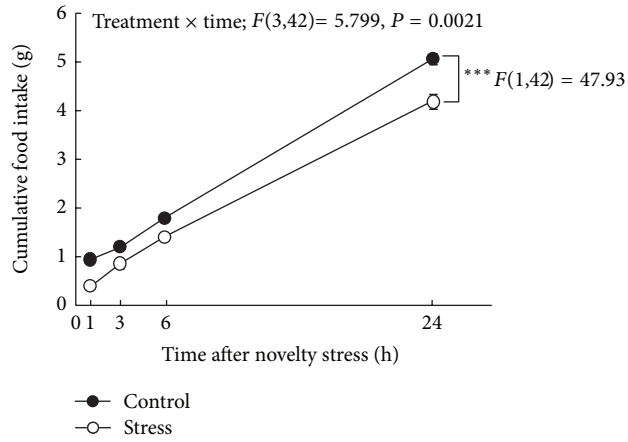

Figure 2: Changes in cumulative food intake after exposure to a novelty stress condition. Data are expressed as the mean ± SEM of 8 mice. $^{***}P < 0.001$ when analyzed by two-factor repeated measures ANOVA.

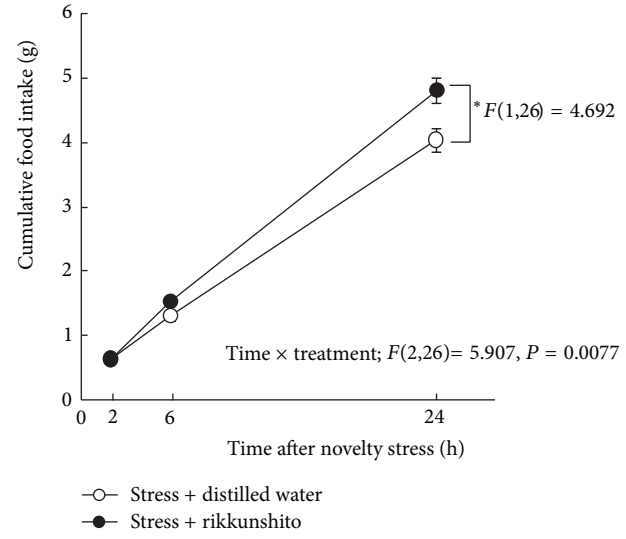

Figure 3: Effect of rikkunshito on food intake under a novelty stress condition. Data are expressed as the mean ± SEM of 7-8 mice. $^{*}P < 0.05$ versus distilled-water-treated mice exposed to novelty stress conditions by two-factor repeated measures ANOVA.

Next, we detected the effects of RKT administration on plasma ghrelin levels under the 24 h fasted condition. RKT administration prevented a decrease in plasma acylated ghrelin levels compared with distilled water 3 h after exposure to novelty stress ($P = 0.0074$, Figure 5). The RKT-treated mice showed a trend toward increased plasma des-acyl ghrelin levels compared with the distilled water-treated stress mice, but the difference was not significant.

3.4. Effects of RKT on mRNA Expression of Orexigenic Factors in Mice Exposed to Novelty Stress. To clarify the effects of RKT on gene expression of orexigenic factors after exposure

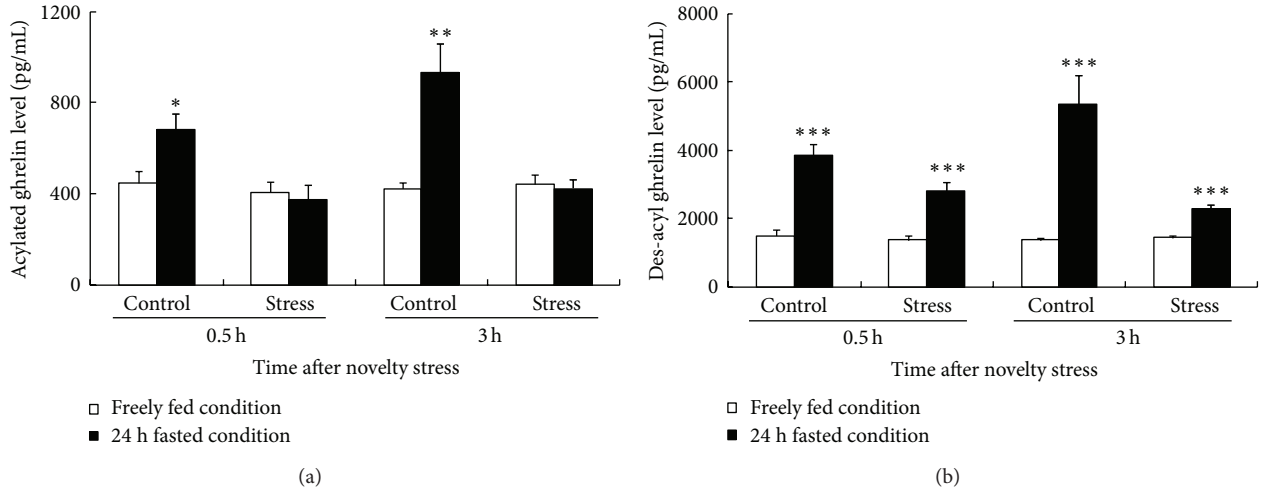

Figure 4: Changes in plasma ghrelin levels under the freely fed or 24 h fasted condition. (a) The plasma acylated ghrelin level. (b) The plasma des-acyl ghrelin level. Data are expressed as the mean ± SEM of 7-8 mice. $^{*}P < 0.05$, $^{**}P < 0.01$, and $^{***}P < 0.001$ versus mice fed freely by Student's t-test or Aspin-Welch's t-test.

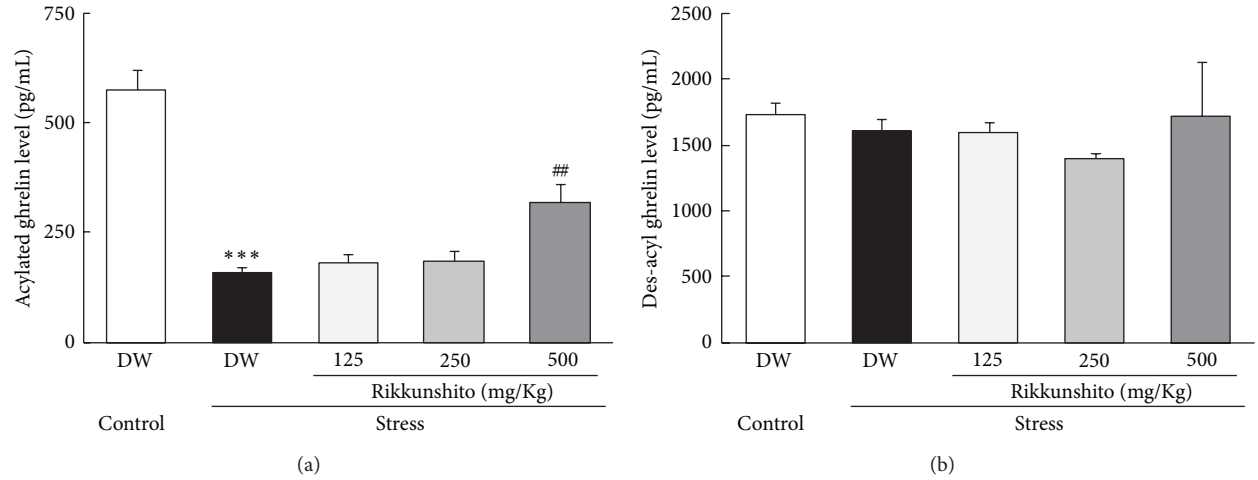

Figure 5: Effect of rikkunshito on plasma ghrelin levels in mice exposed to novelty stress. Plasma ghrelin levels were determined 3 h after onset of novelty stress. (a) Plasma acylated ghrelin level. (b) Plasma des-acyl ghrelin level. Data are expressed as the mean ± SEM of 8 mice. $^{***}P < 0.001$ versus control group by Aspin-Welch's t-test and $^{\#\#}P < 0.01$ versus the distilled-water-treated mice exposed to stress by Dunnett's analysis. DW: distilled water. The partial data of acylated ghrelin level indicated in this figure are derived from [14].

to novelty stress, we evaluated this effect on hypothalamic and gastric mRNA expression 3 h after exposure. In the stress group, hypothalamic NPY and AgRP mRNA showed a trend toward decreased mRNA expression. RKT administration (500 mg/kg, PO) showed a tendency to increase NPY and AgRP mRNA expression compared with stress, but the difference was not statistically significant (Figure 6). Preproghrelin gene expression was significantly increased by RKT treatment ($P = 0.036$), although this remained unchanged 3 h after novelty stress. Levels of ghrelin receptor mRNA in the RKT-treated mice showed an increasing trend, but the difference was not statistically significant. Orexin mRNA expression in the RKT-treated mice was significantly different from that in the distilled-water-treated stress mice ($P = 0.023$). There were no significant changes in leptin receptor and CRF mRNA expression among all groups. In addition, there were no significant changes in gastric preproghrelin mRNA expression among all groups (control group, 1.0 ± 0.03; novelty stress group, 1.1 ± 0.02; stress + RKT group, 1.1 ± 0.03 relative quantity of mRNA; data are not shown in figures and tables).

3.5. Effects of 5-HT$_{2B}$R Antagonists on Food Intake. Cumulative food intake was decreased in the group exposed to novelty stress compared to control mice in the first 6 h after exposure to the stress ($F(1, 80) = 7.647$, $P = 0.0086$, Figure 7). Two-factor repeated measures ANOVA revealed that the effects of stress × time were not significant ($F(2, 80) = 1.789$, $P = 0.17$). Administration of a 5-HT$_{2B}$R antagonist

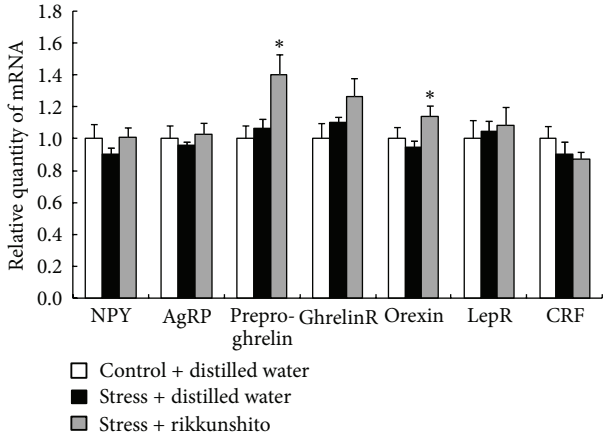

FIGURE 6: Effects of rikkunshito on hypothalamic appetite-related factor gene expression in mice exposed to a novelty stress condition. The hypothalami were collected after a 3 h exposure to novelty stress condition (4 h after rikkunshito 500 mg/kg, PO). The data are expressed as the mean ± SEM of 8 mice. $^{*}P < 0.05$ versus distilled-water-treated mice exposed to a novelty stress condition by Student's *t*-test or Aspin-Welch's *t*-test.

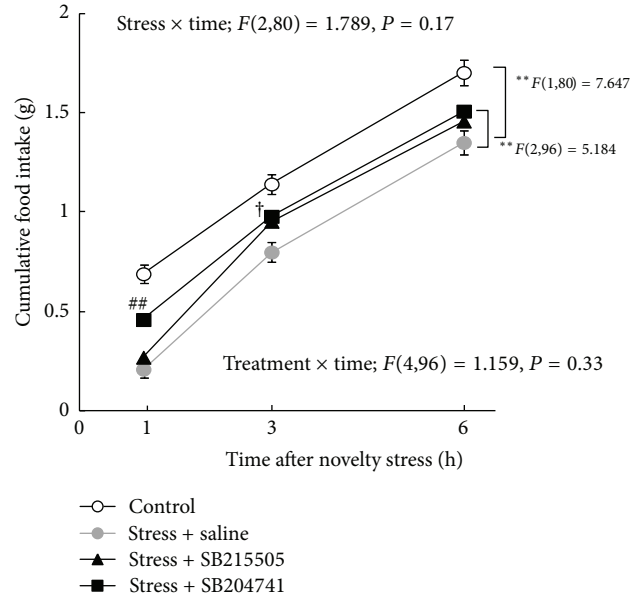

FIGURE 7: Effects of SB215505 or SB204741, 5-HT_{2B} receptor antagonists, on cumulative food intake in mice exposed to a novelty stress condition. Data are expressed as the mean ± SEM of 10–21 mice. $^{**}P < 0.01$ when analyzed by two-factor repeated measures ANOVA. $^{\#\#}P < 0.01$ SB204741 treatment versus saline-treated mice exposed to novelty stress by Dunnett's *post hoc* analysis. $^{\dagger}P < 0.05$ SB215505 treatment versus saline-treated mice exposed to novelty stress by Dunnett's *post hoc* analysis.

(SB215505; 10 mg/kg, IP or SB204741; 10 mg/kg, IP), significantly ameliorated the decrease in food intake ($F(2, 96) = 5.184$, $P = 0.0092$). Administration of SB215505 significantly prevented the decrease in food intake 3 h after exposure to novelty stress ($P = 0.044$), whereas SB204741 prevented the decrease in food intake for 1 h after exposure to stress ($P = 0.0015$).

3.6. Effects of Herbal RKT Components on Food Intake. We investigated the effects of six components of RKT on decreased food intake after exposure to novelty stress. The 6 h cumulative food intake was significantly decreased in the novelty stress-exposed mice compared with that in the control mice ($P = 0.0012$, Figure 8). Isoliquiritigenin administration (4 mg/kg, PO) prevented a decrease in cumulative food intake ($P = 0.045$). Glycycoumarin (4 mg/kg, PO) administration showed a tendency to alleviate decreased food intake in stressed mice, although the effect was not statistically significant. The other RKT components investigated exerted no effects on decreased food intake.

3.7. IC_{50} Values for 5-HT_{2B}R. Table 1 shows the 5-HT_{2B}R-binding inhibitory and cell function activities of isoliquiritigenin contained in RKT. Isoliquiritigenin showed an IC_{50} for 5-HT_{2B}R binding of 6.3 ± 0.0 μmol/L and an inhibitory cell function activity of 2.1 ± 0.2 μmol/L.

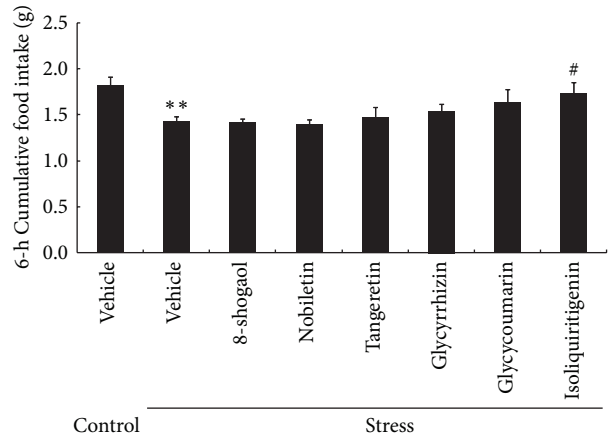

FIGURE 8: Effects of rikkunshito components on 6 h food intake in mice exposed to a novelty stress condition. Data are expressed as the mean ± SEM of 8–16 mice. $^{**}P < 0.01$ versus control mice by Student's *t*-test and $^{\#}P < 0.05$ versus vehicle- (0.5% carboxymethylcellulose-) treated mice exposed to a novelty stress condition by Dunnett's analysis.

4. Discussion

In this study, we demonstrated that the novelty stress decreased food intake and suppressed a physiological increase in plasma acylated ghrelin levels after fasting in mice. Oral RKT administration significantly suppressed this novelty-induced hypophagia and decrease in acylated ghrelin levels during fasting. Furthermore, decreased food intake caused by the novelty stress was significantly suppressed by 5-HT_{2B}R antagonists and isoliquiritigenin, an ingredient of RKT which has 5-HT_{2B}R antagonistic activity *in vitro* that exhibits the same effect.

Table 1: The inhibitory activity for 5-HT_{2B} receptor.

Compound	IC_{50} values for 5-HT_{2B} receptor (μmol/L)	
	Binding	Cell function
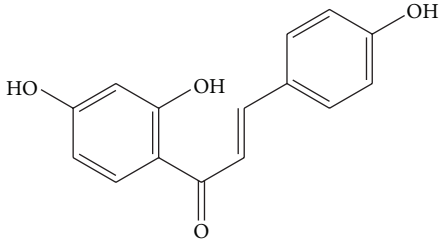 Isoliquiritigenin	6.3 ± 0.0	2.1 ± 0.2

Each value indicated the mean ± SEM of 3 samples.

The effects of drugs on anxiety responses in animal models are generally evaluated by the open field test in novelty environments [22]. In addition, novelty stress models are one of the established methods for evaluating feeding behavior, and novel environmental research using decreased food intake as an index has previously been conducted [7, 23]. Using this methodology, we reported that the acute novel environmental change caused by conversion from group housing to individual housing significantly suppressed feeding behavior in both young [14] and aged mice [24].

During fasting, secretion of acylated ghrelin by the stomach was enhanced, increasing the circulating levels [25]. However, in this study, no increase was observed in the fasting plasma levels of acylated ghrelin in mice exposed to novelty stress. In a previous study, it was clearly demonstrated that exogenous acylated ghrelin supplementation negated decreased food intake in the same model as that used in this study [14]. These results and findings suggest that the transmission of ghrelin signals to the hypothalamic feeding center under the fasting condition is decreased during stress responses caused by novel environmental changes. Although plasma des-acyl ghrelin (a metabolite of acylated ghrelin) levels after 24 h of fasting were significantly enhanced in mice exposed to novelty stress, the intensity of the increase was much lower than that in the nonstress-exposed mice. In addition, novel environmental changes did not cause any significant changes in the expression of gastric preproghrelin or ghrelin-*O*-acyltransferase gene (data are not shown). Therefore, novel environmental stress suppresses the secretion of acylated as well as des-acyl ghrelin, whereas it does not affect the biosynthesis of acylated ghrelin in the stomach during fasting.

NPY and AgRP gene expression in the hypothalamus tended to decrease in the novel environmental change group relative to that in the control group during the 3 h after stress exposure, although no statistically significant difference was observed. Ghrelin is secreted from X/A-like cells in the gastric mucosa and acts on ghrelin receptors in vagus nerve endings, then activating NPY/AgRP neurons in the hypothalamic arcuate nucleus via the vagus nerve [16]. The results of this study did not convincingly verify the attenuation of ghrelin signaling caused by stress when upregulation of hypothalamic NPY/AgRP gene expression was used as an index for ghrelin signaling. The reason why NPY and AgRP mRNA expression were not significantly decreased in mice exposed to novelty stress is unknown. With regard to NPY, there may be interference from mRNA expression in hypothalamic tissue other than the arcuate nucleus. To this end, the *in situ* hybridization technique is required for accurate evaluation of NPY and AgRP mRNA in the arcuate nucleus.

RKT, a Japanese Kampo medicine, is known to increase levels of peripheral acylated ghrelin in humans [26], rodents [13, 27], and dogs [28] as well as increase hypothalamic acylated ghrelin in rodents [29]. RKT also enhances the binding of ghrelin to ghrelin receptors [18, 30], resulting in enhanced and prolonged ghrelin signaling. We have previously reported that RKT administration to mice exposed to novelty stress suppresses a reduction in food intake 1 and 3 h after isolation, and the effects by RKT are abolished by coadministration of RKT with a ghrelin receptor antagonist [14]. The present data regarding the effect of RKT on food intake is almost in agreement with previous findings. In our experiment, RKT significantly reversed the decrease in peripheral acylated ghrelin levels caused by exposure to novelty stress. In contrast, no obvious effect of RKT was observed on des-acyl ghrelin levels after stress. On the basis of these results, we conclude that the increase in peripheral acylated ghrelin level associated with RKT may be mediated through enhanced acylated ghrelin secretion [13] in addition to the inhibition of acylated ghrelin metabolism [27].

In this study, enhanced hypothalamic preproghrelin and orexin mRNA expression and a tendency toward increased ghrelin receptor mRNA expression were observed following RKT administration. Activation of orexin neurons occurs downstream in the ghrelin signaling pathways, and the signal to increase appetite is transmitted to higher-order neurons via orexin gene expression. Enhancement of orexin mRNA by RKT may suggest ghrelin signal-enhancing effects. In addition, RKT promoted the secretion of ghrelin in the hypothalamus in cisplatin-induced hypophagia models [29] and ghrelin receptor gene expression [30]. These results may be supported by other studies indicating enhanced expression of preproghrelin mRNA [26] and ghrelin receptor mRNA

[30], despite differences in models. In addition, no significant changes in the expression of these genes can be confirmed in mice exposed to novelty stress. Our results were obtained 3 h after exposure to stress, but because hypophagia was actually observed 1 h after exposure, it may be necessary to reexamine sampling times.

It is well known that a stress model exhibits higher levels of central 5-HT and expression of 5-HTR, leading to activation of the serotonergic signal [6, 24]. We previously established the involvement of central 5-HT_{2C}R activation in decreased food intake during exposure to novel environmental stress and demonstrated that abnormalities in ghrelin dynamics may partially contribute to this reaction [14]. Contrary to 5-HT_{2C}Rs, 5-HT_{2B}Rs are sparsely expressed in discrete subregions of the central nervous system (CNS) [31], whereas they are heavily expressed in the periphery [32]. In a stomach, 5-HT_{2B}Rs are distributed throughout the gastric submucosa and smooth muscle, and their activation is known to result in contraction of the gastric fundus strip [33]. Although there have been several reports on the association between stress and 5-HT in gastrointestinal organs [34, 35], direct relationship between peripheral 5-HTR activation and novelty stress has not been proven. In the current study, we found that 5-HT_{2B}R antagonism inhibited the decrease in food intake after novelty stress. Because there is no information available on the 5-HT_{2B}R antagonists used in this study in terms of blood-brain barrier permeability, we could not determine whether 5-HT_{2B}R antagonism was effective in the CNS or the peripheral in the present study. Further investigation is required to determine the 5-HT_{2B}R activating site under stress.

5-HT_{2B}R activation by peripheral administration of a 5-HT_{2B}R agonist has been shown to cause a decrease in food intake [12] and inhibition of ghrelin secretion [13]. We also found that peripheral administration of BW723C86, a 5-HT_{2B}R agonist, decreased plasma acylated and des-acyl ghrelin levels in normal rats (see Supplemental Material available online at http://dx.doi.org/10.1155/2013/792940). These findings suggest that 5-HT_{2B}R activation is associated with abnormal ghrelin dynamics.

In the present study, the effects of certain RKT components on food intake in stress models were examined. Administration of isoliquiritigenin (4 mg/kg) significantly improves novelty stress-induced hypophagia. We also found that isoliquiritigenin inhibited binding between 5-HT and 5-HT_{2B}R and confirmed that it has an obvious antagonistic effect on 5-HT_{2B}R using a cell function assay. We previously reported that glycycoumarin, which has an antagonistic effect on 5-HT_{2B}R [13], suppressed decreased food intake 3 h after the application of stress [14]. It seems likely that glycycoumarin may inhibit the decrease in food intake after exposure to novelty stress via 5-HT_{2B}R antagonism. Therefore, multiple RKT ingredients having an antagonistic effect on 5-HT_{2B}R act and are considered to be responsible for its effects.

5. Conclusion

In conclusion, RKT has an ameliorating effect on decreased food intake caused by novel environmental changes. This effect appears to be mediated through improvement of abnormal ghrelin dynamics by 5-HT_{2B}R antagonism.

Acknowledgments

Hiroshi Takeda has received grant support from Tsumura & Co. In addition, Chihiro Yamada, Yayoi Saegusa, Miwa Nahata, Chiharu Sadakane, and Tomohisa Hattori are employed by Tsumura & Co. Furthermore, Koji Nakagawa, Shunsuke Ohnishi, Shuichi Muto, and Naoya Sakamoto have nothing to declare.

References

[1] C. Ó. Luanaigh and B. A. Lawlor, "Loneliness and the health of older people," *International Journal of Geriatric Psychiatry*, vol. 23, no. 12, pp. 1213–1221, 2008.

[2] A. Steptoe, N. Owen, S. R. Kunz-Ebrecht, and L. Brydon, "Loneliness and neuroendocrine, cardiovascular, and inflammatory stress responses in middle-aged men and women," *Psychoneuroendocrinology*, vol. 29, no. 5, pp. 593–611, 2004.

[3] V. Bhatia and R. K. Tandon, "Stress and the gastrointestinal tract," *Journal of Gastroenterology and Hepatology*, vol. 20, no. 3, pp. 332–339, 2005.

[4] C. Lo Sauro, C. Ravaldi, P. L. Cabras, C. Faravelli, and V. Ricca, "Stress, hypothalamic-pituitary-adrenal axis and eating disorders," *Neuropsychobiology*, vol. 57, no. 3, pp. 95–115, 2008.

[5] R. J. Handa, M. K. Cross, M. George et al., "Neuroendocrine and neurochemical responses to novelty stress in young and old male F344 rats: effects of d-fenfluramine treatment," *Pharmacology Biochemistry and Behavior*, vol. 46, no. 1, pp. 101–109, 1993.

[6] H. Miura, H. Qiao, and T. Ohta, "Influence of aging and social isolation on changes in brain monoamine turnover and biosynthesis of rats elicited by novelty stress," *Synapse*, vol. 46, no. 2, pp. 116–124, 2002.

[7] A. J. Bechtholt, T. E. Hill, and I. Lucki, "Anxiolytic effect of serotonin depletion in the novelty-induced hypophagia test," *Psychopharmacology*, vol. 190, no. 4, pp. 531–540, 2007.

[8] J. C. G. Halford, J. A. Harrold, E. J. Boyland, C. L. Lawton, and J. E. Blundell, "Serotonergic drugs: effects on appetite expression and use for the treatment of obesity," *Drugs*, vol. 67, no. 1, pp. 27–55, 2007.

[9] L. H. Tecott, "Serotonin and the orchestration of energy balance," *Cell Metabolism*, vol. 6, no. 5, pp. 352–361, 2007.

[10] L. K. Heisler, N. Pronchuk, K. Nonogaki et al., "Serotonin activates the hypothalamic-pituitary-adrenal axis via serotonin 2C receptor stimulation," *Journal of Neuroscience*, vol. 27, no. 26, pp. 6956–6964, 2007.

[11] J. De Vry and R. Schreiber, "Effects of selected serotonin 5-HT_1 and 5-HT_2 receptor agonists on feeding behavior: possible mechanisms of action," *Neuroscience and Biobehavioral Reviews*, vol. 24, no. 3, pp. 341–353, 2000.

[12] T. Hattori, K. Yakabi, and H. Takeda, "Cisplatin-induced anorexia and ghrelin," *Vitamins & Hormones*, vol. 92, pp. 301–317, 2013.

[13] H. Takeda, C. Sadakane, T. Hattori et al., "Rikkunshito, an herbal medicine, suppresses cisplatin-induced anorexia in rats via 5-HT_2 receptor antagonism," *Gastroenterology*, vol. 134, no. 7, pp. 2004–2013, 2008.

[14] Y. Saegusa, H. Takeda, S. Muto et al., "Decreased plasma ghrelin contributes to anorexia following novelty stress," *American Journal of Physiology: Endocrinology and Metabolism*, vol. 301, no. 4, pp. E685–E696, 2011.

[15] M. Kojima, H. Hosoda, Y. Date, M. Nakazato, H. Matsuo, and K. Kangawa, "Ghrelin is a growth-hormone-releasing acylated peptide from stomach," *Nature*, vol. 402, no. 6762, pp. 656–660, 1999.

[16] Y. Date, N. Murakami, K. Toshinai et al., "The role of the gastric afferent vagal nerve in Ghrelin-induced feeding and growth hormone secretion in rats," *Gastroenterology*, vol. 123, no. 4, pp. 1120–1128, 2002.

[17] M. Nakazato, N. Murakami, Y. Date et al., "A role for ghrelin in the central regulation of feeding," *Nature*, vol. 409, no. 6817, pp. 194–198, 2001.

[18] N. Fujitsuka, A. Asakawa, Y. Uezono et al., "Potentiation of ghrelin signaling attenuates cancer anorexia-cachexia and prolongs survival," *Translational Psychiatry*, vol. 1, article e23, 2011.

[19] N. Fujitsuka, A. Asakawa, M. Hayashi et al., "Selective serotonin reuptake inhibitors modify physiological gastrointestinal motor activities via 5-HT_{2C} receptor and acyl ghrelin," *Biological Psychiatry*, vol. 65, no. 9, pp. 748–759, 2009.

[20] D. W. Bonhaus, C. Bach, A. DeSouza et al., "The pharmacology and distribution of human 5-hydroxytryptamine2B (5-HT_{2B}) receptor gene products: comparison with 5-HT_{2A} and 5-HT_{2C} receptors," *British Journal of Pharmacology*, vol. 115, no. 4, pp. 622–628, 1995.

[21] R. H. P. Porter, K. R. Benwell, H. Lamb et al., "Functional characterization of agonists at recombinant human 5-HT_{2A}, 5-HT_{2B} and 5-HT_{2C} receptors in CHO-K1 cells," *British Journal of Pharmacology*, vol. 128, no. 1, pp. 13–20, 1999.

[22] L. Prut and C. Belzung, "The open field as a paradigm to measure the effects of drugs on anxiety-like behaviors: a review," *European Journal of Pharmacology*, vol. 463, no. 1-3, pp. 3–33, 2003.

[23] S. C. Dulawa and R. Hen, "Recent advances in animal models of chronic antidepressant effects: the novelty-induced hypophagia test," *Neuroscience and Biobehavioral Reviews*, vol. 29, no. 4-5, pp. 771–783, 2005.

[24] M. Nahata, S. Muto, K. Nakagawa et al., "Serotonin 2C receptor antagonism ameliorates novelty-induced hypophagia in aged mice," *Psychoneuroendocrinology*, vol. 38, no. 10, pp. 2051–2064, 2013.

[25] M. Tschop, D. L. Smiley, and M. L. Heiman, "Ghrelin induces adiposity in rodents," *Nature*, vol. 407, no. 6806, pp. 908–913, 2000.

[26] T. Matsumura, M. Arai, Y. Yonemitsu et al., "The traditional Japanese medicine Rikkunshito increases the plasma level of ghrelin in humans and mice," *Journal of Gastroenterology*, vol. 45, no. 3, pp. 300–307, 2010.

[27] C. Sadakane, S. Muto, K. Nakagawa et al., "10-Gingerol, a component of rikkunshito, improves cisplatin-induced anorexia by inhibiting acylated ghrelin degradation," *Biochemical and Biophysical Research Communications*, vol. 412, no. 3, pp. 506–511, 2011.

[28] M. Yanai, E. Mochiki, A. Ogawa et al., "Intragastric administration of rikkunshito stimulates upper gastrointestinal motility and gastric emptying in conscious dogs," *Journal of Gastroenterology*, vol. 48, no. 5, pp. 611–619, 2013.

[29] K. Yakabi, C. Sadakane, M. Noguchi et al., "Reduced ghrelin secretion in the hypothalamus of rats due to cisplatin-induced anorexia," *Endocrinology*, vol. 151, no. 8, pp. 3773–3782, 2010.

[30] K. Yakabi, S. Kurosawa, M. Tamai et al., "Rikkunshito and 5-HT_{2C} receptor antagonist improve cisplatin-induced anorexia via hypothalamic ghrelin interaction," *Regulatory Peptides*, vol. 161, no. 1–3, pp. 97–105, 2010.

[31] A. L. Auclair, A. Cathala, F. Sarrazin et al., "The central serotonin 2B receptor: a new pharmacological target to modulate the mesoaccumbens dopaminergic pathway activity," *Journal of Neurochemistry*, vol. 114, no. 5, pp. 1323–1332, 2010.

[32] D.-S. Choi and L. Maroteaux, "Immunohistochemical localisation of the serotonin 5-HT_{2B} receptor in mouse gut, cardiovascular system, and brain," *FEBS Letters*, vol. 391, no. 1-2, pp. 45–51, 1996.

[33] G. S. Baxter, O. E. Murphy, and T. P. Blackburn, "Further characterization of 5-hydroxytryptamine receptors (putative 5-HT_{2B}) in rat stomach fundus longitudinal muscle," *British Journal of Pharmacology*, vol. 112, no. 1, pp. 323–331, 1994.

[34] S. V. Wu, P.-Q. Yuan, J. Lai et al., "Activation of type 1 CRH receptor isoforms induces serotonin release from human carcinoid BON-1N cells: an enterochromaffin cell model," *Endocrinology*, vol. 152, no. 1, pp. 126–137, 2011.

[35] M. G. Pshennikova, E. V. Popkova, and M. V. Shimkovich, "Adaptation to stress improves resistance to gastric damage during acute stress in Wistar rats and decreases resistance in August rats: role of serotonin," *Bulletin of Experimental Biology and Medicine*, vol. 134, no. 4, pp. 329–332, 2002.

Hindawi Publishing Corporation
BioMed Research International
Volume 2013, Article ID 495319, 8 pages
http://dx.doi.org/10.1155/2013/495319

Research Article

Preparation and Characterization of a Gastric Floating Dosage Form of Capecitabine

Ehsan Taghizadeh Davoudi,[1] Mohamed Ibrahim Noordin,[1] Ali Kadivar,[1] Behnam Kamalidehghan,[1] Abdoreza Soleimani Farjam,[2] and Hamid Akbari Javar[3]

[1] *Department of Pharmacy, Faculty of Medicine, Universiti of Malaya, 50603 Kuala Lumpur, Malaysia*
[2] *Institute of Tropical Agriculture, Universiti Putra Malaysia (UPM), 43400 Selangor, Serdang, Malaysia*
[3] *Department of Pharmaceutics, Faculty of Pharmacy, Tehran University of Medical Sciences (TUMS), Tehran, Iran*

Correspondence should be addressed to Hamid Akbari Javar; akbarijo@sina.tums.ac.ir

Received 30 May 2013; Accepted 8 July 2013

Academic Editor: Ibrahim Banat

Gastrointestinal disturbances, such as nausea and vomiting, are considered amongst the main adverse effects associated with oral anticancer drugs due to their fast release in the gastrointestinal tract (GIT). Sustained release formulations with proper release profiles can overcome some side effects of conventional formulations. The current study was designed to prepare sustained release tablets of Capecitabine, which is approved by the Food and Drug Administration (FDA) for the treatment of advanced breast cancer, using hydroxypropyl methylcellulose (HPMC), carbomer934P, sodium alginate, and sodium bicarbonate. Tablets were prepared using the wet granulation method and characterized such that floating lag time, total floating time, hardness, friability, drug content, weight uniformity, and *in vitro* drug release were investigated. The sustained release tablets showed good hardness and passed the friability test. The tablets' floating lag time was determined to be 30–200 seconds, and it floated more than 24 hours and released the drug for 24 hours. Then, the stability test was done and compared with the initial samples. In conclusion, by adjusting the right ratios of the excipients including release-retarding gel-forming polymers like HPMC K4M, Na alginate, carbomer934P, and sodium bicarbonate, sustained release Capecitabine floating tablet was formulated.

1. Introduction

After cardiovascular disease, cancer is the second reason for death. Prostate, lung, colon, and breast cancers are the most common forms of cancer. The present treatments for cancer include surgery, chemotherapy, hormone therapy, gene therapy, and radiation therapy. Currently, chemotherapeutic drugs are the most common type of cancer treatment. However, the administration of high doses of these drugs leads to some adverse toxic effects. As some reports indicated, many side effects, such as systemic side effects, diarrhea, and gastrointestinal problems will appear in anticancer therapy [1–5].

Many drugs, such as Anthracyclines, Taxanes (Docetaxel, Paclitaxel), Gemcitabine, Vinorelbine, Carboplatin, Trastuzumab, Lapatinib, Cyclophosphamide, Methotrexate, Adriamycin, Epirubicin, Mitoxantrone, Bevacizumab, and Capecitabine, are used in breast cancer. The use of these drugs is strongly recommended to make sure that the side effects and high dosage of these drugs are balanced [4, 6–8].

Capecitabine, 5′-deoxy-5-fluoro-N-((pentyloxy) carbonyl)-cytidine, is a fluoropyrimidine carbamate which has an antineoplastic activity. This chemical is a prodrug of 5′-deoxy-5-fluorouridine (5′-DFUR), which is enzymatically converted *in vivo* to 5-fluorouracil (5-FU). The commercial brand name is Xeloda, which has a biconvex face and a coated film (such as a light peach-colored film for 150 mg Capecitabine and peach-colored film for 500 mg Capecitabine). But both tablets have the same inactive excipients: hydroxypropyl methylcellulose, Croscarmellose sodium, magnesium stearate, microcrystalline cellulose, anhydrous lactose, and purified water. Also, the light peach- or peach-colored film contains talc,

Table 1: Different formulations of tablets with different concentrations (%).

	HPMC	S.A	Car	S.B	Lac	PEG	Mg.St	Cap	Total
F1	20	20	1.6	13.3	35	6.6	3.3	150	300
F2	20	20	3.3	13.3	33.3	6.6	3.3	150	300
F3	20	20	4.6	13.3	32	6.6	3.3	150	300
F4	16.6	16.6	3.3	13.3	40	6.6	3.3	150	300
F5	16.6	20	3.3	13.3	36.6	6.6	3.3	150	300
F6	16.6	23.3	3.3	13.3	33.3	6.6	3.3	150	300
F7	20	16.6	3.3	13.3	36.6	6.6	3.3	150	300
F8	20	20	3.3	13.3	33.3	6.6	3.3	150	300
F9	20	23.3	3.3	13.3	30	6.6	3.3	150	300
F10	23.3	16.6	3.3	13.3	33.3	6.6	3.3	150	300
F11	23.3	20	3.3	13.3	30	6.6	3.3	150	300
F12	23.3	23.3	3.3	13.3	26.6	6.6	3.3	150	300

hydroxypropyl methylcellulose, titanium dioxide, and red and yellow iron oxides [9].

Important problems of Capecitabine as to the current clinical treatment are a short half-life and its rapid metabolism in the liver. Therefore, the administration of high doses of Capecitabine leads to some undesirable side effects [10]. All these problems can be resolved using sustained release. Based on previous research, since the advantages of these systems are to achieve the therapeutic concentration, the desired drug release rate prolonged drug release and reduction of the repeating dosage. Many of these problems can be resolved if sustained release is done [10, 11].

Sustained release (SR) tablets of anticancer drugs could not only provide an optimum plasma concentration with less frequent administration but also help decrease the side effects of conventional dosage forms, such as GIT problems [12]. This could increase the safe administration and improve patient compliance. Nowadays, some pharmaceutical products are considered as controlled-release, which can also be an effective way to deliver different types of drugs into the tissues or cells, such as diltiazem hydrochloride, chlorpheniramine maleate, ciprofloxacin, theophylline, famotidine, and captopril [5, 13–16].

There are several advantages to making sustained release antineoplastic drugs like Capecitabine. These drugs show fewer side effects, have longer half-lives, require less frequent dosages, and improve efficacy. Thus, there would be better patient compliance and less variation in plasma/blood levels [17]. The gastroretentive drug delivery system is formulated to keep the tablet in the stomach for several hours and can improve the drug's solubility and bioavailability and reduce drug waste [5, 18]. This study aimed to prepare the floating dosage form of anticancer drugs, to characterize the sustained release tablet in terms of total floating time, dissolution, friability, hardness, drug content, and weight uniformity, to compare the prepared formulation with the commercial tablet in terms of drug release, and to evaluate the stability of the formulation by accelerating and long term condition according to the International Conference on Harmonization (ICH) procedure.

2. Materials and Methods

2.1. Materials. Capecitabine was a kind gift from Osvah Pharmaceutical Company (Tehran, Iran). The 5 FU was provided from sigma Aldrich (KL, Malaysia). HPMC K4M was supplied by Sigma Chemicals. Sodium alginate and sodium bicarbonate were purchased from R&M chemicals (KL, Malaysia),carbomer934p was purchased from Noveon, polyethylene glycol 3500 from Merck, magnesium stearate from Mallinckrodt, and lactose from HMbG chemicals (United State of America). All reagents were of analytical or pharmaceutical grade.

2.2. Methods

2.2.1. Preparation of Sustained Release Capecitabine. Sustained release tablets were formulated with different types and ratios of polymers using the wet granulation method, and then tablets were compressed directly by a single punch machine. Capecitabine was mixed with carbomer934p as a control release agent, with HPMC K4M as a binder, sodium alginate for gel forming, and sodium bicarbonate to extend floating time. All components were mixed for 10 min, and then Isopropyl alcohol was added dropwise to make a good wet mass of granules. After remixing for 5 min, the granules were passed through a 400 μm mesh sieve. Wet granules were put in a 40°C oven for 40 min to become dry, and then PEG 3500 and magnesium stearate were added to the granules as lubricating agents. Eventually, 300 mg of the mixture was weighted and compressed on an 8 mm flat face by a single punch machine. In this study, 12 formulations were designed with 150 mg of Capecitabine, and the different ratios of polymers are as shown in Table 1.

2.2.2. Kinetic Modeling of Release Profiles. The dissolution results of all formulations in 0.1 N HCl were specified to Higuchi, Korsmeyer-Peppas, Hixson-Crowell, Weibull, and first order and zero order kinetic models. The model with the maximum correlation coefficient was considered to be the best model [19–24].

2.2.3. Determination of Floating Lag Time and Total Floating Time. The floating lag time (FLT) is the time taken for a tablet to rise on medium surface, and total floating time (TFT) is the floating duration that a tablet remained on surface. To determine the floating lag time, tablets ($n = 4$) were put on 100 mL of 0.1 N HCL in a beaker, and the time is required for a tablet to rise on surface was measured. Then, the duration of each formulation that remained on the surface was determined as total floating [15, 25].

2.2.4. Tablet Hardness. To evaluate tablet hardness, 10 tablets of each formulation were tested for diametrical crushing strength using a hardness tester (Dr. schleuniger, 6D-Tablet Tester).

2.2.5. Tablet Friability. The friability of the SR tablets ($n = 10$) was tested by a friabilator (ERWEKA, TAR 10), at a speed of 100 rpm for 5 minutes.

Hardness and friability values were determined and reported as mean ± SD.

2.2.6. Drug Content of the Tablets. To evaluate the drug content through a uniformity test, 10 tablets of each formulation were crushed and suspended in 0.1 N HCL to remove the Capecitabine from the tablets. After 24 hours, media were filtrated and measured by a UV spectrophotometer (Shimadzu 1601) at 214 nm [26, 27].

2.2.7. Tablet Weight Uniformity. An electronic balance (Mettler Toledo, 3-MS-S/MS-L, Switzerland) was used to accurately weigh ten tablets which were randomly selected. The results are expressed as mean values ± SD [26, 27].

2.2.8. In Vitro Release Study. A dissolution test was performed for 24 hours using the ERWEKA DT70 dissolution machine according to American pharmacopeia [25]. Each vessel contained 1000 mL of 0.1 N HCL; the paddle apparatus with 50 rpm speed was also used, while the temperature was kept stable at 37°C. Every two hours till 24 hours, 10 mL of media was withdrawn and measured by UV spectrophotometer at 214 nm (Shimadzu 1601). Furthermore, 10 mL of 0.1 N HCL was replaced to keep the volume stable.

Two formulations (commercial (Xeloda) and prepared tablet) were compared in terms of drug release.

At the end, all results were analyzed using Microsoft Excel. The dissolution test was repeated 4 times for each formulation.

2.2.9. Preparation of Standard Curve. The standard curve was constructed using six different concentrations of Capecitabine, ranging from 100 to 12.5 mg. To make a standard curve, 5 mg of Capecitabine was dissolved in 50 mL of 0.1 N HCL. Then, 3 mL of each dilution was measured by UV spectrophotometer (Shimadzu 1601).

2.2.10. Stability Study Test. To study the quality of the finished product under a variety of conditions (time, humidity, and temperature) and to evaluate the formulation, stability studies were prepared for 6 and 12 months according to the ICH (International Conference on Harmonization) procedures. After storage, all samples were analyzed for their physical characterizations.

Table 2: Storage conditions for tablet stability test.

Type of study	Condition	Time
Accelerated	40°C ± 2°C, 75% RH ± 5% RH	6 months
Long term	25°C±2°C, 60% RH ± 5% RH	12 months

Table 3: Drug release and floating profiles of twelve formulations.

Formulation	Release %	Floating lag time (s)	Total floating time (h)
F1	100	30	20
F2	83.665	70	24
F3	76.3	81	24
F4	100	35	20
F5	90.305	45	24
F6	84.711	60	24
F7	98.286	60	24
F8	83.665	70	24
F9	78.82	85	24
F10	86.666	60	24
F11	80.54	80	24
F12	75.226	200	0.5

s: second; hr: hour.

Tablets ($n = 4$) were used for the stability studies according to ICH long term and accelerated procedure. All tablets were stored in standard condition in WTB binder APT line (Table 2).

All the tablets were packed in polyethylene bags. The bags were clamped using clamping tape and double-packed by putting in cardboard with a plywood lid and the lid was sealed [28–31].

2.2.11. Statistical Analysis. The results were evaluated by one-way analysis of variance (ANOVA) using Duncan's multiple comparison test. Differences were considered significant at P value equal to or less than 0.05 [32, 33].

3. Results and Discussion

3.1. Floating Profile. The sustained release Capecitabine floating tablets were developed using release-retarding gel-forming polymers HPMC K4M, Na alginate, and carbomer934P, accompanied by sodium bicarbonate as a gas-forming agent and lactose as filler.

Table 3 shows the results of the floating and releasing times of 12 prepared formulations over 24 hours.

The investigated gastric floating systems employed sodium bicarbonate ($NaHCO_3$) as a gas-forming agent, which is trapped in a hydrogel matrix (HPMC K4M and Na alginate). The *in vitro* study revealed that most formulations are able to keep the drug buoyant for more than 24 h (Table 3). This suggests that the gel layers, formed by the investigated

polymers, enabled efficient entrapment of the generated CO_2 bubbles.

The floating lag time for most formulations was below 90 seconds, regardless of the content of polymers used (Table 3), indicating significance of the polymers' concentrations (Table 1). The interaction between sodium bicarbonate ($NaHCO_3$) as a gas-generating agent and the dissolution medium (0.1 mol L^{-1} HCl, pH 1.2) generated and entrapped CO_2 inside the jellified polymeric matrices, inducing the tablet to float. A decrease in tablet-specific gravity causes the tablet to float on extended residence time in the stomach, improving absorption.

As the amount of carbomer934P increased, TFT decreased—this could be due to the high affinity of carbomer towards water, which promotes water penetration into polymeric matrices, leading to increased density. As the amount of HPMC K4M increased, the total floating time increased—this is because of the increased gel strength of the matrices, which prevents the escape of involved CO_2 from the matrices, leading to decreased density. As the amount of SA increased, TFT decreased—this is because of the poor gelling strength of SA compared to HPMC K4M that was previously reported [34, 35].

3.2. Drug Release Profiles. Depending on the type and concentration of polymers, variable drug release profiles were successfully tailored.

The dissolution profile of the best formulation (formulation F7) according to standard curve and R2 (Figure 2) was choose and is shown in Figure 1, with appropriate release rate near zero order release kinetic. Drug release involves a combination of swelling, diffusion, and erosion of matrices. This might be due to the water solubility of Capecitabine as well as different characteristics of polymers.

The influence of carbomer934P, HPMC K4M, and Na alginate on the release of capecitabine from the floating tablets in 0.1 N HCl (pH 1.2) at 37 ± 0.5°C was shown in Figures 3, 4, 5, and 6. It is clear that all formulations succeeded in controlling the rate of drug release. However, the drug release rate was dependent on the type and concentration of the collaborated polymers. A higher concentration of HPMC K4M would promote the formation of highly viscous gels upon contact with aqueous fluids. This would promote retardation of the drug release rates. Siepmann and Peppas [36] suggested that drug release from HPMC matrices is sequentially governed as follows: at the initial time, when the tablet contacts the media, water can penetrate into the polymeric complex, and due to water absorption, HPMC will swell and increase the dimensions of the complex. Then, drug will dissolve and diffuse out due to the concentration of the polymers.

The results of t_{50} (time required for 50% drug release) showed wide variations. From the results of multiple regression analysis, it was found that the dependent variable, t_{50}, is strongly dependent on the independent variables (carbomer934P, HPMC, and Na alginate). As the amount of HPMC K4M and carbomer934P increased, t_{50} decreased and floating lag time increased; again, this may be due to the high affinity of HPMC and carbomer934P towards water, which promotes water penetration into polymeric matrices, leading to solubility of Capecitabine. As the amount of Na alginate increased, t_{50} decreased probably because of the poor water affinity of Na alginate compared to HPMC K4M and carbomer934P.

As this and previous studies [5, 37, 38] have shown that, upon contact with aqueous media, polymers would produce strong barriers that would effectively reduce the burst release. Taking into consideration the aim of the research of achieving a compromise between excellent floating behavior (short floating lag time and long total floating time) and sustained

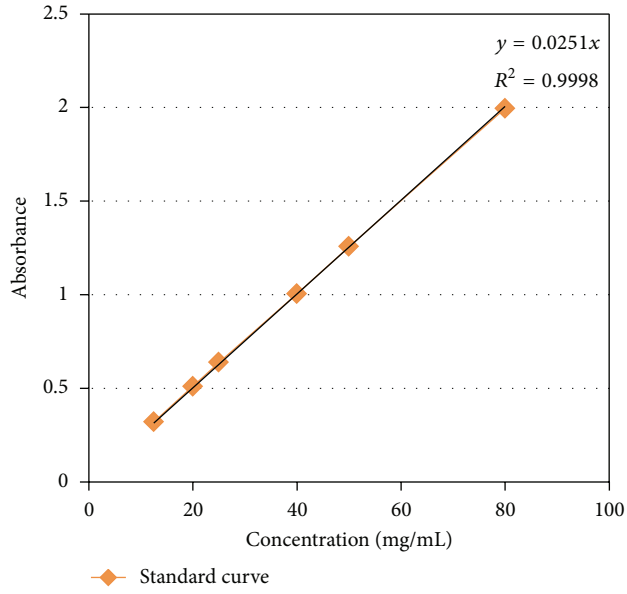

Figure 1: Calibration curve of Capecitabine in HCL 0.1 N.

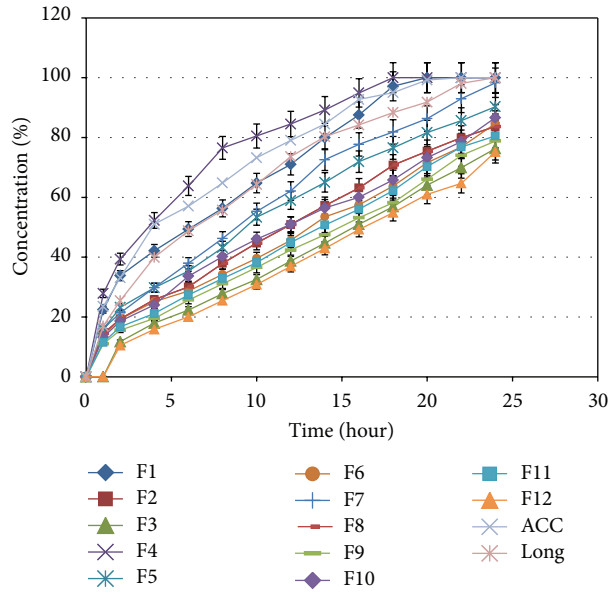

Figure 2: *In vitro* release profiles of various Capecitabine floating formulations in 0.1 N HCl (pH 1.2) at 37 ± 0.5°C (n = 4).

Table 4: Mathematical release modeling of sustained release capecitabine floating tablets.

Formulations code	Zero order R^2	First order R^2	Higuchi R^2	Hixson-Crowell R^2	Korsmeyer-Peppas
F1	0.964	0.818	0.983	0.908	0.482
F2	0.996	0.972	0.977	0.990	0.576
F3	0.992	0.959	0.970	0.980	1.606
F4	0.871	0.974	0.962	0.940	0.413
F5	0.989	0.968	0.988	0.993	0.558
F6	0.996	0.926	0.954	0.963	0.564
F7	0.989	0.851	0.988	0.960	0.596
F8	0.996	0.972	0.977	0.990	0.575
F9	0.997	0.943	0.955	0.969	0.625
F10	0.993	0.936	0.980	0.973	0.590
F11	0.998	0.951	0.962	0.976	0.621
F12	0.992	0.954	0.967	0.976	1.644
Acc	0.922	0.857	0.986	0.955	0.464
Long	0.955	0.894	0.997	0.918	0.464

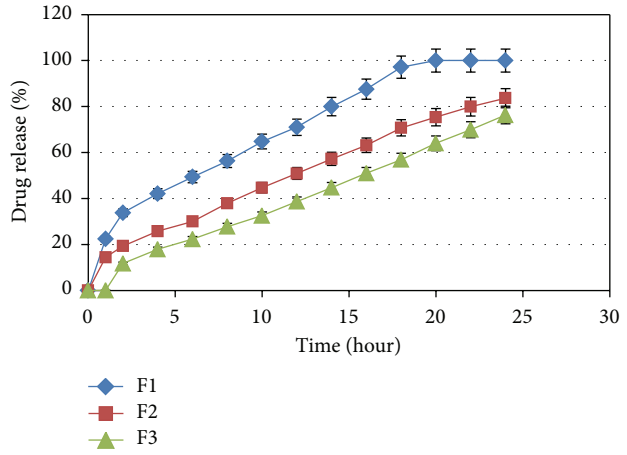

Figure 3: The influence of carbomer934P on the release of Capecitabine from the SR tablets in 0.1 N HCl (pH 1.2) at 37 ± 0.5°C ($n = 4$).

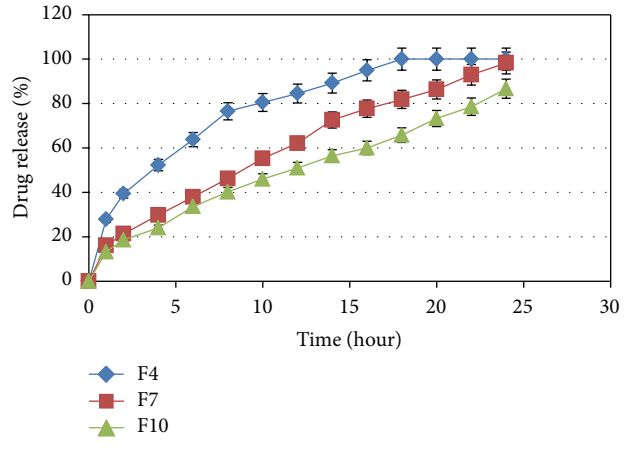

Figure 4: The influence of HPMC K4M in F4, F7, and F10 on the release of Capecitabine from the SR tablets in 0.1 N HCl (pH 1.2) at 37 ± 0.5°C ($n = 4$).

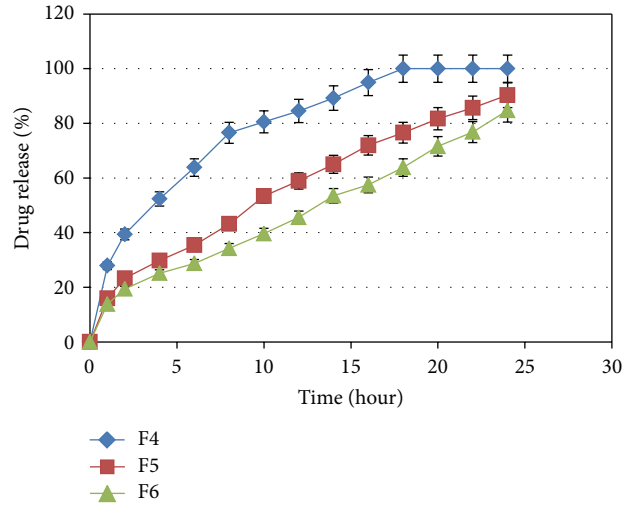

Figure 5: The influence of Na alginate in F4, F5, and F6 on the release of Capecitabine from the SR tablets in 0.1 N HCl (pH 1.2) at 37 ± 0.5°C ($n = 4$).

drug release characteristics, formula F7 was chosen for further studies.

An immediate release rate was achieved following the dissolution of a commercial brand of Capecitabine 150 mg tablets in 0.1 N HCl. Indeed, 100% of the drug was released within 40 min (Figure 7). There was a significant difference between immediate release and sustained release ($P < 0.05$). The rate of immediate release significantly increased and most of the drug was released within the first 30 minutes, but in sustained release, the drug release increased gradually during 24 hours (Figure 7).

3.3. Kinetic Results. To establish the mechanism of drug release, all data from the dissolution studies of floating tablets were obtained and fitted in kinetic models (Table 4) [19, 23, 24, 39]. The correlation coefficient (R^2) was used as an

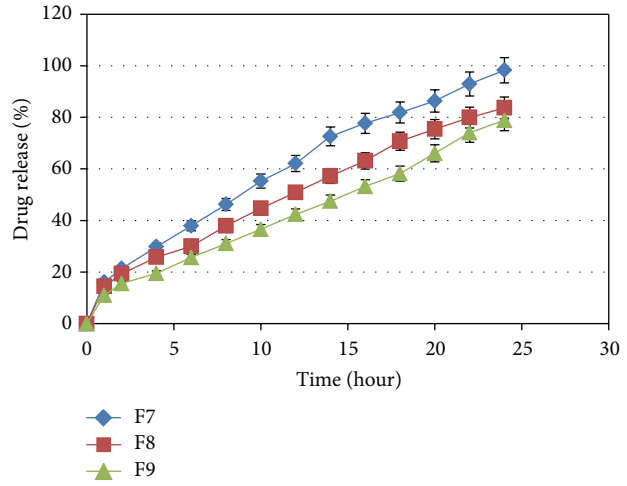

Figure 6: The influence of Na alginate in F7, F8, and F9 on the release of Capecitabine from the SR tablets in 0.1 N HCl (pH 1.2) at 37 ± 0.5°C ($n = 4$).

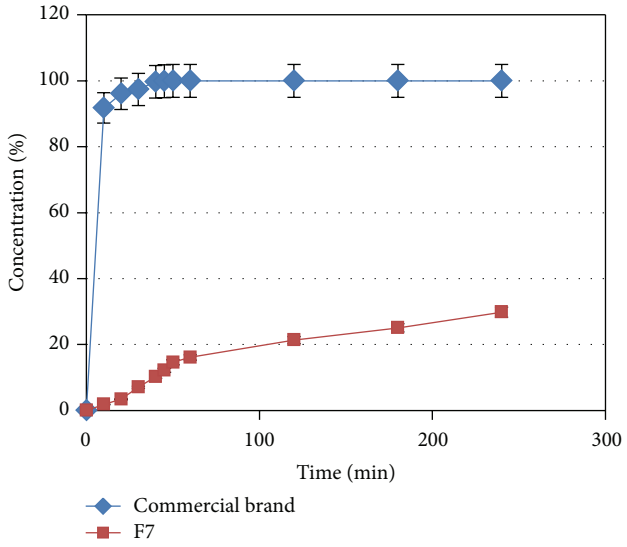

Figure 7: Release profiles of a commercial brand of Capecitabine and F7 ($n = 4$).

indicator for best fitting, in which all formulation regression values were between (R^2) = 0.998 to 0.871 zero order. By comparing the regression values of different models, the zero order model was found to be the best model for optimum formulation (F7) (Table 4). According to the results, it could be predicted that the drug release model of the prepared tablet was of the diffusion type.

3.4. Physical Properties. Previous studies have reported that tablet hardness not only had a slight effect on drug release profiles but was also a determining factor with regards to buoyancy of the tablets. Increasing the hardness would possibly lead to prolongation of the floating lag time by affecting the rate of the tablet penetration by the dissolution medium. Also, the percentage friability for all formulae was less than

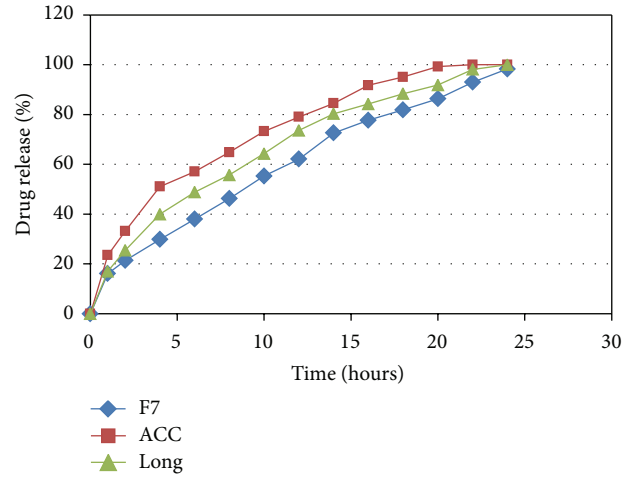

Figure 8: Comparison of the release profiles of F7 and stored tablets ($n = 4$).

Table 5: Comparison of physical properties of all formulations.

	Hardness (N)	Friability (%)	Drug content (%)	Weight uniformity (mg)
F1	57	0.35	99.33 ± 0.81	299 ± 0.89
F2	76	0.26	98.61 ± 1.13	300 ± 0.75
F3	81	0.22	99.45 ± 0.19	301 ± 0.82
F4	55	0.35	99.83 ± 0.88	298 ± 1.04
F5	62	0.29	98.17 ± 1.05	299 ± 0.79
F6	68	0.25	99.05 ± 0.71	299 ± 0.9
F7	69	0.31	99.79 ± 0.48	299 ± 0.18
F8	76	0.26	98.61 ± 1.13	298 ± 0.62
F9	80	0.21	99.86 ± 0.36	300 ± 0.25
F10	95	0.19	99.25 ± 0.51	298 ± 0.72
F11	104	0.11	98.48 ± 0.19	300 ± 0.43
F12	112	0.103	99.01 ± 0.47	299 ± 1.09

1%, indicating good mechanical resistance. The physicochemical properties of the tablets are as summarized in Table 6.

All tablet formulae showed (Table 5) acceptable physicochemical properties and complied with the pharmacopoeia specifications [25, 26] for weight variation, drug content and friability. The weight of the tablets ranged from 298 to 301 mg.

Drug uniformity results were found to be good among different formulations, where the percentage of drug content ranged from 98.06% to 99.86%.

3.5. Drug Release and Physical Profile in Stability Condition. The optimum formulation (F7) was packed according the standard procedures, and was analyzed by dissolution and physical characterization procedures after storage (Tables 2 and 6 and Figure 8).

The drug release of the stored samples was slightly affected by the different storage conditions, indicating that either heat or humidity affected the permeability of the polymeric matrix.

Table 6: Drug release and physical properties of stored tablet.

Formulation	Release %	Floating lag time	Total floating time	Hardness (N)	Friability (%)	Drug content (%)	Weight uniformity (mg)
ACC	99.216	80 s	20 h	57	0.30	98.06 ± 0.61	298 ± 0.41
Long	100	65 s	23 h	65	0.33	99.37 ± 0.82	299 ± 0.16

Accelerated test (which carried out at 40°C and 75% humidity) affected the floating ability of tablets by slight decrease in floating time.

3.6. Statistical Analysis Results. Before and after conducting the stability studies, statistical analyses of the results for storage months were carried out by one-way ANOVA. No significant difference (P value > 0.05) was observed in the drug release.

F7 stability test after 6 months: there was no significant effect of accelerated term on F7 stability conditions at the $P < 0.05$ level for the three conditions ($F(1, 26) = 1.108138$, $P = 0.302173$, and Fcrit = 4.225201).

F7 stability test after 12 months: there was no significant effect in release rate and stability of F7 after 12 months at the $P < 0.05$ level for the three conditions ($F(1, 26) = 0.285179$, $P = 0.597864$, and Fcrit = 4.225201).

F7 stability test in 6 and 12 months: there was no significant effect of 6 months and 12 months on stability condition at the $P < 0.05$ level for the three conditions ($F(1, 26) = 0.260494$, $P = 0.614087$, and Fcrit = 4.225201).

4. Conclusion

The purpose of this study was to prepare a sustained release tablet of Capecitabine with a 24-hour gradual release with concurrent floating. In doing so, various polymers, such as HPMC K4M, sodium alginate, and sodium bicarbonate, were tested. Also, characterization tests such as floating lag time, total floating time, release measurements, hardness, friability, content uniformity, and weight uniformity were performed. Comparisons of all release studies showed that the drug release depended on the ratio of two polymers—HPMC K4M, which was used as a binder; and sodium alginate, which created gel-forming capabilities in the tablet.

Abbreviations

μg: Microgram
ACC: Accelerated time
API: Active pharmaceutical ingredient
BP: British pharmacopeia
Cap: Capecitabine
Car: Carbomer934p
FDA: Food and Drug Administration
HPMC: Hydroxypropyl methylcellulose
Lac: Lactose
Long: Long term
mg: Milligram
Mg.St: Magnesium stearate
Min: Minute
mm: Millimeter
°C: Degree Celsius
PEG: PolyEthylene glycol
RH: Relative humidity
S.A: Sodium alginate
S.B: Sodium bicarbonate
USP: United States of pharmacopeia
UV: Ultraviolet.

Conflict of Interests

There is no conflict of interests in this project.

Acknowledgments

This study was supported by research a Grant from IPPP, Universiti of Malaya, Malaysia (Grant no. PS202/2010B). The authors thank Osvah Pharmaceutical Company, Tehran, Iran, for their gift of Capecitabine and also Mrs. Fatemeh Allah Bedashti for her friendship and assistance.

References

[1] J. D. Cook, M. Carriaga, S. G. Kahn, W. Schalch, and B. S. Skikne, "Gastric delivery system for iron supplementation," *The Lancet*, vol. 335, no. 8698, pp. 1136–1139, 1990.

[2] G. J. Yoo, E. G. Levine, C. Aviv, C. Ewing, and A. Au, "Older women, breast cancer, and social support," *Supportive Care in Cancer*, vol. 18, no. 12, pp. 1521–1530, 2010.

[3] S. Miyazaki, H. Yamaguchi, C. Yokouchi, M. Takada, and W.-M. Hou, "Sustained-release and intragastric-floating granules of indomethacin using chitosan in rabbits," *Chemical and Pharmaceutical Bulletin*, vol. 36, no. 10, pp. 4033–4038, 1988.

[4] R. C. F. Leonard and T. P. Pwint, "Therapeutic aspect of metastatic breast cancer: chemotherapy," in *Metastasis of Breast Cancer*, R. E. Mansel, Ed., pp. 373–388, Springer, Berlin, Germany, 2007.

[5] S. Arora, J. Ali, A. Ahuja, R. K. Khar, and S. Baboota, "Floating drug delivery systems: a review," *AAPS PharmSciTech*, vol. 6, no. 3, pp. 372–390, 2005.

[6] H. A. Gezairy, *Guidelines for Management of Breast Cancer*, EMRO, 2006.

[7] Minestry of Health Malaysia, *Clinical Practice Guidlines: Management of Breast Cancer*, Minestry of Health Malaysia, Putrajaya, Malaysia, 2002.

[8] R. C. F. Leonard and T. P. Pwint, "Therapeutic aspect of metastatic breast cancer: chemotherapy," in *Metastasis of Breast Cancer*, R. E. Mansel, Ed., pp. 373–388, Springer, Berlin, Germany, 2007.

[9] Roche, *Capecitabine*, Food and Drug Administration (FDA), London, UK, 2000.

[10] J. Khurana, *Development and Characterization of Polymeric Nanoparticulate Delivery System for Hydrophillic Drug: Gemcitabine*, Creighton University, Omaha, Neb, usa, 2009.

[11] S. Patel, "Oral sustained release formulation of anti cancer drug comptothecin using hydroxyl propyle methyl cellulose," 2008, Long Island.

[12] G. B. Jacobson, R. Shinde, C. H. Contag, and R. N. Zare, "Sustained release of drugs dispersed in polymer nanoparticles," *Angewandte Chemie*, vol. 47, no. 41, pp. 7880–7882, 2008.

[13] A. V. Mayavanshi and S. S. Gajjar, "Floating drug delivery systems to increase gastric retention of drugs: a review," *Research Journal of Pharmacy and Technology*, vol. 1, no. 4, pp. 345–348, 2008.

[14] C. Sauzet, M. Claeys-Bruno, M. Nicolas, J. Kister, P. Piccerelle, and P. Prinderre, "An innovative floating gastro retentive dosage system: formulation and in vitro evaluation," *International Journal of Pharmaceutics*, vol. 378, no. 1-2, pp. 23–29, 2009.

[15] M. Jaimini, A. C. Rana, and Y. S. Tanwar, "Formulation and evaluation of famotidine floating tablets," *Current Drug Delivery*, vol. 4, no. 1, pp. 51–55, 2007.

[16] R. S. Rathi, V. R. Patil, M. M. Patel, B. A. Patil, A. G. Shankhpal, and S. D. Barhate, "Formulation and evaluation of matrix floating tablet of Famotidine," *Journal of Pharmacy Research*, vol. 2, no. 3, pp. 531–533, 2009.

[17] A. Savaser, Y. Özkan, and A. Isımer, "Preparation and in vitro evaluation of sustained release tablet formulations of diclofenac sodium," *Il Farmaco*, vol. 60, pp. 171–177, 2005.

[18] H. Garse, M. Vij, M. Yamgar, V. Kadam, and R. Hirlekar, "Formulation and evaluation of a gastroretentive dosage form of labetalol hydrochloride," *Archives of Pharmacal Research*, vol. 33, no. 3, pp. 405–410, 2010.

[19] D. Ray and A. K. Prusty, "Designing and in-vitro studies of gastric floating tablets of tramadol hydrochloride," *International Journal of Applied Pharmaceutics*, vol. 2, no. 4, pp. 12–16, 2010.

[20] S. Londhe, S. Gattani, and S. Surana, "Development of floating drug delivery system with biphasic release for verapamil hydrochloride: in vitro and in vivo evaluation," *Journal of Pharmaceutical Science and Technology*, vol. 2, no. 11, pp. 361–367, 2010.

[21] R. C. Nagarwal, D. N. Ridhurkar, and J. K. Pandit, "In vitro release kinetics and bioavailability of gastroretentive cinnarizine hydrochloride tablet," *AAPS PharmSciTech*, vol. 18, no. 1, pp. 294–303, 2010.

[22] M. I. Tadros, "Controlled-release effervescent floating matrix tablets of ciprofloxacin hydrochloride: development, optimization and in vitro-in vivo evaluation in healthy human volunteers," *European Journal of Pharmaceutics and Biopharmaceutics*, vol. 74, no. 2, pp. 332–339, 2010.

[23] V. S. Patil, P. D. Gaikwad, V. H. Bankar, and S. P. Pawar, "Formulation and evaluation of floating matrix tablet of locally acting h2-antagonist," *International Journal of Pharmacy & Technology*, vol. 2, no. 3, pp. 528–540, 2010.

[24] S. Zeenath, R. Gannu, S. Bandari, and M. Y. Rao, "Development of gastroretentive systems for famotidine: in vitro characterization," *Acta Pharmaceutica Sciencia*, vol. 52, no. 4, pp. 494–504, 2010.

[25] United States Pharmacopeia, *USP32-NF27*, vol. 2, The United States Pharmacopeial Convention, 2010.

[26] British Pharmacopoeia, *Uniformity of Content, Volume 5*, Stationery Office on Behalf of the (MHRA), London, UK, 2010.

[27] A. Pare, S. K. Yadav, and U. K. Patil, "Formulation and evaluation of effervescent floating tablet of amlodipine besylate," *Research Journal of Pharmacy and Technology*, vol. 1, no. 4, pp. 526–530, 2008.

[28] I. Ahmad and R. H. Shaikh, "Effect of temperature and humidity on hardness and friability of packaged Paracetamol tablet formulations," *Pakistan Journal of Pharmaceutical Sciences*, vol. 7, no. 2, pp. 69–78, 1994.

[29] K. A. Russo, "The Role of USP Monographs in Stability Testing," in *Pharmaceutical Stability Testing to Support Global Markets: Pharmasp*, K. Huynh-Ba, Ed., pp. 51–60, American Association of Pharmaceutical Scientists, Arlington, Va, USA, 2010.

[30] M. Łaszcz, K. Trzcińska, K. Filip, A. Szyprowska, M. Mucha, and P. Krzeczyński, "Stability studies of capecitabine," *Journal of Thermal Analysis and Calorimetry*, vol. 105, no. 3, pp. 1015–1021, 2011.

[31] U. S. Department of Health and Human Services, *Guidance for Industry Q1A(R2) Stability Testing of New Drug Substances and Products*, Food and Drug Administration, Silver Spring, Md, USA, 2003.

[32] E. A. Klausner, E. Lavy, D. Stepensky, M. Friedman, and A. Hoffman, "Novel gastroretentive dosage forms: evaluation of gastroretentivity and its effect on riboflavin absorption in dogs," *Pharmaceutical Research*, vol. 19, no. 10, pp. 1516–1523, 2002.

[33] F. A. A. AI-khaled, "Bioadhesive and floating formulations as sustained release dosage form verapamil hydrochloride," in *Pharmaceutics*, King Saud University, Riyadh, Saudi Arabia, 2002.

[34] S. El Samaligy, *Floating Systems for Oral Controlled Release Drug Delivery*, University of Berlin, Berlin, Germany, 2010.

[35] S. T. Prajapati, L. D. Patel, and D. M. Patel, "Gastric floating matrix tablets: design and optimization using combination of polymers," *Acta Pharmaceutica*, vol. 58, no. 2, pp. 221–229, 2008.

[36] J. Siepmann and N. A. Peppas, "Modeling of drug release from delivery systems based on hydroxypropyl methylcellulose (HPMC)," *Advanced Drug Delivery Reviews*, vol. 64, pp. 163–174, 2012.

[37] B. Y. Choi, H. J. Park, S. J. Hwang, and J. B. Park, "Preparation of alginate beads for floating drug delivery system: effects of CO_2 gas-forming agents," *International Journal of Pharmaceutics*, vol. 239, no. 1-2, pp. 81–91, 2002.

[38] A. O. Nur and J. S. Zhang, "Captopril floating and/or bioadhesive tablets: design and release kinetics," *Drug Development and Industrial Pharmacy*, vol. 26, no. 9, pp. 965–969, 2000.

[39] R. C. Nagarwal, D. N. Ridhurkar, and J. K. Pandit, "In vitro release kinetics and bioavailability of gastroretentive cinnarizine hydrochloride tablet," *AAPS PharmSciTech*, vol. 11, no. 1, pp. 294–303, 2010.

Hindawi Publishing Corporation
BioMed Research International
Volume 2013, Article ID 681027, 10 pages
http://dx.doi.org/10.1155/2013/681027

Research Article

Preventive Inositol Hexaphosphate Extracted from Rice Bran Inhibits Colorectal Cancer through Involvement of Wnt/β-Catenin and COX-2 Pathways

Nurul Husna Shafie,[1] Norhaizan Mohd Esa,[1,2] Hairuszah Ithnin,[3,4] Abdah Md Akim,[5] Norazalina Saad,[3] and Ashok Kumar Pandurangan[2]

[1] *Laboratory of Molecular Biomedicine, Institute of Bioscience, Universiti Putra Malaysia, 43400 Serdang, Selangor, Malaysia*
[2] *Department of Nutrition and Dietetics, Faculty of Medicine and Health Sciences, Universiti Putra Malaysia, 43400 Serdang, Selangor, Malaysia*
[3] *UPM-MAKNA Cancer Research Laboratory, Institute of Bioscience, Universiti Putra Malaysia, 43400 Serdang, Selangor, Malaysia*
[4] *Department of Pathology, Faculty of Medicine and Health Sciences, Universiti Putra Malaysia, 43400 Serdang, Selangor, Malaysia*
[5] *Department of Biomedical Sciences, Faculty of Medicine and Health Sciences, Universiti Putra Malaysia, 43400 Serdang, Selangor, Malaysia*

Correspondence should be addressed to Norhaizan Mohd Esa; nhaizan@upm.edu.my

Received 4 June 2013; Revised 4 August 2013; Accepted 29 August 2013

Academic Editor: Mahmood Ameen Abdulla

Nutritional or dietary factors have drawn attention due to their potential as an effective chemopreventive agent, which is considered a more rational strategy in cancer treatment. This study was designed to evaluate the effect of IP_6 extracted from rice bran on azoxymethane- (AOM-) induced colorectal cancer (CRC) in rats. Initially, male Sprague Dawley rats were divided into 5 groups, with 6 rats in each group. The rats received two intraperitoneal (*i.p.*) injections of AOM in saline (15 mg/kg body weight) over a 2-week period to induce CRC. IP_6 was given in three concentrations, 0.2% (w/v), 0.5% (w/v), and 1.0% (w/v), via drinking water for 16 weeks. The deregulation of the Wnt/β-catenin signaling pathway and the expression of cyclooxygenase (COX)-2 have been implicated in colorectal tumorigenesis. β-Catenin and COX-2 expressions were analysed using the quantitative RT-PCR and Western blotting. Herein, we reported that the administration of IP_6 markedly suppressed the incidence of tumors when compared to the control. Interestingly, the administration of IP_6 had also markedly decreased β-catenin and COX-2 in colon tumors. Thus, the downregulation of β-catenin and COX-2 could play a role in inhibiting the CRC development induced by IP_6 and thereby act as a potent anticancer agent.

1. Introduction

Inositol hexaphosphate (IP_6) is a dietary component that constitutes approximately 1 to 5% of the weight of most cereals, nuts, oil seeds, legumes, and grains [1, 2]. In particular, approximately 9.5 to 14.5% of the weight of rice bran is composed of IP_6. Phytic acid or IP_6 is a polyphosphorylated carbohydrate with six phosphate groups, each attached to a carbon atom [3]. *Myo*inositol is the parent compound of IP_6. The phosphate grouping in positions 1, 2, and 3 (axial-equatorial-axial) is unique for IP_6 and suggests tremendous chelating potential [3], thereby it has a potential role as anticancer agent. According to previous research, IP_6 exhibits a variety of chemopreventive properties, including antioxidant and anticancer properties [4, 5]. Matejuk and Shamsuddin suggested that IP_6 acts as a protective agent in cancer development [6].

Preclinical studies have been conducted to evaluate the potential anticancer properties and tolerability of IP_6 in cancer treatment [6]. However, because these studies have not evaluated the anticancer potential and toxicity effects of IP_6 extracted from rice bran, its specific mechanism of action

as an anticancer agent remains unexplored. Furthermore, the antiproliferative activity of IP_6 is most likely mediated through the coordinated activity of a number of molecules, although the exact signaling network involved in eliciting this response is unclear. Therefore, our study aims to evaluate the anticancer potential of IP_6 extracted from rice bran and to determine its mechanism of actions.

Furthermore, Singh et al. [7] have previously analyzed the anticancer efficacy of oral IP_6 against human prostate carcinoma xenograft *in vivo*, in which IP_6 suppressed the tumor growth without any toxicity. IP_6 also has been found to be effective in animal tumorigenesis models of other cancer types without any toxicity [8]. In addition, our earlier study has reported that no toxic effect has been found in liver and kidney after the administration of IP_6 to treat colorectal cancer (CRC) in AOM-induced rats [9].

CRC is ranked as the third most prevalent cancer and the second leading cause of disease-related deaths in the US [10]. CRC results in, when normal glandular epithelial cells accumulate acquired genetic and epigenetic changes that transform the cells into invasive adenocarcinomas. In other words, when normal epithelium transforms into an adenoma, it can eventually invade nearby colon tissue and metastasizes [11]. Carcinogenesis may be targeted at multiple points during its sequence to prevent the development of adenocarcinoma. Potential preventive agents that help suppress colon carcinogenesis can lead to chemoprevention of the disease [12]. To date, many chemopreventive agents from natural products and their phytochemical constituents are known to interact with diverse molecular targets during carcinogenesis [13]. A broad range of nutraceutical compounds possess remarkable therapeutic properties; therefore, we aimed to examine the development of an alternative compound from Malaysian sources, particularly rice bran. Rice bran which is composed of pericarp, seed coat, nucellus, aleurone layers, and germ is a byproduct of rice milling in the production of white rice.

Abnormal activation of the Wnt/β-catenin pathway has been implicated in human CRC [14]. This activation occurs due to the overexpression of the Wnt ligand and/or mutations in the downstream molecules of the Wnt signaling cascade, such as the *APC* and *β-catenin* genes [15]. Therefore, the Wnt/β-catenin pathway is considered a therapeutic target for the prevention and treatment of CRC.

Spychalski et al. [14] reported that, in addition to excessive β-catenin, overexpression of COX-2 and increased prostaglandin (PG) production from free arachidonic acid also contribute to CRC development. Overexpression of cyclooxygenase-2 (COX-2) has been reported in approximately 90% of colon tumors and premalignant colorectal adenomas [16, 17]. COX-2 is an inducible prostaglandin G/H synthase and was identified to have a vital function in prostaglandin (PG) synthesis. In addition to the COX-2/PGE2 signaling pathway, a lot of natural products and their active phytochemicals have been proven to have chemopreventive potential that can modulate various signal transduction pathways underlying colon carcinogenesis [13]. This was proven by Reddy et al. [18] who have shown that wheat bran fractions play a role in reducing iNOS and COX-2 expressions in CRC. Moreover, reduction in transcriptional activity of COX-2 has been shown after administration of anthocyanin-rich extracts of bilberry and grape in AOM-induced rat [19]. Bakhle [20] has previously reported that the COX-2 protein is normally absent in cells. To the best of our knowledge, the effects of IP_6 in altering the expression of β-catenin and COX-2 have not been described earlier. Hence, we intend to investigate the effects of IP_6 for the first time on these two pathways during colon tumorigenesis.

2. Materials and Methods

2.1. Chemicals. Hexane and hydrochloric acid (HCl) were purchased from Merck (Darmstadt, Germany). Iron chloride ($FeCl_3$), azoxymethane, and sodium hydroxide (NaOH) were purchased from Sigma (St. Louis, MO, USA). Western blotting reagents were purchased from Bio-RAD (CA, USA). Dimethylformamide (DMF) was purchased from Fermentas (Lithuania, EU). Other chemicals used in this study were of the highest commercial grade.

2.2. Preparation of IP_6. Freshly milled raw rice bran samples from mixed local varieties (MR 84 and MR 219) were kindly supplied by the BERNAS Milling Plant (Selangor, Malaysia). The bran was microwaved immediately and stabilized according to the method used by Ramezanzadeh et al. [21]. Then, 2 mL of hexane was added to every 0.5 g of rice bran and soaked overnight to produce defatted rice bran [22]. The rice bran was then filtered and dried by evaporation using a vacuum pump apparatus. After that, IP_6 was extracted as follows: using a slight modification to previously described methods [23]. The defatted rice bran was combined with hydrochloric acid (0.5 M HCl) and continuously shaken in an orbital mixer for 2 hours at room temperature. The mixture was then centrifuged at 17,300 g for 30 minutes at 15°C, and the supernatant containing IP_6 was collected. To neutralize the sample, $FeCl_3$ was added to the IP_6, and the mixture was placed in a boiling water bath to allow complete precipitation of the ferric phytate complexes. Ferric phytate was then heated with NaOH and centrifuged to obtain ferum (III), hydroxide (pellet), and sodium phytate (supernatant) [24]. Finally, the supernatant was collected and freeze dried. We successfully extracted and obtained the pure IP_6 from rice bran in our laboratory. The determination of IP_6 was done by HPLC analysis [23].

2.3. Animals. Male Sprague Dawley rats weighing approximately 50 g were acclimatized for seven days and fed on normal rat chow, according to the AIN 76-A guidelines, and tap water was provided *ad libitum*. Rats were housed in individual cages, which were fully ventilated and maintained at room temperature on a 12-hour light-dark cycle. All of the experimental protocols involving animals were approved by the Animal Care and Use Committee of the Faculty of Medicine and Health Sciences, Universiti Putra Malaysia (UPM), Serdang, Selangor, Malaysia.

2.4. Experimental Design. Rats were acclimatized for seven days and randomized into experimental and control

groups. The animals were injected intraperitoneally with azoxymethane (AOM), a specific carcinogen that was diluted in saline, once per week (15 mg/kg body weight), over a 2-week period to induce colonic tumors [9, 25]. Rats were divided into 5 groups ($n = 6$). Group 1 was the control group. Groups 2–5 received intraperitoneal (*i.p.*) injections of AOM once per week, for two consecutive weeks at a dose of 15 mg/kg body weight, as mentioned above. Starting one week after the second dosing with AOM, groups 3–5 received various concentrations of IP_6 [0.2% (w/v), 0.5% (w/v), and 1.0% (w/v)] in their drinking water for a period of 16 weeks. These concentrations were achievable physiologically in rat tumor models considering the doses used which give rise to inhibition of tumor incidence [9, 26]. All of the rats were carefully observed on a daily basis, and their body weights were recorded weekly. At the end of the experiment, all of the rats were euthanized by cervical decapitation, and the whole colon tissues were collected, weighed, and processed immediately for further analysis.

2.5. Detection of Aberrant Crypt Foci (ACF) and Tumor Assessment. The colons were resected and flushed with 10% neutralized formalin to remove residual bowel contents, cut open longitudinally and submerged overnight in 10% (v/v) neutralized formalin. The tissue samples were dehydrated in an ascending series of alcohol dehydration, cleared with xylene, and wax impregnated with paraffin wax for 14 hours in an automatic tissue processor machine. Sections (3 μM) were stained with hematoxylin and eosin (H & E).

ACF were identified using a published set of criteria which distinguishes these lesions from normal crypts [25]. Tumor assessment parameters have been previously described by Bird [25]. Briefly, tumor incidence is the percentage of total animals with tumors as follows:

$$\text{tumor incidence} = \frac{\text{total animals with adenoma and/or adenocarcinoma}}{\text{total animals}}. \quad (1)$$

2.6. Analysis of β-Catenin and COX-2 Expression by Real-Time PCR. The extraction of total RNA from fresh whole colon tumor tissue was performed using TRI Reagent (Sigma, MO, USA). Tissue disruption and homogenization were performed such that the colon tumor tissue was weighed out (20–30 mg), immediately placed in liquid nitrogen, and homogenized using a tissue grinder. The tissue powder and liquid nitrogen were decanted into an RNase-free, 2 mL microcentrifuge tube, and the liquid nitrogen was allowed to evaporate. Then, the tissue samples were homogenized in 1 mL of TRI Reagent per 50–100 mg of tissue for 10 minutes. RNA extraction was then performed according to the manufacturer's instructions, and 1 μg of the total RNA sample was reverse transcribed using the GeneAmp Gold RNA PCR Core Kit (Applied Biosystems, California, USA) in a final reaction volume of 20 μL, according to the manufacturer's protocol. The reverse transcription reaction was carried out at 42°C for 30 minutes in an authorized thermal cycler (Eppendorf, NY, USA), followed by a 10-minute step at 99°C to denature the enzyme; then, it was cooled to 4°C. This cDNA was then used as a template for amplification in real-time PCR reactions. Quantitative real-time PCR was performed in a reaction volume of 20 μL, according to the manufacturer's instructions for the KAPA SYBR Green FAST qPCR kits (Kapa Biosystems, Boston, MA, USA). Nucleotides primer sequences of rat origin were used (Table 1). Briefly, 18.2 μL of master mix, 0.8 μL of primer assay (10x), and 1 μL of template cDNA (20 ng) were added to each well. After a brief centrifugation, the PCR plate was subjected to 40 cycles of the following conditions: (i) PCR activation at 95°C for 20 seconds, (ii) denaturation at 95°C for 3 seconds, and (iii) annealing/extension at 60°C for 20 seconds. All samples and controls were run in triplicate on a Mastercycler realplex system (Eppendorf, NY, USA). The quantitative RT PCR data were analyzed using a comparative threshold (Ct) method, and the fold inductions of the samples were compared with the untreated samples. β-actin was used as an internal reference gene to normalize the expression of the target genes.

2.7. Western Blot Analyses of β-Catenin and COX-2. The fresh colon tumor tissue disruption and homogenization steps for extracting proteins were similar to those described for total RNA extraction. The samples were homogenized in Buffer RLT using a QIAshredder homogenizer. Protein extraction was performed using the AllPrep DNA/RNA/Protein Mini Kit, according to the manufacturer's protocol (Qiagen, Duesseldorf, Germany). Next, the protein concentration was determined by the Bradford assay, according to the manufacturer's protocol (Bio-RAD, CA, USA). The protein (50 μg) was separated by 12% sodium dodecyl sulfate polyacrylamide gel electrophoresis (SDS-PAGE) and transferred onto a piece of PVDF membrane using transfer buffer (25 mM Tris base, 190 mM glycine, and 20% (v/v) methanol, pH 8.3). After transfer, the PVDF membrane was blocked at room temperature with blocking solution (25 mM Tris base, 0.3 M NaCl, and 5% milk diluent) (Bio-RAD, CA, USA) for 30 minutes. The membrane was then incubated overnight with primary antibodies at a 1 : 1000 dilution (β-catenin rabbit monoclonal antibody and COX-2 rabbit monoclonal antibody from Santa Cruz Biotechnology, CA, USA), followed by a 1-hour incubation with alkaline phosphatase-labeled goat anti-mouse secondary antibody (Santa Cruz Biotechnology, TX, USA) at a 1 : 10000 dilution in Tris-buffered saline (TBS) and 0.5% Tween 20. Immunodetection was performed by the addition of a developing solution. The developing solution for alkaline phosphatase conjugated antibodies consisted of 10 mL alkaline phosphatase buffer (100 mM Tris HCl, 100 mM NaCl, and 5 mM $MgCl_2$; pH 9.5), 33 μL BCIP (0.5 g 5-bromo-4-chloro-3-indolylphosphate-p-toluidine salt (Fermentas, Lithuania, EU) in 10 mL of 100% (v/v) dimethylformamide (DMF)), and 66 μL NBT (0.75 g nitroblue tetrazolium chloride (Fermentas, Lithuania, EU) in 10 mL of 70% (v/v) DMF). The reaction was stopped when the desired protein band appeared. Densitometric analysis of band intensities obtained from western blotting experiments were carried out using ImageJ software (National Institutes of Health (NIH), USA).

Table 1: Nucleotide sequence for PCR primers for amplification and sequence-specific detection.

Pair no.	Primer name	Accession no.	Oligonucleotides (5′-3′) sequence	Product size (bp)
1	β-catenin	NM-001165902	F-ACAGCACCTTCAGCACTCT R-AAGTTCTTGGCTATTACGACA	168
2	COX-2	L25925	F-ACAGGAGAGAAAGAAATGGCTGCAGAGT R-CAGTATTGAGGAGAACAGATGGGATT	198
3	β-actin	NM-031144	F-TCACCCACACTGTGCCCATCTATGA R-GTCACGCACGATTTCCCTCTCAGC	180

2.8. Statistical Analysis. Data were expressed as the mean ± standard deviation (SD) and statistically analyzed using SPSS version 10, with a one-way ANOVA with Tukey's test and a significance level of $P < 0.05$.

3. Results

3.1. Identification of IP_6. IP_6 was analyzed by reversed-phase high-performance liquid chromatography (HPLC). HPLC chromatograms were compared with those of standard phytic acid. As we reported earlier [9, 23], based on the HPLC chromatogram data, two peaks were represented as pure inositol hexaphosphate.

3.2. Body Weight. Figure 1 represents the changes in the rat body weights during the experiment. Body weights were compared between all groups (normal, AOM only, AOM + 0.2% (w/v) of IP_6, AOM + 0.5% (w/v) of IP_6, and AOM + 1% (w/v) of IP_6). The plotted graph in Figure 1 shows that the body weights of all of the rats increased over time. When compared with the normal group, the IP_6-fed groups (AOM + 0.2% (w/v) of IP_6, AOM + 0.5% (w/v) of IP_6, and AOM + 1% (w/v) of IP_6) showed no significant differences in body weight, even after 16 weeks of IP_6 treatment. However, there was a significant ($P < 0.05$) difference between the body weight of the positive control group (AOM only) and the body weight of the rats in the IP_6-fed and normal groups. In addition, the body weight of the AOM-only group was significantly lower than that of the IP_6-fed and normal groups; these results support the expectation that exposure to the carcinogen AOM would cause weight loss. Additionally, administration of IP_6 during the early treatment may boost growth (Figure 1). However, the mechanism is unknown. These data clearly showed that daily consumption of IP_6 even for longer duration of treatment was not toxic to normal rats and also maintained or even increased the body weight of AOM-treated rats versus normal rats, potentially inhibiting abnormal growths in the colon, which were further examined by histopathological analyses.

3.3. Incidence of ACF and Tumors. ACF is a preneoplastic lesion which can be characterized by clusters of mucosal cells with an enlarged and thicker layer of epithelia compared to the surrounding normal crypts. ACF may progress into polyps, later develop into adenomas, and eventually become invasive carcinomas [27]. Although not all ACF may develop into cancer, but all colon cancers arise from ACF as evidenced

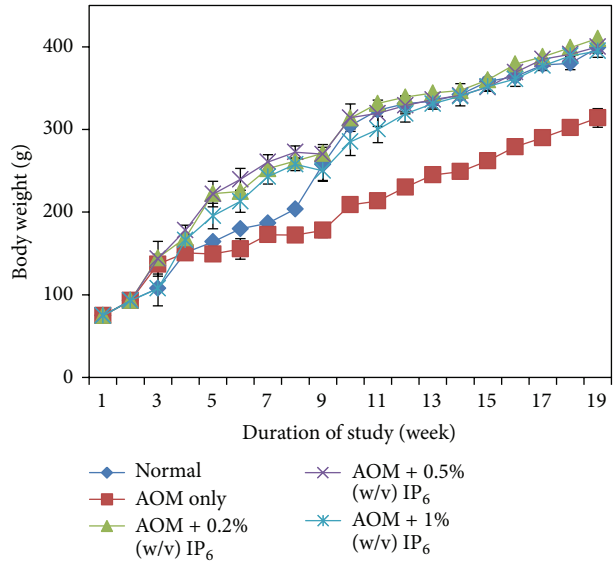

Figure 1: General observation on body weight of experimental rats throughout the study. IP_6 increases the body weight in all IP_6-fed groups relative to the normal group. Groups are normal, AOM only, AOM + 0.2% (w/v) of IP_6, AOM + 0.5% (w/v) of IP_6, and AOM + 1% (w/v) of IP_6. (AOM = azoxymethane, IP_6 = inositol hexaphosphate).

by several studies [27]. Jen et al. [28] proposed that only dysplastic ACF progress to adenoma and adenocarcinoma. The beneficial effect of various dosages of phytic acid (IP_6) (0.2% (w/v), 0.5% (w/v), and 1% (w/v)) on the reduction of ACF development was further demonstrated. As shown in Figure 2, the analysis of ACF formation incidence demonstrated that the administration of rice bran IP_6 significantly reduced the total number of ACF ($P < 0.05$) in all IP_6-fed groups in comparison with the untreated rats and AOM-only group, thereby leading to the inhibition of ACF formation which may or may not develop into the invasive carcinoma. Figure 3 summarized the histological analysis of aberrant crypt foci (ACF) with surrounding normal tissue using H & E staining. The images (Figure 3) represented the incidence of ACF taken from group of rats induced with AOM only (without treatments of IP_6).

An adenoma is defined as a benign tumor of glandular origin. Colonic adenoma consists of proliferation on colonic glands lined by neoplastic colonic epithelium, while an adenocarcinoma is a malignant tumor originating in glandular epithelium. Colonic adenocarcinoma is composed of

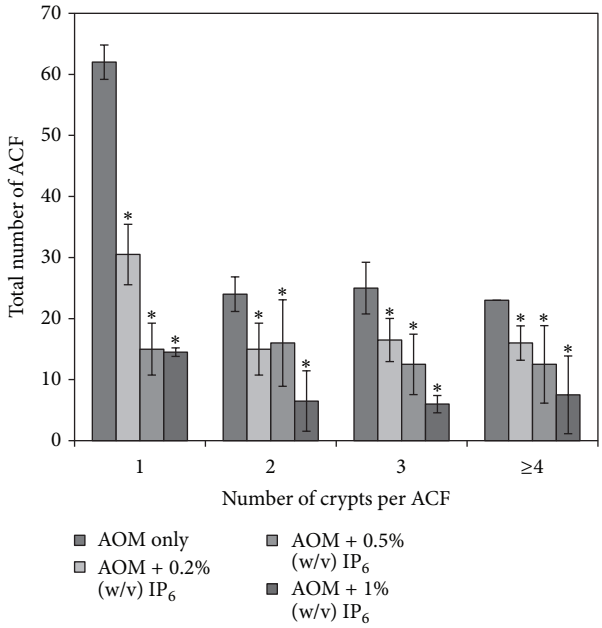

Figure 2: Effect of IP_6 on AOM-induced colonic aberrant crypt foci (ACF) in rats. IP_6 decreases the number of ACF in all IP_6-fed groups relative to the AOM-only group. Each value expressed as mean ± SD ($n = 6$). *Indicates significant difference by Tukey's test ($P < 0.05$). Groups are AOM only, AOM + 0.2% (w/v) of IP_6, AOM + 0.5% (w/v) of IP_6, and AOM + 1% (w/v) of IP_6. (AOM = azoxymethane, ACF = aberrant crypt foci, IP_6 = inositol hexaphosphate).

invasive glands lined by pleomorphism and hyperchromatic epithelium. Figure 4 showed the histopathology of colonic lesions developed by AOM-induced CRC in rats. The images (Figure 4) represented the incidence of adenoma and adenocarcinoma taken from rats induced with AOM only (without treatments of IP_6).

The incidence of adenoma, adenocarcinoma, and total tumors (adenoma + adenocarcinoma) in different study groups is summarized in Table 2. The highest incidence of adenoma, adenocarcinoma, and total tumors occurred in the AOM-only group. However, administration with IP_6 (0.2, 0.5, and 1% (w/v)) significantly reduced the incidence of tumors in a dose-dependent manner when compared with the results of the AOM-only group (no IP_6 treatment) ($P < 0.05$). None of the rats in the normal group developed colon tumor. Additionally, not all rats consist of both adenoma and adenocarcinoma, namely, total tumors (Table 2), and in accordance with our previous study which demonstrated that both adenoma and adenocarcinoma are developed in some of the rats [9]. Altogether, the administration of IP_6 appeared to reduce the incidence of adenoma, adenocarcinoma, and total tumors.

3.4. IP_6 Downregulated the mRNA Levels of β-Catenin and COX-2. Our study successfully demonstrates that inhibition of tumor growth in AOM-induced rat CRC using IP_6 treatment is accompanied by the downregulation of β-catenin. Figure 5(a) shows that, compared with the controls, IP_6-treated rats expressed less β-catenin at the mRNA level, especially for rats treated with the highest concentration of IP_6, 1% (w/v). After treatment with 0.2%, 0.5%, and 1% (w/v) of IP_6, β-catenin was significantly downregulated by 0.93-, 0.514-, and 0.385-fold, respectively, demonstrating a dose-dependent relationship ($P < 0.05$).

Moreover, based on the fold changes relative to the control, IP_6 also significantly inhibited the expression of COX-2 in AOM-induced rat colon carcinogenesis ($P < 0.05$). As shown in Figure 5(b), after treatment with IP_6 (0.2%, 0.5%, and 1% (w/v)), COX-2 mRNA expression was significantly downregulated by 0.783-, 0.661-, and 0.426-fold, showing a dose-dependent relationship ($P < 0.05$).

3.5. IP_6 Reduced the Expressions of β-Catenin and COX-2. The expression levels of β-catenin and COX-2 proteins for the control and experimental group of rats are presented in Figure 6. The results from the Western blot show that β-catenin and COX-2 were both overexpressed in the AOM-induced rats. As shown in Figure 6(a), β-catenin was detected as a 92-kDa band in AOM-induced rat colon carcinogenesis. Significant reduction in β-catenin protein expression was observed after treatment with IP_6 (0.2%, 0.5%, and 1%) by 0.272-, 0.189-, and 0.045-fold relative to the control in a dose-dependent manner ($P < 0.05$).

Furthermore, as shown in Figure 6(b), the immunoreactive bands of COX-2 were detected at 72 kDa (the molecular weight of COX-2) in AOM-induced rats. Similarly, because COX-2 expression was inhibited by IP_6 at the mRNA level, it was also downregulated at the protein level. COX-2 protein expression in AOM-induced rat colon carcinogenesis was significantly decreased by 0.38-, 0.102-, and 0.031-fold after treatment with 0.2%, 0.5%, and 1% (w/v) of IP_6, respectively, compared with the control group, thus showing a dose-dependent relationship ($P < 0.05$). All together, these results showed that the regulation or stability of β-catenin and COX-2 protein levels should be affected by IP_6.

4. Discussion

The primary parameters used in cancer chemoprevention studies to assess the toxicity of a test compound include body weight gain profiles. Accordingly, changes in animal body weight, as a result of IP_6 administration during the 16-week study period, were assessed to evaluate potential adverse health effects of the treatment. As mentioned earlier, all of the IP_6-fed groups experienced body weight gain that was similar to the normal group and, therefore, did not show any significant differences. These results were also observed by Norazalina et al. [9] who previously studied the anticancer efficacy of AOM-induced CRC in rats; their results included the body weights of the rats that were treated with IP_6 from rice bran. Similar findings were observed in the suppression of prostate cancer growth for IP_6-fed mice [26].

A significant reduction in the body weight of AOM-induced group was observed when compared with the other groups; the body weights observed for the normal and IP_6-fed groups were reliable because, according to Alfin-Slater

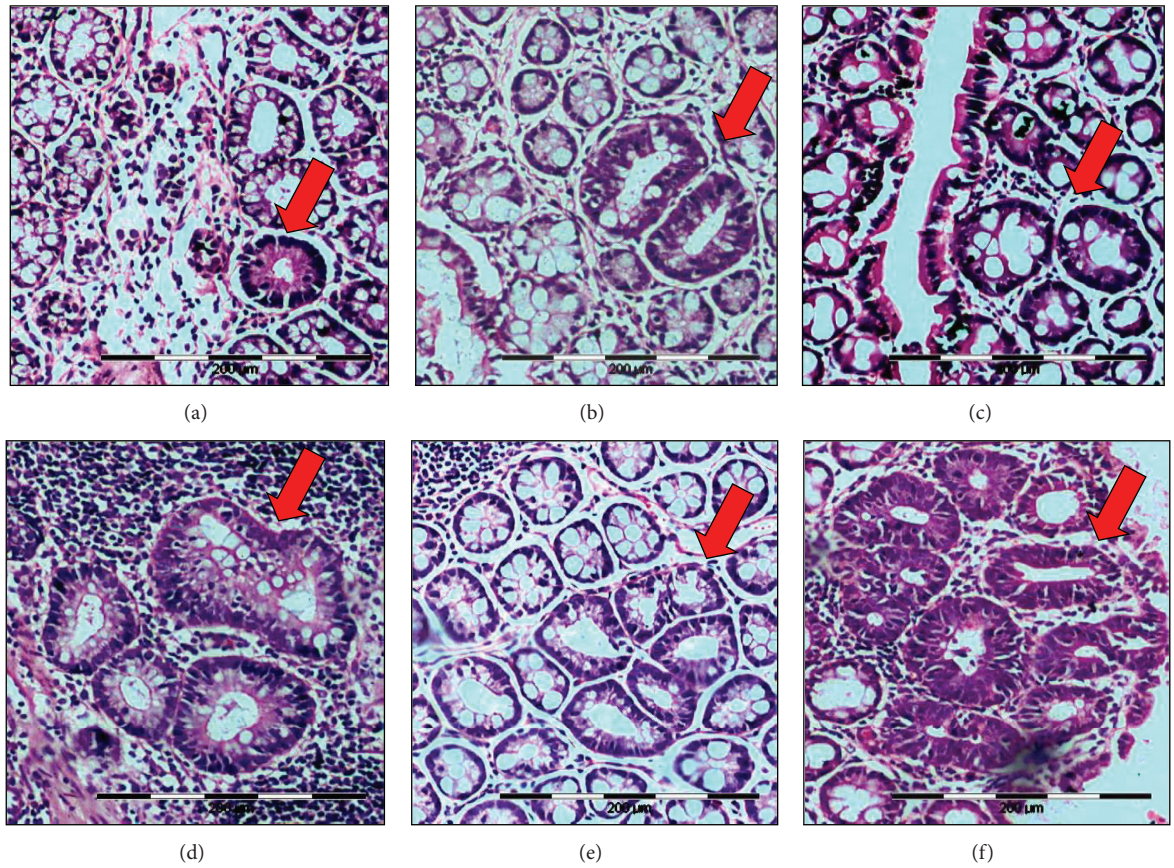

Figure 3: Histological analysis of aberrant crypt foci (ACF) (magnification, 400x). (a) small ACF containing 1 crypt, (b) small ACF containing 2 crypts, (c) medium ACF containing 3 crypts, and (d, e, f) large ACF containing more than 4 crypts. (ACF = aberrant crypt foci).

Table 2: Incidence of tumor of the IP_6-treated rats with AOM-induced colon carcinogenesis.

Group no.	Treatment	No. of rats	Incidence (%) of adenoma and/or adenocarcinoma		
			Adenoma	Adenocarcinoma	Total
1	Normal	6	0	0	0
2	AOM only	6	4/6 (67%)[a]	5/6 (83%)[b]	5/6 (83%)[b]
3	AOM + 0.2% (w/v) IP_6	6	3/6 (50%)[c]	3/6 (50%)[c]	4/6 (67%)[d]
4	AOM + 0.5% (w/v) IP_6	6	1/6 (17%)[e]	2/6 (33%)[f]	3/6 (50%)[g]
5	AOM + 1% (w/v) IP_6	6	1/6 (17%)[e]	1/6 (17%)[e]	2/6 (33%)[f]

Groups: normal, AOM only, AOM + 0.2% (w/v) of IP_6, AOM + 0.5% (w/v) of IP_6, AOM + 1% (w/v) of IP_6, and (IP_6: inositol hexaphosphate, AOM: azoxymethane). Values in the same column with different superscript indicate significant difference by the Tukey's test ($P < 0.05$). Adenoma is defined as a benign tumor of glandular origin. Adenocarcinoma is a malignant tumor originating in glandular epithelium. Total tumor consists of both adenoma and adenocarcinoma in the colon tumor tissue.

and Kritchevsky [29], the weight loss that accompanies tumor development is thought to be associated with a reduction of not only body fat stores but also body mass. There is increasing evidence that the tumor directly affects the host's protein metabolism. Specifically, the protein turnover process is altered in the cancer-bearing host, and there is a net loss of nitrogen from nonmalignant tissues because protein degradation exceeds protein synthesis. Moreover, it is interesting to highlight that in all of the IP_6-fed groups, even though all of the rats were initially treated with the carcinogen (AOM), their body weights showed no significant difference compared with that of the normal rats after 16 weeks of continuous IP_6 treatment. Thus, the administration of IP_6 appears to have an inverse effect on the reduction in body weight seen with AOM alone. However, the mechanism behind this effect is unknown.

The current data shows that the administration of IP_6 in drinking water suppressed the number of ACF and thereby leading to the inhibition of tumor incidence in the colons of the IP_6-fed groups as compared with the AOM-induced group. IP_6 has been shown to reduce the number and size of colon adenomas, which are the precursor lesions of CRC. Our

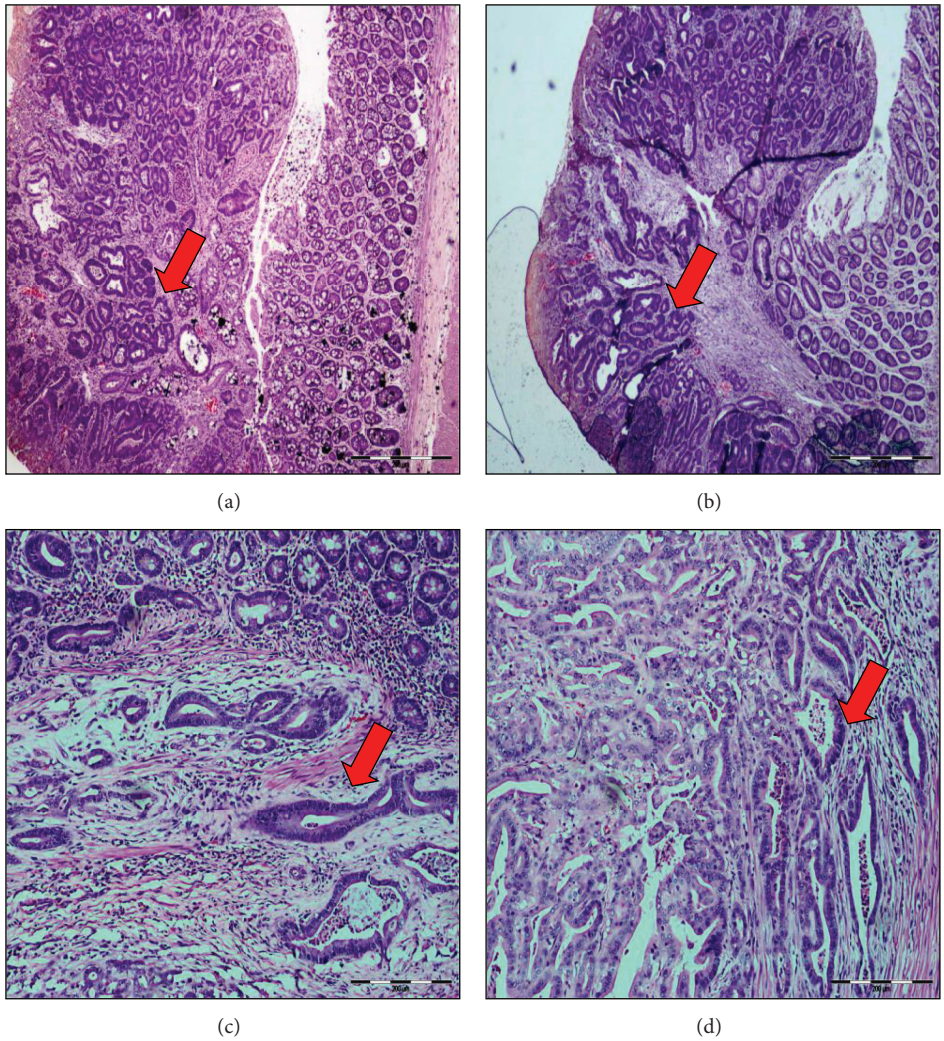

Figure 4: Histopathology of colonic lesions developed in rats' group treated with AOM only. (a) Adenomatous polyps originated from the colon of a few rats (a and b). The polyps are located in the mucosal layer only. (b) Adenocarcinoma (c and d) showing the invasive gland in the submucosa and muscular layer (magnification 400x).

study suggests that IP_6 extracted from rice bran might reduce the formation of tumors in the colon. The tumor inhibition action of IP_6 has been supported by previous studies, which showed that the addition of IP_6 to drinking water had a chemopreventive effect on CRC [9, 30, 31]. Furthermore, our earlier studies have shown the potential antiproliferative effects of IP_6 from rice bran on CRC and hepatic cancer *in vitro* [32, 33].

Alterations in the *APC* or *β-catenin* gene are regarded as early critical events during CRC and are therefore considered to play a gate keeper role in the development of CRC in both humans and preclinical models [34–36]. Mutations in the *APC* or *β-catenin* gene were proved to repress the degradation of the protein and generate *β*-catenin accumulations in the cytosol [37, 38]. The excessive *β*-catenin functions as a transcriptional activator when complexed with members of the T-cell factor (TCF) family of DNA binding proteins [39, 40]. Furthermore, target genes of *β-catenin* signaling pathway, such as *c-myc* and *cyclin D1*, are growth-promoting genes, suggesting that this pathway is potentially an oncogenic pathway [41, 42]. Expression of non-p-*β*-catenin was elevated in AOM-induced experimental CRC [43], also colon adenocarcinoma cells [44]. Other natural compounds have the ability to reduce the expression of non-p-*β*-catenin during colon tumorigenesis [43–45]. Our present study further supported previous reports on the expression of *β*-catenin which was increased while induction with AOM [46]. We assumed that IP_6 might be involved in regulation or stability of *β*-catenin level in CRC as a previous study has also reported the role of inositol polyphosphates in Wnt signaling pathway, by which IP_5 accumulates in response to Wnt3a, thereby playing an essential component of signaling of the canonical pathway to the level of *β*-catenin accumulation [47].

Interestingly, we demonstrated that the inhibition of CRC by IP_6 may be mediated through inactivation of *COX-2*

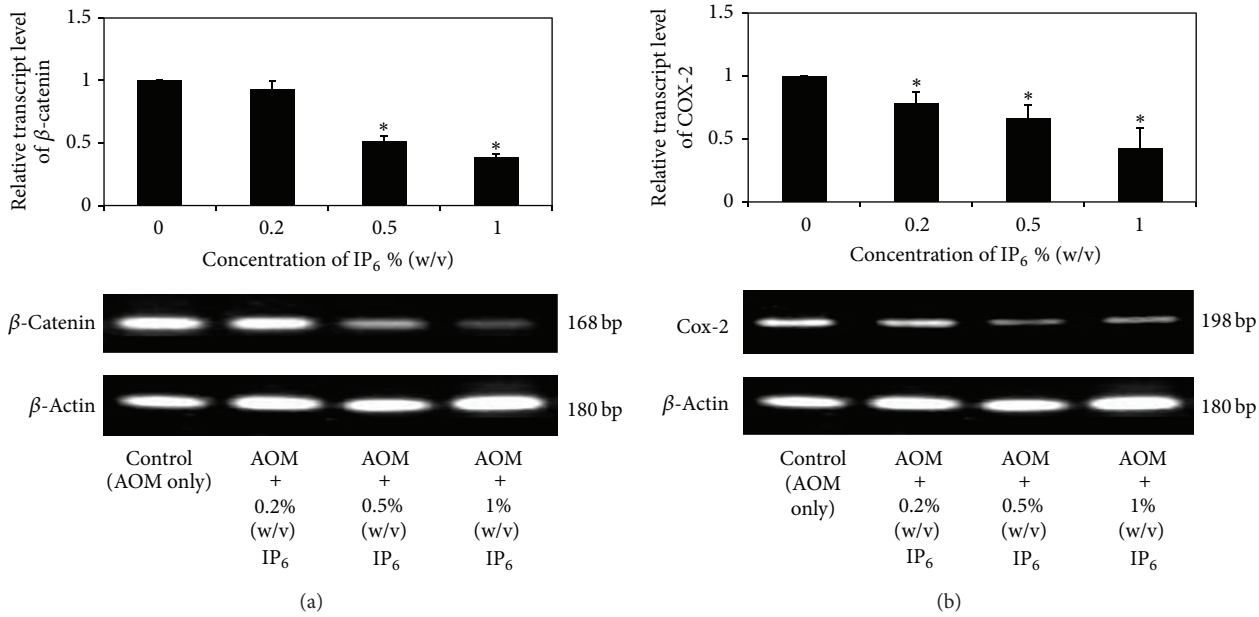

Figure 5: Expression of β-catenin and COX-2 at the mRNA level in rats with AOM-induced colon carcinogenesis after treatment with IP_6. The expressions of β-catenin and COX-2 mRNA were assessed by quantitative RT PCR. IP_6 downregulates the expression of (a) β-catenin and (b) COX-2 in a dose-dependent manner. The results show a typical pattern from the 3 experiments performed. *Indicates significant difference by Tukey's test ($P < 0.05$) relative to their respective control.

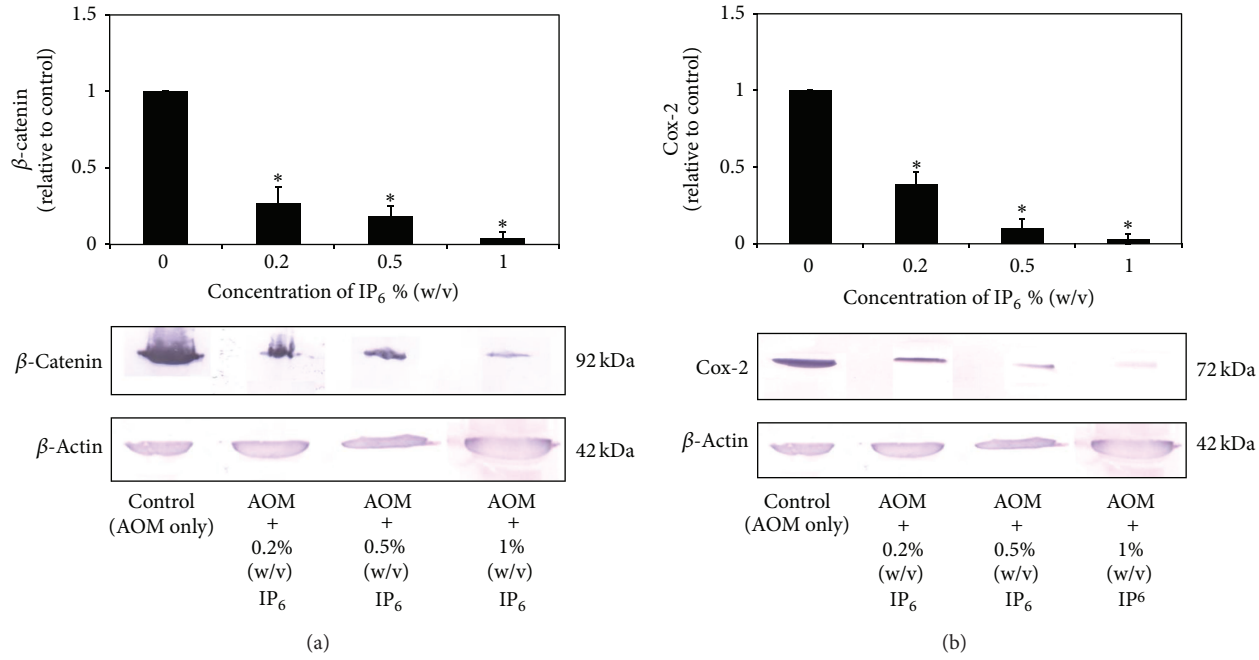

Figure 6: The effect of IP_6 on the protein levels of β-catenin and COX-2 in rats with AOM-induced colon carcinogenesis. IP_6 decreases the protein expression of β-catenin (a) and COX-2 (b) in a dose-dependent manner. Protein expression was normalized to the β-actin control. The results show a typical pattern from the 3 experiments performed. *Indicates significant difference by Tukey's test ($P < 0.05$) relative to their respective control.

gene. The results showed a dose-dependent reduction in the level of COX-2 in IP_6-treated rats with AOM-induced CRC. Although the mechanism underlying how IP_6 modulates the expression of the COX-2 is still unknown, it is likely that the downregulation of COX-2 might be the cause of repressed tumor growth and subsequent tumor cell death. The current data indicate that oral administration of IP_6 was associated with a decreased incidence of CRC through reductions in the number and size of adenomas and invasive carcinomas. These observations suggest the protective effects of IP_6 against AOM-induced colon cancer in animal models.

Our data demonstrate that the anticancer action of IP_6 occurs via a reduction in tumor incidence, which subsequently leads to tumor suppression and the depletion of COX-2 and β-catenin expressions, whereby all of these are implicated in AOM-induced colon carcinogenesis. These data further support previous studies suggesting that IP_6 acts as an anticancer agent by reversing the proliferative effects of carcinogens [2].

Interestingly, several studies have shown that COX-2 may be regulated by the Wnt/β-catenin signaling pathway [48–50]. It seems likely that IP_6 may downmodulate Wnt signaling via the inhibition of β-catenin, thus reducing levels of COX-2. This effect was shown by a marked inhibition of COX-2 expression after treatment with IP_6. Real-time PCR determination of the COX-2 mRNA level in IP_6-treated rats with AOM-induced CRC indicates that COX-2 is significantly downregulated; this effect correlates with the observed protein levels as well. Therefore, COX-2 expression may be suppressed via inhibition of Wnt/β-catenin signaling. The pharmacological inhibition of COX-2 may therefore provide an effective chemoprotective method against CRC. To further support this finding and previous studies that correlate β-catenin with COX-2, we suggest that the underlying inhibitory mechanism of IP_6 occurs via the suppression of β-catenin expression through COX-2 regulation or vice versa. This correlation at the mRNA and protein levels strongly supports the reduction of intestinal neoplasia by β-catenin and COX-2 inhibitions, suggesting that IP_6 may play a therapeutic role in CRC and may contribute to new strategies in the prevention and treatment of this disease.

5. Conclusion

The observed modulatory influences of rice bran IP_6 at the level of cell proliferation, by inhibiting β-catenin and COX-2 during AOM-induced CRC, have not been noted previously and suggest that the intake of rice bran IP_6 may be used in future clinical chemopreventive trials to monitor the responsiveness of the CRC development to the chemopreventive agents.

Acknowledgments

The authors are thankful to Faculty of Medicine and Health Sciences, Institute of Bioscience, UPM for their facilities and are indebted to the Ministry of Agriculture (MOA) for funding the project with Grant no. (05-01-04-SF0856).

References

[1] A. M. Shamsuddin, I. Vucenik, and K. E. Cole, "IP_6: a novel anticancer agent," *Life Sciences*, vol. 61, no. 4, pp. 343–354, 1997.

[2] U. Schlemmer, W. Frølich, R. M. Prieto, and F. Grases, "Phytate in foods and significance for humans: food sources, intake, processing, bioavailability, protective role and analysis," *Molecular Nutrition and Food Research*, vol. 53, no. 2, pp. 330–375, 2009.

[3] I. Vucenik and A. M. Shamsuddin, "Protection against cancer by dietary IP_6 and inositol," *Nutrition and Cancer*, vol. 55, no. 2, pp. 109–125, 2006.

[4] M. E. Norhaizan, S. K. Ng, M. S. Norashareena, and M. A. Abdah, "Antioxidant and cytotoxicity effect of rice bran phytic acid as an anticancer agent on ovarian, breast and liver cancer cell lines," *Malaysian Journal of Nutrition*, vol. 17, no. 3, pp. 367–375, 2011.

[5] R. J. Jariwalla, "Rice-bran products: phytonutrients with potential applications in preventive and clinical medicine," *Drugs under Experimental and Clinical Research*, vol. 27, no. 1, pp. 17–26, 2001.

[6] A. Matejuk and A. Shamsuddin, "IP_6 in cancer therapy: past, present and future," *Current Cancer Therapy Reviews*, vol. 6, no. 1, pp. 1–12, 2010.

[7] R. P. Singh, G. Sharma, G. U. Mailikarjuna, S. Dhanalakshmi, C. Agarwal, and R. Agarwal, "In vivo suppression of hormone-refractory prostate cancer growth by inositol hexaphosphate: induction of insulin-like growth factor binding protein-3 and inhibition of vascular endothelial growth factor," *Clinical Cancer Research*, vol. 10, no. 1 I, pp. 244–250, 2004.

[8] R. P. Singh and R. Agarwal, "Prostate cancer and inositol hexaphosphate: efficacy and mechanisms," *Anticancer Research*, vol. 25, no. 4, pp. 2891–2904, 2005.

[9] S. Norazalina, M. E. Norhaizan, I. Hairuszah, and M. S. Norashareena, "Anticarcinogenic efficacy of phytic acid extracted from rice bran on azoxymethane-induced colon carcinogenesis in rats," *Experimental and Toxicologic Pathology*, vol. 62, no. 3, pp. 259–268, 2010.

[10] A. Jemal, F. Bray, M. M. Center, J. Ferlay, E. Ward, and D. Forman, "Global cancer statistics," *CA Cancer Journal for Clinicians*, vol. 61, no. 2, pp. 69–90, 2011.

[11] E. R. Fearon and B. Vogelstein, "A genetic model for colorectal tumorigenesis," *Cell*, vol. 61, no. 5, pp. 759–767, 1990.

[12] K. L. Krzystyniak, "Current strategies for anticancer chemoprevention and chemoprotection," *Acta Poloniae Pharmaceutica*, vol. 59, no. 6, pp. 473–478, 2002.

[13] S. Rajamanickam and R. Agarwal, "Natural products and colon cancer: current status and future prospects," *Drug Development Research*, vol. 69, no. 7, pp. 460–471, 2008.

[14] M. Spychalski, L. Dziki, and A. Dziki, "Chemoprevention of colorectal cancer: a new target needed?" *Colorectal Disease*, vol. 9, no. 5, pp. 397–401, 2007.

[15] H. H. Luu, R. Zhang, R. C. Haydon et al., "Wnt/β-catenin signaling pathway as novel cancer drug targets," *Current Cancer Drug Targets*, vol. 4, no. 8, pp. 653–671, 2004.

[16] S. L. Kargman, G. P. O'Neill, P. J. Vickers, J. F. Evans, J. A. Mancini, and S. Jothy, "Expression of prostaglandin G/H synthase-1 and -2 protein in human colon cancer," *Cancer Research*, vol. 55, no. 12, pp. 2556–2559, 1995.

[17] H. Sano, Y. Kawahito, R. L. Wilder et al., "Expression of cyclooxygenase-1 and -2 in human colorectal cancer," *Cancer Research*, vol. 55, no. 17, pp. 3785–3789, 1995.

[18] B. S. Reddy, Y. Hirose, L. A. Cohen, B. Simi, I. Cooma, and C. V. Rao, "Preventive potential of wheat bran fractions against experimental colon carcinogenesis: implications for human colon cancer prevention," *Cancer Research*, vol. 60, no. 17, pp. 4792–4797, 2000.

[19] G. Lala, M. Malik, C. Zhao et al., "Anthocyanin-rich extracts inhibit multiple biomarkers of colon cancer in rats," *Nutrition and Cancer*, vol. 54, no. 1, pp. 84–93, 2006.

[20] Y. S. Bakhle, "Cox-2 and cancer: a new approach to an old problem," *British Journal of Pharmacology*, vol. 134, no. 6, pp. 1137–1150, 2001.

[21] F. M. Ramezanzadeh, R. M. Rao, W. Prinyawiwatkul, W. E. Marshall, and M. Windhauser, "Effects of microwave heat, packaging, and storage temperature on fatty acid and proximate compositions in rice bran," *Journal of Agricultural and Food Chemistry*, vol. 48, no. 2, pp. 464–467, 2000.

[22] S. Zullaikah, E. Melwita, and Y. H. Ju, "Isolation of oryzanol from crude rice bran oil," *Bioresource Technology*, vol. 100, no. 1, pp. 299–302, 2009.

[23] S. Norazalina, M. E. Norhaizan, I. Hairuszah, and S. Nurul Husna, "Optimization of optimum condition for phytic acid extraction from rice bran," *African Journal of Plant Sciences*, vol. 5, pp. 168–175, 2011.

[24] A. L. Camire and F. M. Clydesdale, "Analysis of phytic acid in foods by HPLC," *Journal of Food Sciences*, vol. 47, pp. 575–578, 1982.

[25] R. P. Bird, "Aberrant crypt foci to study cancer preventive agents in the colon," in *Tumor Marker Protocol*, M. Hanaucek and Z. Walaszek, Eds., pp. 465–474, Human Press, New Jersey, NJ, USA, 1998.

[26] R. P. Singh, G. Sharma, G. U. Mailikarjuna, S. Dhanalakshmi, C. Agarwal, and R. Agarwal, "In vivo suppression of hormone-refractory prostate cancer growth by inositol hexaphosphate: induction of insulin-like growth factor binding protein-3 and inhibition of vascular endothelial growth factor," *Clinical Cancer Research*, vol. 10, no. 1 I, pp. 244–250, 2004.

[27] M. S. Cappell, "From colonic polyps to colon cancer: pathophysiology, clinical presentation, screening and colonoscopic therapy," *Minerva Gastroenterologica e Dietologica*, vol. 53, no. 4, pp. 351–373, 2007.

[28] J. Jen, S. M. Powell, N. Papadopoulos et al., "Molecular determinations on aberrant crypt foci from human colons," *Cancer Research*, vol. 54, pp. 5527–5530, 1994.

[29] R. B. Alfin-Slater and D. Kritchevsky, *Cancer and Nutrition*, Plenum Press, New York, NY, USA.

[30] A. Ullah and A. M. Shamsuddin, "Dose-dependent inhibition of large intestinal cancer by inositol hexaphosphate in F344 rats," *Carcinogenesis*, vol. 11, no. 12, pp. 2219–2222, 1990.

[31] T. P. Pretlow, M. A. O'Riordan, T. G. Pretlow, and T. A. Stellato, "Aberrant crypts in human colonic mucosa: putative preneoplastic lesions," *Journal of Cellular Biochemistry Supplement*, vol. 16, pp. 55–62, 1992.

[32] S. Nurul-Husna, M. E. Norhaizan, I. Hairuszah, M. A. Abdah, S. Norazalina, and I. Norsharina, "Rice bran phytic acid (IP_6) induces growth inhibition, cell cycle arrest and apoptosis on human colorectal adenocarcinoma cells," *Journal of Medicinal Plant Research*, vol. 4, no. 21, pp. 2283–2289, 2010.

[33] S. Norazalina, M. E. Norhaizan, I. Hairuszah, A. R. Sabariah, S. N. Husna, and I. Norsharina, "Antiproliferation and apoptosis induction of phytic acid in hepatocellular carcinoma (HEPG2) cell lines," *African Journal of Biotechnology*, vol. 10, no. 73, pp. 16646–16653, 2011.

[34] S. M. Powell, N. Zilz, Y. Beazer-Barclay et al., "APC mutations occur early during colorectal tumorigenesis," *Nature*, vol. 359, no. 6392, pp. 235–237, 1992.

[35] P. Polakis, "The adenomatous polyposis coil (APC) tumor suppressor," *Biochimica et Biophysica Acta*, vol. 1332, no. 3, pp. F127–F147, 1997.

[36] M. Takahashi, K. Fukuda, T. Sugimura, and K. Wakabayashi, "β-catenin is frequently mutated and demonstrates altered cellular location in azoxymethane-induced rat colon tumors," *Cancer Research*, vol. 58, no. 1, pp. 42–46, 1998.

[37] H. Aberle, A. Bauer, J. Stappert, A. Kispert, and R. Kemler, "β-catenin is a target for the ubiquitin-proteasome pathway," *EMBO Journal*, vol. 16, no. 13, pp. 3797–3804, 1997.

[38] P. J. Morin, A. B. Sparks, V. Korinek et al., "Activation of β-catenin-Tcf signaling in colon cancer by mutations in β-catenin or APC," *Science*, vol. 275, no. 5307, pp. 1787–1790, 1997.

[39] M. Molenaar, M. van de Wetering, M. Oosterwegel et al., "XTcf-3 transcription factor mediates β-catenin-induced axis formation in xenopus embryos," *Cell*, vol. 86, no. 3, pp. 391–399, 1996.

[40] J. Behrens, J. P. Von Kries, M. Kühl et al., "Functional interaction of β-catenin with the transcription factor LEF-1," *Nature*, vol. 382, no. 6592, pp. 638–642, 1996.

[41] T. C. He, A. B. Sparks, C. Rago et al., "Identification of c-MYC as a target of the APC pathway," *Science*, vol. 281, no. 5382, pp. 1509–1512, 1998.

[42] O. Tetsu and F. McCormick, "β-catenin regulates expression of cyclin D1 in colon carcinoma cells," *Nature*, vol. 398, no. 6726, pp. 422–426, 1999.

[43] P. Ashokkumar and G. Sudhandiran, "Luteolin inhibits cell proliferation during Azoxymethane-induced experimental colon carcinogenesis via Wnt/ β-catenin pathway," *Investigational New Drugs*, vol. 29, no. 2, pp. 273–284, 2011.

[44] A. K. Pandurangan, P. Dharmalingam, S. K. Ananda Sadagopan et al., "Luteolin induces growth arrest in colon cancer cells through involvement of Wnt/β-catenin/GSK-3β," *Journal of Environmental Pathology, Toxicology and Oncology*, vol. 32, no. 2, pp. 131–139, 2013.

[45] A. Kumar, A. K. Pandurangan, F. Lu et al., "Chemopreventive sphingadienes downregulate wnt signaling via a PP2A/Akt/GSK3β pathway in colon cancer," *Carcinogenesis*, vol. 33, no. 9, pp. 1726–1735, 2012.

[46] S. Norazalina, M. E. Norhaizan, and I. Hairuszah, "Suppression of β-catenin and cyclooxygenase-2 expression and cell proliferation in azoxymethane-induced colonic cancer in rats by rice bran phytic acid (PA)," *Asian Pacific Journal of Cancer Prevention*, vol. 14, pp. 3093–3099, 2013.

[47] Y. Gao and H. Y. Wang, "Inositol pentakisphosphate mediates Wnt/β-catenin signaling," *Journal of Biological Chemistry*, vol. 282, no. 36, pp. 26490–26502, 2007.

[48] Y. Araki, S. Okamura, S. P. Hussain et al., "Regulation of cyclooxygenase-2 expression by the WNT and ras pathways," *Cancer Research*, vol. 63, no. 3, pp. 728–734, 2003.

[49] J. Dimberg, A. Hugander, A. Sirsjö, and P. Söderkvist, "Enhanced expression of cyclooxygenase-2 and nuclear β-catenin are related to mutations in the APC gene in human colorectal cancer," *Anticancer Research*, vol. 21, no. 2 A, pp. 911–916, 2001.

[50] S. J. Kim, D. S. Im, S. H. Kim et al., "β-Catenin regulates expression of cyclooxygenase-2 in articular chondrocytes," *Biochemical and Biophysical Research Communications*, vol. 296, no. 1, pp. 221–226, 2002.